ความว่องไวของไททาเนียขนาดนาโนเมตรที่สังเคราะห์โดยการสลายตัวด้วยความร้อน
ของไททาเนียมนอร์มัลบิวทอกไซด์สำหรับการย่อยสลายซึ่งถูกเร่งด้วยแสงของยาปราบ
ศัตรูพืชแบบฟีนิลยูเรีย

นางสาวจิตลดา คล่องดี

ACTIVITY OF NANOSIZED TITANIA SYNTHESIZED BY THERMAL

DECOMPOSITION OF TITANIUM N-BUTOXIDE FOR PHOTOCATALYTIC

DEGRADATION OF PHENYLUREA HERBICIDES

Miss Jitlada Klongdee

A Thesis Submitted in Partial Fulfillment of the Requirements

for the Degree of Master of Engineering Program in Chemical Engineering

Department of Chemical Engineering

Faculty of Engineering

Chulalongkorn University

Academic Year 2006

Thesis Title ACTIVITY OF NANOSIZED TITANIA SYNTHESIZED BY
THERMAL DECOMPOSITION OF TITANIUM N-BUTOXIDE
FOR PHOTOCATALYTIC DEGRADATION OF PHENYLUREA
HERBICIDES
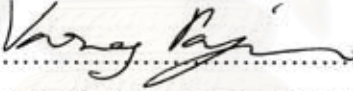By Miss Jitlada Klongdee
Field of Study Chemical Engineering
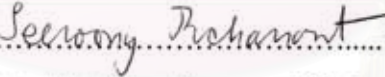Thesis Advisor Assistant Professor Varong Pavarajarn, Ph.D.

Accepted by the Faculty of Engineering, Chulalongkorn University in Partial
Fulfillment of the requirements for the Master's Degree

.... Dean of the Faculty of Engineering
(Professor Direk Lawansiri, Ph.D.)

THESIS COMMITTEE

.... Chairman
(Associate Professor Suttichai Assabumrungrat, Ph.D.)

.... Thesis Advisor
(Assistant Professor Varong Pavarajarn, Ph.D.)

.... Member
(Assistant Professor Seeroong Prichanont, Ph.D.)

.... Member
(Akawat Sirisuk, Ph.D.)

.... Member
(Okorn Mekasuvandumrong, D.Eng)

จิตลดา   คล่องดี: ความว่องไวของไททาเนียขนาดนาโนเมตรที่สังเคราะห์โดยการสลายตัวด้วย
ความร้อนของไททาเนียมนอร์มัลบิวทอกไซด์สำหรับการย่อยสลายซึ่งถูกเร่งด้วยแสงของยาปราบ
ศัตรูพืชแบบฟีนิลยูเรีย (ACTIVITY OF NANOSIZED TITANIA SYNTHESIZED BY
THERMAL DECOMPOSITION OF TITANIUM N-BUTOXIDE FOR PHOTOCATALYTIC
DEGRADATION OF PHENYLUREA HERBICIDES) อ. ที่ปรึกษา: ผศ.ดร.วรงค์ ปวราจารย์,
156 หน้า. ISBN: 974-14-2038-2

อานาเทสไททาเนียเตรียมได้ด้วยวิธีการสลายตัวด้วยความร้อนของไททาเนียมนอร์มัลบิวทอกไซด์
ในตัวกลางอินทรีย์ อันได้แก่ 1,4-บิวเทนไดออล โทลูอีน และมิเนอรัลออยล์ สมบัติเชิงกายภาพของไท
ทาเนียถูกตรวจวัดด้วยเทคนิค XRD SEM TEM และ พื้นที่ผิว BET อานาเทสไททาเนียเกิดขึ้นในเครื่อง
ปฏิกรณ์ที่อุณหภูมิ 270 องศาเซลเซียสโดยไม่มีเฟสอื่นปน เฟสอสัณฐานและการเกาะตัวกันของอนุภาค
ลดลงเมื่ออุณหภูมิในการสังเคราะห์สูงขึ้น   การเผาที่อุณหภูมิสูงจะช่วยเพิ่มความเป็นผลึกของไททาเนีย
ไททาเนียที่เตรียมใน 1,4-บิวเทนไดออลจะให้ลักษณะความเป็นผลึกที่สูงกว่า และมีการเกาะตัวกันของ
อนุภาคน้อยกว่าไททาเนียที่เตรียมในโทลูอีนและมิเนอรัลออยล์   ความว่องไวของการเป็นตัวเร่ง
ปฏิกิริยาของไททาเนียที่สังเคราะห์ได้ถูกทดสอบด้วยการใช้เป็นตัวเร่งปฏิกิริยาเชิงแสงในการสลายตัวของ
สารประกอบ ฟีนิลยูเรีย ได้แก่ ไดยูรอน ลินูรอน และไอโซโปรทูรอน ไททาเนียที่ถูกเผาที่อุณหภูมิสูงให้
ความว่องไวกว่าไททาเนียที่ไม่ได้เผา ซึ่งอธิบายได้จากความเป็นผลึกที่เพิ่มขึ้นของไททาเนีย ไททาเนียที่
เตรียมใน   1,4-บิวเทนไดออลมีความว่องไวสูงกว่าที่เตรียมในโทลูอีนและมิเนอรัลออยล์ เนื่องจาก
ลักษณะความเป็นผลึกที่สูงกว่าและการเกาะตัวกันที่น้อยกว่า   โครงสร้างและความเสถียรของ
สารประกอบฟีนิลยูเรียมีผลต่ออัตราการสลายตัว ไอโซโปรทูรอนมีโครงสร้างที่ว่องไวมากกว่าและมีความ
เสถียรน้อยกว่าจึงทำให้เกิดอัตราการสลายตัวที่เร็วกว่าไดยูรอนและลินูรอน เกิดสารมัธยันต์ขึ้นในระหว่าง
กระบวนการ ปฏิกิริยาการสลายตัวซึ่งถูกเร่งด้วยแสงของสารประกอบฟีนิลยูเรีย สารที่เกิดขึ้นเกิดจากการ
เข้าทำปฏิกิริยาอนุมูลของไฮดรอกซีที่ตำแหน่งต่างๆของสารประกอบฟีนิลยูเรีย โดยปฏิกิริยาออกซิเดชันที่
ตำแหน่งยูเรติกเป็นปฏิกิริยาหลักของกระบวนการนี้

ภาควิชา.............วิศวกรรมเคมี....................   ลายมือชื่อนิสิต......................................
สาขาวิชา.............วิศวกรรมเคมี....................   ลายมือชื่ออาจารย์ที่ปรึกษา......................................
ปีการศึกษา.......2549......................

JITLADA KLONGDEE: ACTIVITY OF NANOSIZED TITANIA SYNTHESIZED BY THERMAL DECOMPOSITION OF TITANIUM N-BUTOXIDE FOR PHOTOCATALYTIC DEGRADATION OF PHENYLUREA HERBICIDES. THESIS ADVISOR: ASSISTANT PROFESSOR VARONG PAVARAJARN, Ph.D. 156 pp. ISBN: 974-14-2038-2

Anatase titania was synthesized by thermal decomposition of titanium (IV) n-butoxide in organic medium, i.e. 1,4-butanediol, toluene and mineral oil. Physical properties of titania were characterized by XRD, SEM, TEM and BET surface area techniques. Anatase titania was formed at temperature of 270°C in an autoclave without contamination of other phases. Amorphous phase and agglomeration was decreased with an increase in temperature synthesis. Crystallinity of titania was improved by calcination at high temperature. Titania synthesized in 1,4-butanediol showed higher crystallinity and less agglomeration than that synthesized in toluene and mineral oil. Photocatalytic degradation of phenylurea herbicides (PUHs), i.e. diuron, isoproturon and linuron, was used to investigate catalytic activity of the synthesized titania. The calcined titania exhibited higher activity than uncalcined titania, which can be explained by the increased crystallinity. Titania synthesized in 1,4-butanediol showed higher activity than that synthesized in toluene and mineral oil, because of higher crystallinity and lower degree of agglomeration. Chemical structure and stability of PUH affected the rate of degradation. The higher activity and less stability of structure of isoproturon give higher rate of degradation than that diuron and linuron. Degradation intermediates of PUH generated intermediates during photocatalytic process, which were formed by reaction of hydroxyl radical attacking to several sites of phenylurea structure. Oxidation at uretic group was found to be the main reaction.

Department...Chemical Engineering....... Student's Signature.....*Jitlada Klongdee*

Field of Study ...Chemical Engineering... Advisor's Signature............

Academic Year.....2006.....................

ACKNOWLEDGEMENTS

CONTENTS

Page

LIST OF TABLES

Table **Page**

LIST OF FIGURES

Figure   **Page**

Figure   **Page**

CHAPTER I

INTRODUCTION

Titanium (IV) oxide or titania (TiO_2) is one of the most common metal oxides recognized in various industries. Due to its good physical and chemical properties, such as catalytic activity (Coulter 1995), photocatalytic activity (Wakanabe 1993), good stability toward adverse environment (Tonejc 1996), sensitivity to humidity and gas (Traversa 1996), dielectric characteristic (Ohtani 1993), nonlinear optical characteristic (O'Regan 1991) and photoluminescence (Liu 1997), titania has been used in many fields of application including the use as catalysts, catalyst supports, electronics, cosmetics, pigments and filler coating. Nevertheless, photocatalyst is one of the most important applications of titania. Titania is known to have three natural polymorphs, i.e. rutile, anatase, and brookite, but only anatase is generally accepted to have significant photocatalytic activity (Nishimoto 1985; Fox 1993; Tanaka 1993).

Many factors affect the photocatalytic activity of titania. Particle size is one of the most important factors. It has been reported that photocatalytic activity is increased with the decrease in titania particle size, especially into nanometer-scale, because of high surface area and short interface migration distances for photoinduced holes and electrons (Sato 1996; Uchida 1997; Xu 1999). Nanocrystalline titania can be synthesized by many methods, such as sol-gel method, hydrothermal method, vapor-phase hydrolysis, laser-induced decomposition, chemical vapor decomposition and molten salt method. In this work, nanocrystalline anatase titania was synthesized via the thermal decomposition of titanium alkoxide in organic solvent, which has been employed to synthesize various nanocrystalline metal-oxides (Inoue 1988; Inoue 1992

; Inoue 1993; Kominami 1997; Kominami 1999; Kongwudthiti 2003; Mekasuwandumrong 2003).

Hydrothermal method has been widely applied for the synthesis of variety of ceramic materials. Synthesis of metal oxides which uses organic solvent instead of water in hydrothermal method, at temperature high than boiling point of the solvent is called solvothermal synthesis. Many researchers have also explored the synthesis of inorganic materials in glycols in the same fashion and called "Glycothermal method" (Bibby 1978; Cruickshack 1985; Inoue 1991; Kominami 1999). Nevertheless, these methods are all based on the thermal decomposition of precursor, which is often metal-oxides, in the reaction medium. By solvothermal method, nanocrystalline titanium (IV) oxide can be produced. It has been demonstrated that the activity of titania synthesized by this method is much higher than that of commercially available titania for photocatalytic decomposition of simple compound, such as acetic acid, in aqueous solution (Kominami 1997). However, it has never been used for the decomposition of more complex substance. In this study, photodegradation of complex substance, i.e. diuron [3-(3,4-dichlorophynyl)-1,1-dimethylurea], linuron [1-methoxy-1-methyl-3-(3,4-dichlorophenyl)urea] and isoproturon [N-(4-isopropylphenyl)-N′,N′-dimethylurea], is employed to investigate the activity of titania prepared by this method.

Phenylurea herbicides (PUHs) have been widely used throughout the world for long time. However it has resulted in residue in crops, soil and surface water (Liska 1996; Simon, 1998), which consequently inhibits photosynthesis in crops and affects

human and animal health. Diuron, linuron and isoproturon are common herbicides belonging to this group, yet their properties and chemical stability are varied.

In this study, it is intended to investigate the photocatalytic degradation of these phenylurea herbicides by using nanocystalline titania synthesized via the thermal decomposition of titanium alkoxide in organic solvents. The results are compared with reference catalyst from the Catalysis Society of Japan.

The objectives of this research are listed as following:

1. To study the thermal decomposition of titanium alkoxide in organic solvents for the synthesis of nanocrystalline titania. Effects of catalyst preparation conditions on chemical and physical properties of the synthesized titania are investigated.

2. To investigate the photocatalytic degradation of phenylurea herbicides mentioned earlier, using titania as catalyst. Effect of photocatalytic reaction conditions on the degradation activity are also subject to study in this research.

The present thesis is arranged as follows:

Chapter II explains the basic theory about titania such as the general properties of titania, various preparation methods to obtain the ultrafine titania and phenylurea herbicides.

Chapter III shows experimental systems and procedures for the preparation of titania by thermal decomposition method, and the photocatalytic degradation experiments.

Chapter IV presents the experimental results and discussion.

In the last chapter, the overall conclusions of this research and recommendations for the future work are given.

Crystallite size determination and GC-MS data are included in Appendices at the end of this thesis.

CHAPTER II

THEORY AND LITERATURE REVIEWS

The theory relating to titania synthesis, properties of phenylurea herbicides and photocatalytic degradation of organic compounds will be explained in this chapter.

2.1 Physical and Chemical Properties of Titania

Titanium (IV) oxide or titania has great potential for many industrial applications. Therefore, many researches have focused on its fabrication and characterizatio. Titania has been used in many fields of application such as catalyst, catalyst support, electronics, cosmetic pigment and filter coating (Nishimoto 1985; Fox 1993; Tanaka 1993). In recent years, main attention has been devoted to its photocatalytic activity and photoinduced superhydrophilicity. Since titania has relatively wide band gap (3.2 eV), charge carriers, i.e. electrons and holes, are produced when titania is excited. Consequently, highly reactive radicals are generated and oxidation-reduction reaction of species adsorbed on the surface of titania can occur (Zeman 2003). Basic thermochemical data of titania are shown in Table 2.1.

Titania is thermally stable with a melting point of 1855°C. It also has resistance to many chemical attacks. The reactivity of titania towards acids is very dependent on preparation route and thermal history.

Table 2.1 Thermochemical data for formation of titanium oxide compound

Compound	State	Heat of formation ΔH_f^o, kJ/mol		Free energy of formation ΔG_f^o, kJ/mol		Entropy S, J/mol.K	
		At 298 K	At 1300 K	At 298 K	At 1300 K	At 298 K	At 1300 K
TiO	Crystal	-519.6	-515.9	-495.1	-417.1	50.2	127.0
TiO$_2$							
-Anatase	Crystal	-933.0	-930.0	-877.6	-697.4	49.9	150.6
-Rutile	Crystal	-944.7	-942.4	-889.5	-707.9	50.3	149.0

For instance, titania prepared by precipitation from titanium (IV) solution and gently heated to remove water is soluble in concentrated hydrochloric acid. However, if titania is heated to temperature approximately 900°C, its solubility in acids is considerably reduced. Titania can be slowly dissolved in hot concentrated sulfuric acid, whereas the rate of salvation is increased by the addition of ammonia sulfate. Another acid that can dissolve titania is hydrofluoric acid, which is used extensively in the analysis of titanium (IV) oxide trace elements. Aqueous alkalines have virtually no effect on titania, but molten sodium and potassium hydroxides, carbonates and borates dissolve titania readily.

Titania occurs in three crystalline forms, i.e. anatase, rutile and brookite. Rutile is a thermodynamically-stable phase of titania that can be found in igneous rock. It is one of two most important ores of titanium. Anatase is a metastable phase, which tends to be more stable at low temperature. For brookite, it is formed under hydrothermal conditions and usually found only in mineral. Brookite has been produced by heating amorphous titania, which is prepared from the reaction between alkyl titanates with sodium or potassium hydroxide in an autoclave at 200 to 600°C for several days (Li 2004). Among all crystalline phases of TiO_2, anatase is the most photoactive phase and has been employed as photocatalyst for long time.

The crystallographic characteristic of these varieties are shown in Table 2.2. Although anatase and rutile are both tetragonal, they are not isomorphous (Figure 2.1). Anatase usually occurs in near-regular octahedral form, while rutile forms slender prismatic crystals that are frequently twinned. Nevertheless, both anatase and rutile are anisotropic of which physical properties vary according to direction relative

to the crystal axes. However in most applications using these substances, the distinction between crystallographic direction is lost because of the random orientation from large number of small particles or grains in the article.

Table 2.2 Cystallographic characteristic of anatase, brookite and rutile.

Properties	Anatase	Brookite	Rutile
Crystal Structure	Tetragonal	Orthorhombic	Tetragonal
Optical	Uniaxial, negative	Biaxial, positive	Uniaxial, negative
Density, g/cm^3	3.9	4.0	4.23
Hardness, Mohs scale	$5\frac{1}{2}$ - 6	$5\frac{1}{2}$ - 6	7- $7\frac{1}{2}$
Unit cell	$D_4a^{19}.4TiO_2$	$D_2h^{15}.8TiO_2$	$D_4h^{12}.3TiO_2$
Lattice parameter, nm			
a	0.3758	0.9166	0.4584
b		0.5436	
c	0.9514	0.5135	2.953

(a)   (b)   (c)
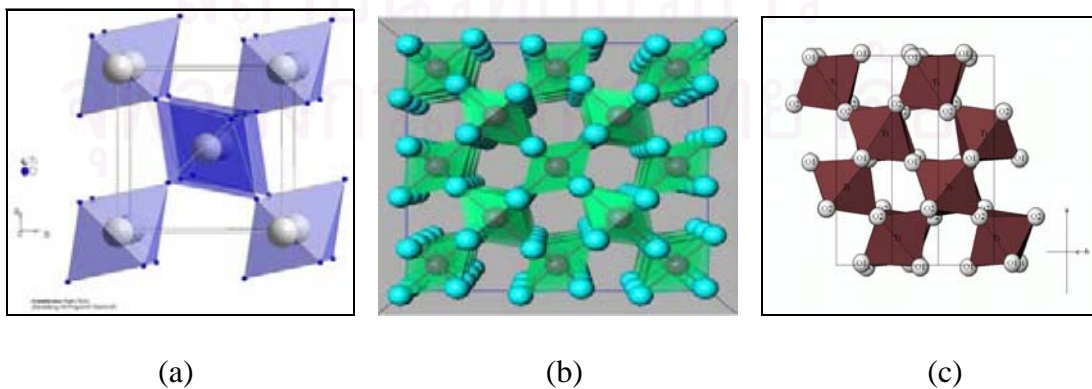
Figure 2.1 Crystal structure of TiO_2; (a) Rutile, (b) Anatase, (c) Brookite.

Three allotropic forms of titania have been prepared artificially, but only rutile has been obtained in the form of transparent large single crystal. The transformation from anatase to rutile is accompanied by evolution of ca. 12.6 kJ/mol (3.01 kcal/mol). The rate of phase transformation is greatly affected by temperature and by presence of other substances which may either catalyze or inhibit the transformation. The lowest temperature at which the conversion from anatase to rutile takes place at a measurable rate is approximately 500-550°C (Depero 1993). The change is not reversible and it has been shown that ΔG for the transformation from anatase to rutile is always negative.

2.2 Titania Synthesis Methods

There are several methods that can be used to synthesize anatase titania. In general, methods which have been reported for anatase synthesis are: sol-gel method, chemical vapor deposition, thermal decomposition method and precipitation method.

2.2.1 Sol-gel method

This method can be performed at relatively low temperature to prepare a solid. Sol is first prepared from suitable reactants in suitable liquid. Sol preparation can be either simply the dispersion of insoluble solids in liquid or addition of precursor which reacts with the solvent to form a colloidal product. A typical example of the former approach is the dispersion of oxides or hydroxides in water with the pH adjusted so that the solid particles remain in suspension rather than precipitate out. A typical example of the later approach is the addition of metal alkoxide to water. The alkoxides are hydrolyzed giving the oxide as a colloidal product. The sol is then either

treated or simply left to form a gel. To obtain a final product, the gel is heated. This heating serves several purposes. It removes the solvent, decomposes anions such as alkoxides or carbonates to give oxides, allows rearrangement of the structure of the solid and allows crystallization. For the synthesis of titania, the process starts with the mixing of titanium alkoxide with alcohol. Acidic aqueous solution is subsequently added to the mixture (Jung 1999). This technique can be adapted by using ultrasonication to aid dispersion, which can result in titania with higher surface area and better thermal stability than titania prepared by using stirring method (Awati 2003). The average crystal size of titania synthesized by this method has been reported to be in the range of $4 - 8$ nm with BET surface area in the range of 91-120 m^2/g, depending on calcination temperature. However the limit of this method is that strong reactivity of alkoxide toward water often results in uncontrolled precipitation.

2.2.2 Chemical vapor deposition method

This method involves the formation of noncrystalline (amorphous) titania by hydrolysis and condensation of titanium alkoxide (Watson 2003). The preparative process is conducted in an aerosol reactor, which is made of two concentric glass tubes, externally heated in a vertical furnace. Titanium precursor is evaporated in separated reactor to control its vapor pressure before it is carried by N_2 gas into the reactor. Water vapor is then introduced into the reactor by using dry air as the carrier. Precursor vapor and water vapor are mixed rapidly and react to form TiO_2 aerosol at atmospheric pressure. Consequently, the product is collected by thermophoresis and filter. The as-prepared TiO_2 powder is then put into furnace for heat treatment.

2.2.3 Precipitation method

Ultrafine crystalline titania powder can be prepared by heating and stirring of $TiOCl_2$ aqueous solution with Ti^{+4} concentration of 0.5 mol/l from room temperature up to 100°C under normal atmospheric pressure (Nam 1998). Crystalline phase of the synthesized titania can be controlled from the reaction temperature. Titania crystals in pure rutile phase precipitated at temperature below 65°C. On the other hand TiO_2 precipitates in anatase phase at temperature higher than 65°C. The direct formation of TiO_2 crystalline precipitates from aqueous $TiOCl_2$ solution is the result from the existence of the OH^- ions in water which cause the crystallization of $TiOCl_2$ into TiO_2 without hydrolyzation to $Ti(OH)_4$. Conventionally, rutile phase is synthesized at much higher temperature. However, in this study a stable rutile phase TiO_2 was obtained by a simple method at temperature close to room temperature.

2.2.4   Chloride process

Ultrafine titania particles are produced routinely on large scale by the oxidation of titanium tetrachloride ($TiCl_4$) vapor. The reaction take place in gas phase at temperature in the range of 700 to 1400°C, resulting in the formation and growth of fine titania particles. Titania synthesized by this method is commonly used in coating to provide maximum light scattering without absorption. It has been shown that the product is primarily anatase but fraction of rutile increases with increasing reaction temperature. Moreover, the average particle size increases with the increase in both inlet $TiCl_4$ concentration and residence time.

2.2.5   *Thermal decomposition method*

Thermal decomposition method has been developed for the synthesis of metal oxide and binary metal oxide by decomposition of precursor, often metal-oxides, in the reaction medium, e.g. organic solvent or glycol. It is a modification of hydrothermal method, in which the reaction takes place in water under moderately high temperature and pressure. The use of glycol or solvent instead of water produces the different form of the intermediate phase of which the stability is not so strong. Instability of the intermediate phase gives a large driving force to the formation of product under quite mild condition. This method has been used to successfully synthesize various types of nanosized metal oxides, including titania, with large surface area, high crystallinity and high thermal stability (Payakgul 2005). Titanium precursor such as titanium alkoxide, was used as starting material for titania synthesis. Titanium precursor was first suspended in organic solvent in a cavity of an autoclave. The crystalline titania was formed at temperature in the range of 200-300°C in the autoclave. It has been reported that physiochemical properties of the synthesized titania depend on the reaction conditions as well as the calcination temperature. This method was selected to prepare titania in this work.

2.3 Photocatalysis on Anatase Titania

Photocatalysis can be defined as the acceleration of photoreaction by presence of catalyst. Photocatalysis over a semiconductor oxide such as TiO_2 is initiated by the absorption of photon with energy equal to or greater than the band gap of the semiconductor (3.2 eV for TiO_2), producing electron-hole (e^-/h^+) pairs. The holes can

react with water to produce highly reactive hydroxyl radicals, which are the key for further reaction. Following irradiation, the TiO_2 particles can act as either an electron donor or acceptor for molecules in the surrounding media. However, the photoinduced charges in bare TiO_2 particles have a very short lifetime because of the quick charge recombination. Therefore, for effective photocatalytic process, it is important to prevent hole-electron recombination before designated chemical reaction occurs on the TiO_2 surface (Popielarski 1998).

Heterogeneous photocatalysis has been used to decompose various pollutants (Herrmann 1999). The process can be carried out in various medias, i.e. gas, organic liquid or aqueous solution. Titania is one of the most of frequently used semiconductor catalysts. Nevertheless anatase is the only crystalline form of titania that has effective photocatalytic activity. The photocatalytic reaction on anatase TiO_2 has attracted attention for application in decomposition and elimination of various organic pollutant in air and water (Inagaki 2004). Photocatalysis based on TiO_2 are promising for water decontamination (Macounova 2003). Many organic substances have been mineralized to CO_2, H_2O and corresponding mineral acids using TiO_2 under irradiation (Fox 1993). As mentioned earlier the processes of photocatalytic degradation are induced by absorption of photons by titania particles, which consequently results in the photogeneration of separated charge carriers, i.e. electrons and holes. The positive holes can be trapped by surface hydroxyl groups forming highly reactive hydroxyl radicals. These highly oxidizing species react rapidly with almost every organic molecule and thus initiate its oxidative decomposition. The electrons are typically transferred to dioxygen yielding superoxide radical anion ($\bullet O_2^-$). The dissolved dioxygen is an essential reaction component of the

photocatalysis, which also participates further in steps of degradation. It can repeatedly react with organic radicals originated from the primary OH⁻ attacks leading to peroxyl radicals of various structures. There are two typical ways of these transformations: an elimination of hydroperoxyl radical (•OOH) and a bimolecular recombination of two peroxyl radicals. In the latter case, the initially formed tetraoxides represent unstable intermediates that usually decompose producing two oxygen-containing compounds. The repetition of these processes leads to gradual oxidation of the original organic compound, to get CO_2, which is a substance with the highest oxidation level of carbon, as product.

The detailed mechanism of photocatalytic degradation of aqueous organic compound on anatase titania can be expressed by a series of advanced oxidation process (AOP) as following (Houas 2001).

1) Absorption of efficient photons ($h\nu \geq E_G = 3.2$ eV) by titania

$$(TiO_2) + h\nu \rightarrow e^-_{CB} + h^+_{VB} \qquad (2.1)$$
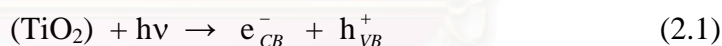
2) Oxygen ionosorption (first step of oxygen reduction)

$$(O_2)_{ads} + e^-_{CB} \rightarrow O_2^{\bullet-} \qquad (2.2)$$
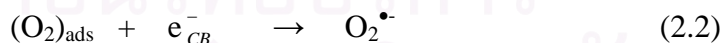
3) Neutralization of OH⁻ groups by photoexcited holes

$$(H_2O \Leftrightarrow H^+ + OH^-)_{ads} + h^+_{VB} \rightarrow H^+ + OH^\bullet \qquad (2.3)$$
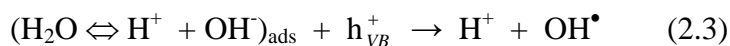
4) Neutralization of $O_2^{\bullet-}$ by protons

$$O_2^{\bullet-} + H^+ \rightarrow HO_2^\bullet \qquad (2.4)$$

5) Transient hydrogen peroxide formation

$$2\ HO_2^{\bullet}\ \rightarrow\ H_2O_2\ +\ O_2 \tag{2.5}$$

6) Decomposition of H_2O_2 and second reduction of oxygen

$$H_2O_2\ +\ e^-\ \rightarrow\ OH^{\bullet} + OH^- \tag{2.6}$$

7) Oxidation of the organic reactant via successive attack by $OH^{\bullet}$ radical

$$R\ +\ OH^{\bullet}\ \rightarrow\ R'^{\bullet}\ +\ H_2O \tag{2.7}$$

8) Direct oxidation by reaction with holes

$$R\ +\ h^+\ \rightarrow\ R^{+\bullet}\ \rightarrow \text{degradation products} \tag{2.8}$$

It has been generally accepted that nanometer-sized particles have different physical and chemical properties from bulk materials. When used as catalysts, their catalytic activity is expected to be enhanced not only because of their increased surface area, but also because of the change of surface properties such as surface defects. For the photocatalysis on titania, it has been reported that photocatalytic activity is increased with the decrease in titania particle size into nanometer scale because of the short interface migration distance for photoinduced hole and electron (Sato 1996; Uchida 1997; Xu 1999).
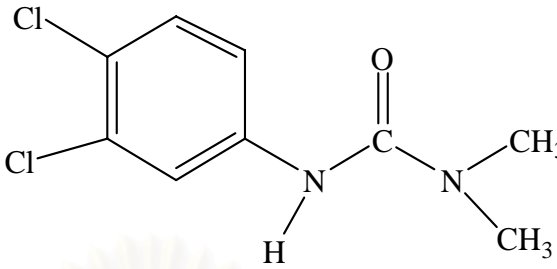
2.4. Phenylurea Herbicides

In the present day, tropical countries of the world still use herbicide in agriculture. It is the cause of many problems about toxic contamination in environment. Phenylurea herbicide is one group of herbicide which has been widely used throughout the world to eliminate general weed for various crops such as citrus, asparagus and bush fruit (Pena 2002). Phenylurea herbicide functions as photosynthesis inhibitor. However, only less than 1% of total applied herbicide reaches the target plant. The vast majority being dispersed ends up contaminating land, air and mainly water. Examples of herbicide in this group are diuron, isoproturon, linuron, monuron and fenuron. In this work, diuron, isoproturon and linuron are selected as representatives for an investigation of phenylurea degradation by photocatalytic reaction.

2.4.1 Diuron

Diuron [3-(3,4-dichlorophenyl)-1,1-dimethylurea) or N´-(3,4-dichlorophenyl)-N,N-dimethyl urea] is one of the most commonly used herbicide for more than 40 years. It is largely used for selective control of germinating grass and broad-leaved weed in many crops. It is also used for total weed control in non-cultivated area (Tomlin 2000). It has been shown to inhibit plant photosynthesis by blocking light reaction (Cawse 1980). Diuron is bio-recalcitrant and chemically stable with half-life in soil over 300 days. Since diuron is slightly soluble (solubility of 36.4 mg/l at 25 °C), it can slowly penetrate through soil and contaminate underground water (Macounova 2003). Physical properties of diuron are shown in Table 2.3.

Table 2.3 Physicochemical properties of diuron.

Chemical structure	
Molecular formula	$C_6H_{10}Cl_2N_2O$
Molecular weight	233.10
Melting point	158 – 159°C
Vapor pressure	0.0041 Pa at 30°C
Appearance	White crystalline solid
Synonyms	Cekiuron, Crisuron, Dailon, Diater Di-on, Derex4L, Diurex, Diurol Dynex, etc.
Solubility	42 ppm in water at 25°C
Toxicity	The concentrated material may cause irritation to the eyes and mucous membrane, but a 50% water paste was not irritating to the intact skin of mammal
Half-life	Over 300 days in soil

(Malato 2003) studied the technical feasibility, mechanisms, and performance of the degradation of aqueous diuron in pilot scale, using two well-defined photocatalytic systems, i.e. heterogeneous photocatalysis with titania and homogeneous photocatalysis by photo-fenton. Equivalent pilot scale and field

conditions used for both techniques allowed adequate comparison for degree of mineralization and toxicity achieved as well as the transformation products generated en route to mineralization by both systems. Total disappearance of diuron was attained by both phototreatments in 45 min, where 100 % of chlorine was recovered as chloride, but total recovery of nitrogen as inorganic ions was not attained. About 90% of mineralization was reached after 200 min of photocatalytic treatment. Transformation products evaluated by LC-IT-MS by direct injection of the samples were the same in both cases. The main differences between the two processes were in the amount of transformation product generated.

(Konstantinou 2003) studied the reaction pathway of TiO_2 photocatalysis of many phenylurea herbicides such as diuron. The reaction pathways are hydroxylation, oxidation and decarboxylation that can result in given the transformation products as hydroxyl-phenylurea, phenyl-hydroxyurea and aniline derivatives, respectively. Because the solubility of diuron in water at ambient temperature is very low and many analytical technique was not suitable for detecting such weak concentration, the photocatalyzed mineralization of diuron was carried out in organic (CH_3CN) and in semi-aqueous (CH_3CN-H_2O) media (Bouquet-Somrani 2000). The experiments showed that diuron degradation was faster in CH_3CN than CH_3CN-H_2O. After about 8 h of irradiation in acetronitrile, the disappearance of diuron was complete, whereas in acetronitrile-water, it was not totally achieved even after 48 h.

(Madani 2006) studied the practical elimination of diuron from water by photocatalysis using two commercial titania photocatalysts (Degussa P25 (50 m^2/g)) and Millennium PC500 (340 m^2/g). These two catalysts were compared as suspension

in slurry reactor. Their activities were determined, based on the rate of diuron disappearance. In particular, comparison was made on their initial activities, which was independent of the influence of intermediates formed. Under identical conditions, Degussa P25 appeared to be substantially more active than Millennium PC500. The equilibrium was reached within less than 30 min in both cases. It was observed that diuron was fully degraded in less than 45 min by titania Degussa P25, whereas, with titania PC500, ca. 7% of diuron remained after 106 min of irradiation. In case of the P25/PC500 mixture, an irradiation time of 60 min was sufficient to degrade 100% of diuron existing in solution.
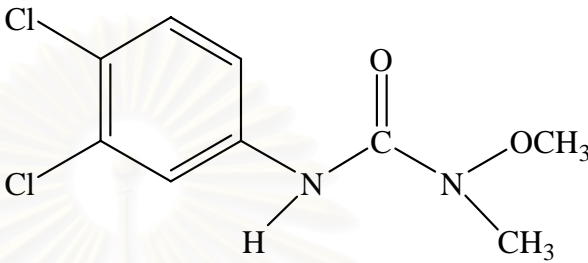
(Macounova 2003) studied the kinetic of photocatalytic degradation of diuron in aqueous colloidal solution of Q-TiO_2 nanoparticles by applying a model of parallel consecutive reactions in the first-order. The mechanism was compared with the reaction pathways of electrochemically assisted photoprocesses on illuminated TiO_2 layers, polarized by external voltage, in various solvents. While a reductive dechlorination on benzene ring of diuron represented the major pathway in acetonitrile, a consecutive oxidative demethylation on the aliphatic side chain was mainly observed in water.

2.4.2 Linuron

Linuron [3-(3,4-dichlorophenyl)-1-methoxy-1-methyl urea or N´-(3,4-dichlorophenyl) N´-methoxy- N´-methyl urea] is a selective herbicide belonging to the phenylurea group with pre- and post-emergence activity. It is widely used in different types of cultivation. Linuron tends to be strongly absorbed by soil and therefore its mobility is low (Sanchez-Martin 1996). Linuron is used to control weed

in many vegetations including potatoes, peas, carrot, bean, wheat, celery, parsnip and parsley. Its properties are shown in Table 2.4.

Table 2.4 Physicochemical properties of linuron.

Chemical structure	

Molecular formula	$C_9H_{10}Cl_2N_2O_2$
Molecular weight	249.17
Melting point	85 - 94°C
Vapor pressure	0.0020 Pa at 24°C
Appearance	White crystalline solid
Synonyms	Afalon, Lorox, Linex, Linurex, Markman1, Rotalin, etc.
Solubility	75 ppm in water at 25°C
Toxicity	Excessive exposure to Linuron may affect the blood, and may cause cancer, vary to aquatic organism and likely to be harmful to other wildlife, low toxicity herbicide
Half-life	3-4 months in most soils
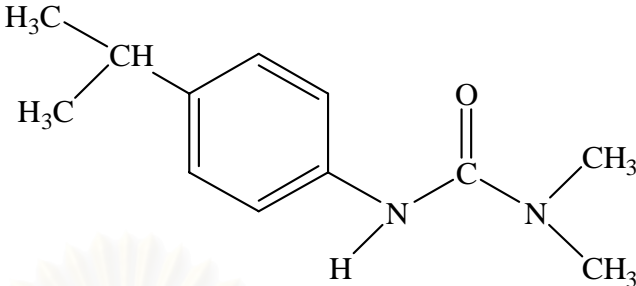
(Katsumata 2005) studied the photodegradation of linuron, which was carried out in the presence of Fenton reagent. The degradation rate was strongly influenced

by the pH and initial concentrations of H_2O_2 and Fe(II). An initial linuron concentration of 10 mg/L was completely degraded after 20 min under the optimum conditions. The decrease of TOC as a result of mineralization of linuron was observed during the photo-Fenton process. The degree of linuron mineralization was about 90% under UV irradiation after 25 h. The formations of chloride, nitrate and ammonium ions as end-products were observed during the photocatalytic system. The decomposition of linuron gave eight kinds of intermediate products. The first step of decomposition pathway of linuron was initiated by the attack on the aromatic ring by OH• radicals without dechlorination or alkyl chains. The next step involved a series of oxidation processes that eliminated alkyl groups and chlorine atoms. The last step involved oxidative opening of the aromatic ring, leading to small organic ions and inorganic species. The degradation mechanism of linuron was proposed based on the evidence of the identified intermediates.

2.4.3 *Isoproturon*

Isoproturon [3-(4-isopropylphenyl)-1,1-dimethylurea or 3-p-cumenyl-1,1-dimethylurea] is a selective herbicide acting by inhibition of photosynthesis (Tomlin 1994). It has been used for pre-and post-emergence control of annual grass, wild oats, annual meadow grass and many broad leaf weeds, etc. Isoproturon can be mobile in soil and has been detected in both surface water and ground water. In water, its half-life is about 30 days. Its properties are shown in Table 2.5.

Table 2.5 Physicochemical properties of isoproturon

Chemical structure	
Molecular formula	$C_{12}H_{18}N_2O$
Molecular weight	206.29
Melting point	155 – 156°C
Vapor pressure	0.003 mPa at 20°C
Appearance	White crystalline solid
Solubility	72 ppm in water at 20°C
Toxicity	Low toxic, acute oral to mouse is over 10000 mg/kg
Half-life time	30 days in water , 6.5 to 30 days in soil

(Farre 2005) studied Photo-Fenton/ozone (PhFO) and TiO_2-photocatalysis/ozone (PhCO) coupled systems using as advanced oxidation processes for the degradation of biorecalcitrant pesticides, such as alachlor, atrazine, chlorfenvinfos, diuron, isoproturon and pentachlorophenol. The degradation process of the different pesticides that occurred through oxidation of the organic molecules by means of their reaction with generated OH radical followed a first and zero-order kinetics, when PhFO and PhCO were applied, respectively. These two advanced oxidation processes, together with the traditional ozone +UV, have been used to investigate TOC reduction of the different pesticide aqueous solutions. Best results of

pesticide mineralization are obtained when PhFO is applied. With the use of this advanced oxidation process the aqueous pesticide solutions became detoxified except in the case of atrazine and alachlor aqueous solutions, for which no detoxification was achieved at the experimental conditions, at least after 2 and 3 h of treatment, respectively. The reaction constants in the first order kinetics for degradation of isoproturon, i.e. k_{PhFO} and k_{PhCO} are 6.2 and 6.0, respectively.

(Parra 2002) studied the degradation of metobromuron, isoproturon, chlortoluron, and chlorbromuron in heterogeneous photocatalytic solution via TiO_2. The influence of parameters such as TiO_2 and herbicide concentration was investigated and the optimal conditions for the abatement of the herbicides were found. The primary degradation of the herbicides was measured by HPLC analysis. A systematic study of their photodegradation was conducted to assess structure–photoreactivity relationship. Correlation analysis showed that photoreactivity was associated with the molecular dipolar moment, which depended on the differences in electronegativity of the substituents in the aromatic ring of each herbicide. The effect of the molecular charge distribution encoded in the dipolar moment was confirmed by the calculation of electrostatic potential contour maps. It was also found that photoreactivity was inversed to the adsorption capability of these compounds on TiO_2. Indeed, as confirmed in this study, the extent of adsorption was not necessarily decisive in the evolution of the photochemical process and the photocatalytic reactions could occur independently of the degree of adsorption of the herbicides on TiO_2.

(Haque 2003) studied heterogeneous photocatalysed degradation of a herbicide derivative, N-(4-isopropylphenyl)-N′,N′-dimethylurea or isoproturon in aqueous suspension of titania by monitoring the change in absorption intensity and depletion in Total Organic Carbon content as a function of irradiation time. The degradation kinetics was studied under different conditions such as pH, catalyst concentration, substrate concentration, and different types of TiO_2 and in the presence of electron acceptors such as hydrogen peroxide (H_2O_2), potassium bromate ($KBrO_3$) and potassium persulphate ($K_2S_2O_8$). The degradation rate was found to be strongly influenced by all of the above parameters. The photocatalyst Degussa P25 was found to be more efficient, comparing to other photocatalysts. An attempt was made to identify the degradation product through GC-MS analysis technique.

CHAPTER III

EXPERIMENTAL

3.1 Preparation of Titania

3.1.1 Chemicals

1. Titanium (IV) n-butoxide (TNB, Ti[O(CH$_2$)$_3$CH$_3$]$_4$), 97% available from Aldrich

2. 1,4-butanediol (1,4-BG, (HO(CH$_2$)$_4$OH), 99% available from Aldrich

3. Toluene (C$_6$H$_5$CH$_3$), 100% available from Finechem

4. Paraffin liquid (Mineral oil), 100% available from Finechem

5. Methanol

6. Acetone

3.1.2 Equipments

The equipment for the synthesis of titania consisted mainly of a 300 cm^3 autoclave reactor, as shown in Figure 3.1. The autoclave was connected to a heater and a temperature readout as shown in Schematic diagram in Figure 3.2
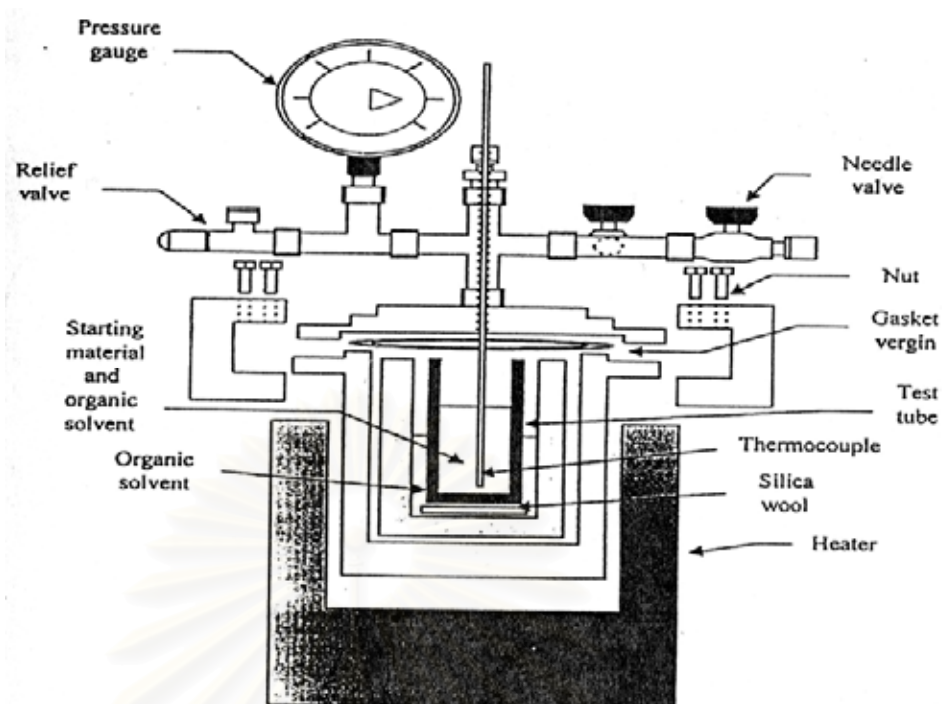
Figure 3.1 Autoclave reactor
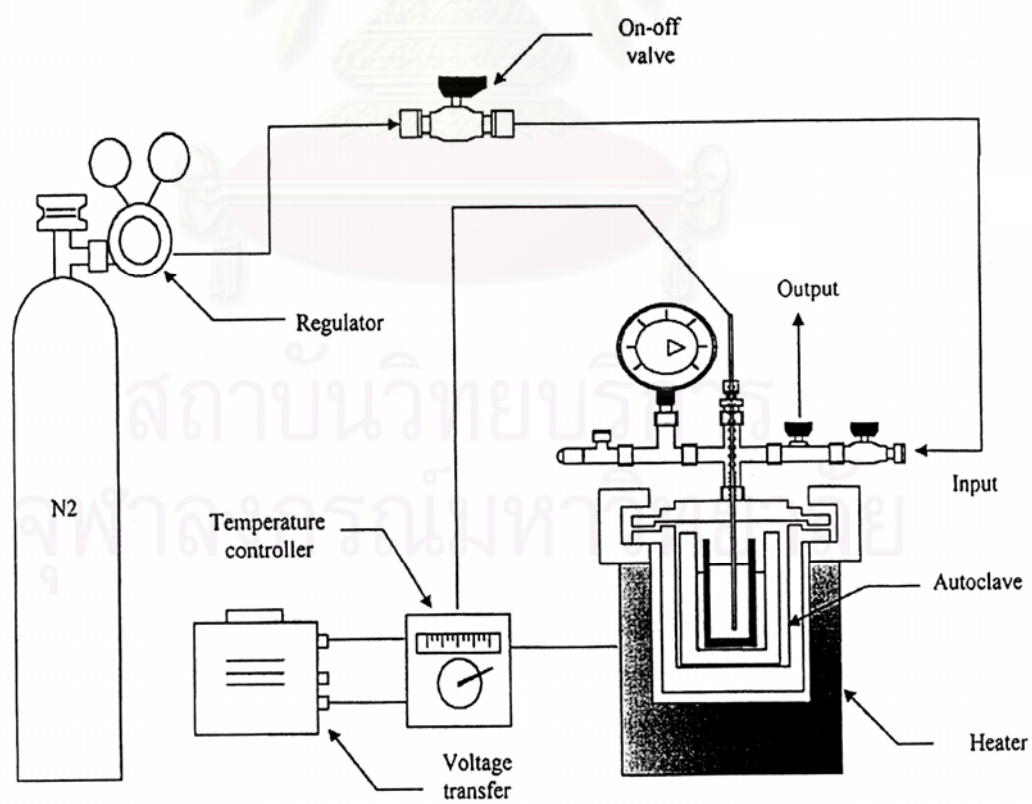
Figure 3.2 Diagram of the reaction equipment for synthesis of titania

*3.1.3 Preparation procedure*s

Titania was synthesized by using titanium (IV) n-butoxide (TNB) as starting material. About 15 g of TNB was suspended in 100 ml of solvent in a test tube. The test tube was then placed in another test tube, which contained 30 ml of the same solvent. Therefore, the gap between two test tubes was filled the solvent. The test tubes then placed in the autoclave. The autoclave was purged completely by nitrogen before heating up to desired temperature (270°C or 300°C) at the rate of 2.5°C/min. Autogeneous pressure during the reaction gradually increased as temperature was raised. The system was held at the desired temperature for 2 hours before cooling down to room temperature. The resulting powders in the test tube were repeatedly washed with methanol by centrifugation. They were then dried in air.

The calcination of the thus-obtained product was carried out in the box furnace. The product was heated at rate of 10°C/min to desired temperature (400°C – 600°C) and held at that temperature for 2 hours.

3.1.4   *Characterizations of titania*

3.1.4.1 X-ray diffraction (XRD)

The XRD analysis of powder was performed by Siemens D5000 X-ray diffractometer at the Center of Excellence on Catalysis and Catalytic Reaction Engineering, Chulalongkorn University. The measurements were carried out by using Ni-filtered CuKα radiation. The crystallite size was estimated from line broadening

according to the Scherrer equation (see Appendix A), using α-Al_2O_3 as standard.

3.1.4.2 Scanning electron microscopy (SEM)

Morphology and size of secondary particles of the samples were observed by Scanning electron microscope (SEM), JEOL JSM-5410LV at the Scientific and Technological Research Equipment Center, Chulalongkorn University (STREC).

3.1.4.3 Surface area measurement

The BET surface area of the samples was measured by a Pulse Chemisorption System: Micrometrics Chemisorp 2750 at the Center of Excellence on Catalysis and Catalytic Reaction Engineering, Chulalongkorn University. Using nitrogen as the adsorbate. The operating conditions are as follows:

Sample weight   ~ 0.3 g

Degas temperature   200°C

Vacuum pressure   < 10 mmHg

3.1.4.4 Transmission electron microscopy (TEM)

Morphology and size of primary particles of the samples were observed by Transmission electron microscopy (TEM) model JEM-100SX at the Scientific and Technological Research Equipment Center, Chulalongkorn University (STREC).

3.2 Photocatalytic Degradation of Phenylurea Herbicides

3.2.1 Herbicides

1. Diuron (3-(3,4-dichlorophenyl)-1,1-dimethylurea or N´-(3,4-dichlorophenyl)-N,N-dimethyl urea), 98% available from Sigma

2. Linuron (3-(3,4-dichlorophenyl)-1-methoxy-1-methyl urea or N´-(3,4-dichlorophenyl)N´-methoxy- N´-methyl urea), 99% available from Chem Service

3. Isoproturon (3-(4-isopropylphenyl)-1,1-dimethylurea or 3-p-cumenyl-1,1-dimethylurea), 99% available from Chem Service

3.2.2 Experimental procedures

Photocatalytic degradation of phenylurea herbicides, i.e. diuron, isoproturon and linuron, in aqueous solution was employed to investigate the photocatalytic activity of the synthesized titania. The initial concentrations of herbicides used were 1, 5 and 10 ppm, respectively. The solution was mixed with titania in the ratio of 1 mg titania to 10 mg of solution and kept in the dark for at least 15 minutes to allow the complete adsorption of herbicide on the surface of titania. The photocatalytic reaction was initiated by exposing test tubes to light from UV lamps (Phillips Cleo 15 W). The diagram of the equipment setup for photocatalytic reaction is shown in Figure 3.3.
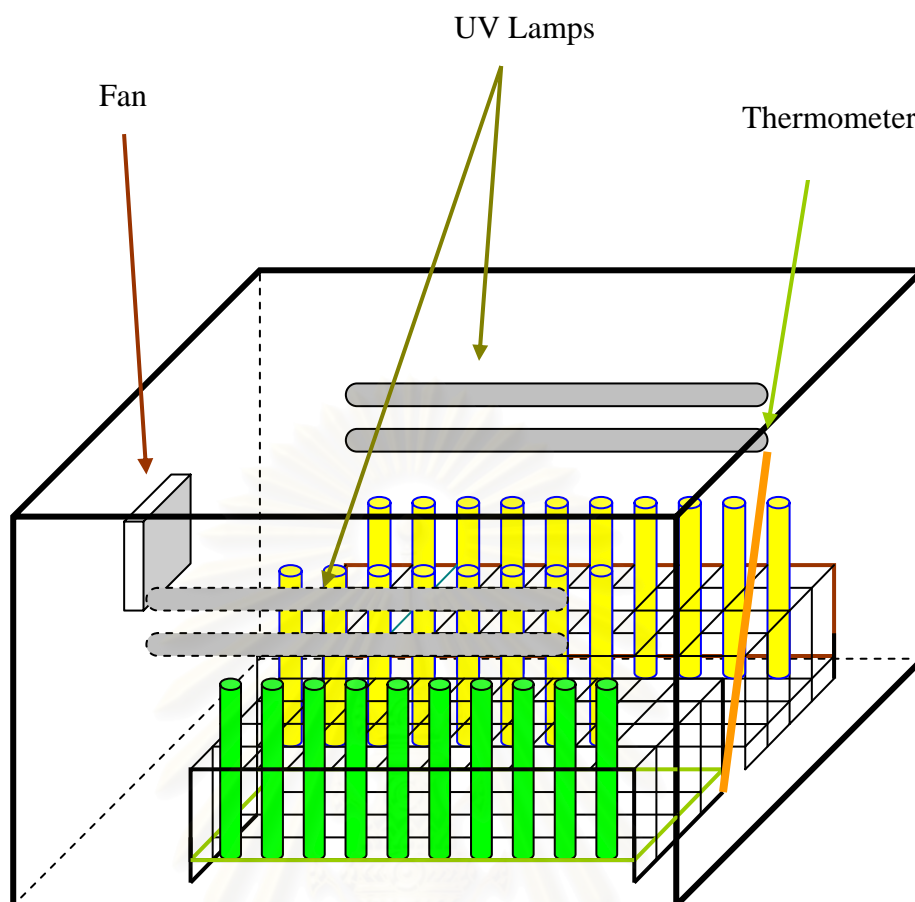
Figure 3.3 Diagram of the equipment setup for photocatalytic reaction.

The herbicide degradation was periodically monitored by using reverse phase liquid chromatography system, with UV detector (HPLC-UV, Agilent Technologies, series 1100) and C-18 column (ZORBAX Eclipse XDS-C18 PrepHT, 7μm particle size, 21.5×250 mm). The solution of 70% acetronitrile-29.5% water-0.5% phosphoric acid was used as mobile phase (flow rate 20 ml/min). The sample injection volume was 5 ml.

Intermediate products from the photocatalytic reaction of herbicides were fractionated from the HPLC system and identified by gas chromatography-mass

spectroscopy (GC-MS) system. The MS system was an Agilent G2589A series (Agilent Technologies) quadrupole mass spectroscopy equipped with an electron ionization (EI) source. The instrument was operated in the positive ionization mode. The operating conditions for EI were as followed: methane and helium gas were used at pressure of 414 KPa; drying gas flow of 10.0 l/min; capillary voltage of 4000 V and gas temperature of 350°C.

CHAPTER IV

RESULTS AND DISCUSSION

The photocatalytic reaction on titania can be applied to degrade many organic compounds. Many literatures have investigated such degradation. In this study, anatase titania was prepared by thermal decomposition method in various organic solvents. Physical properties of the synthesized titania were investigated by many techniques. Chemical properties were also investigated by photocatalytic decomposition reaction of organic compounds.

4.1 Titania Synthesis

Titania was synthesized by thermal decomposition in many organic solvents i.e. 1,4-butanediol, mineral oil and toluene, at temperature of 270 and 300°C. Characterization techniques such as XRD, SEM, TEM and BET were used to observe physical properties of as-synthesized titania as well as calcined titania.

4.1.1 Synthesis in 1,4-butanediol

Thermal decomposition of alkoxides in glycol is usually referred to as glycothermal reaction. In the glycothermal reaction of titanium (IV) n-butoxide (TNB), TNB is easily converted to glycoxide. Then, thermal decomposition of the glycoxide molecule occurs by intermolecular interaction from the remaining hydroxyl

group of glycol moiety, which subsequently forms ≡Ti-O- anion. The nucleophilic

attraction among these ions results in crystallization of titanium (IV) oxide (Payakgul

2002). Mechanism of the glycothermal reaction of TNB in 1,4-butanediol can be

presented in Figure 4.1
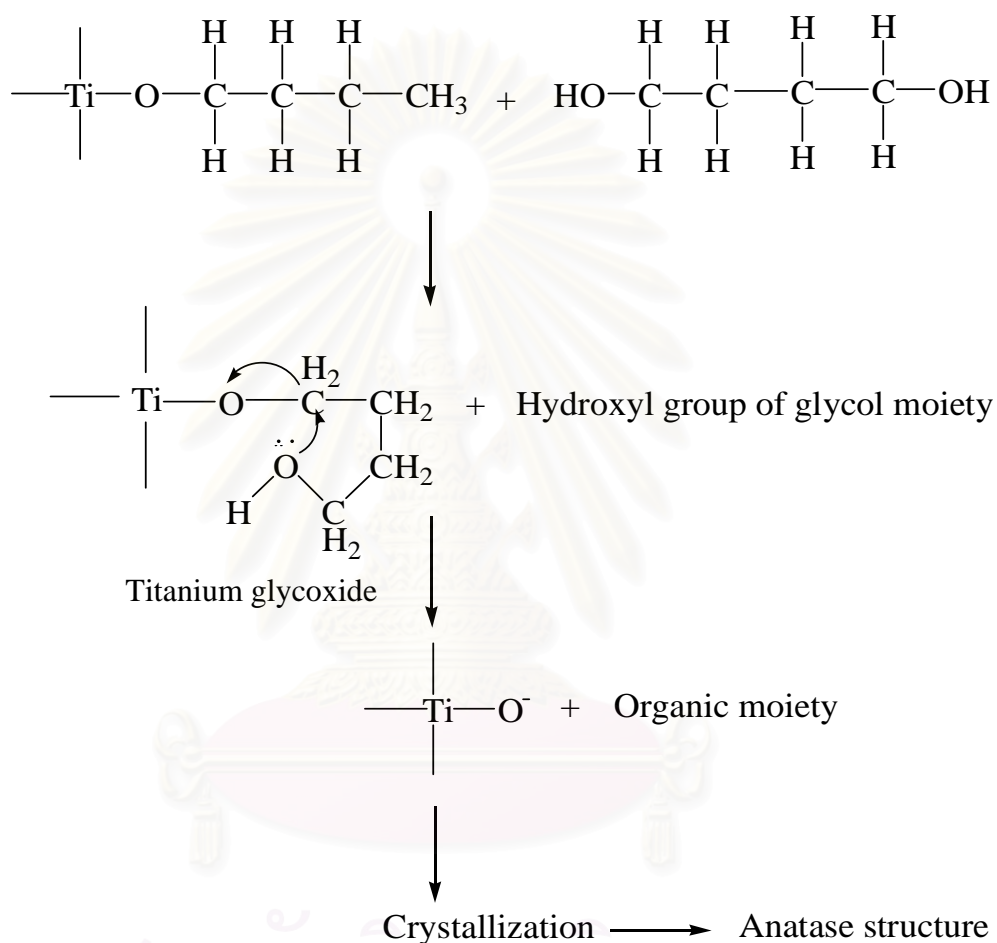
Figure 4.1 Mechanism of the glycothermal reaction for anatase formation (Payakgul
2002).

Titania synthesis was conducted in an autoclave at 270ºC and 300ºC. The

XRD patterns of the as-synthesized products (Figure 4.2) confirmed that titania are

formed in anatase phase without contamination from other crystalline phases. It has

been reported that, for titania synthesis in 1,4-butanediol, anatase crystals are from by

crystallization when the temperature in the autoclave reaches 250ºC (Payakgul 2005).

XRD analysis also showed that the calcined titania was still in anatase phase, which

proved that anatase titania synthesized by this method is thermally stable. The

crystallite sizes of the as-synthesized and calcined products calculated from the

Scherrer equation were shown in Table 4.1. The as-synthesized titania at both 270 and

300°C has same crystallite size of 6 nm. After calcinations at high temperature, i.e.

400, 500, and 600°C, the crystallite size of titania was increased with increasing

calcination temperature, due to crystal growth. SEM micrographs in Figure 4.3 and

4.4 revealed that titania crystals agglomerated into micrometer-sized secondary

particles. It was also found that the secondary particles formed at 300°C was larger

than that synthesized at 270°C. TEM micrographs of the as-synthesized and the

calcined products (Figure 4.5) confirmed that the synthesized products were a

collection of nanosized single crystal titania.

The BET surface areas of titania measured by nitrogen absorption (S_{BET}) are

also shown in Table 4.1. The BET surface area of the products remained roughly

unchanged, even after calcinations at 500°C. However, the surface area was notably

decreased after the products were calcined at 600°C, due to the sintering of the

agglomerated primary particles. It should also be note that the change in the BET

surface area of titania synthesized at 270°C was more significant than that synthesized

at 300°C. This suggested that nanocrystalline anatase titania formation was not

completed at the synthesis temperature of 270°C, even though it has been reported

that anatase crystals are formed by crystallization in 1,4-butanediol when the

temperature reached about 250°C (Payakgul 2005).
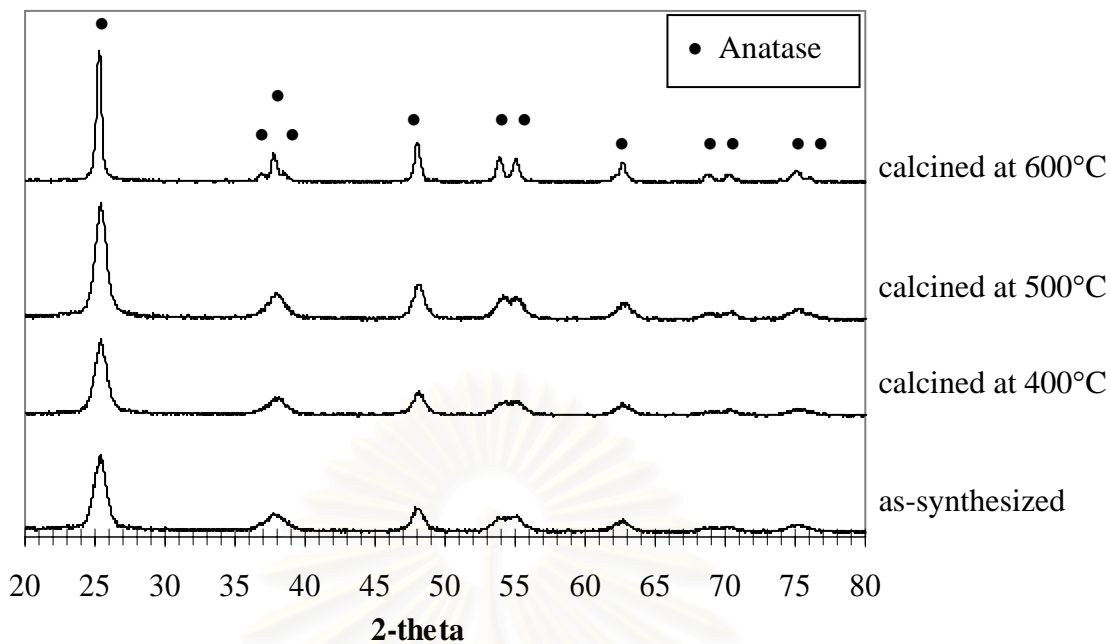
(a)
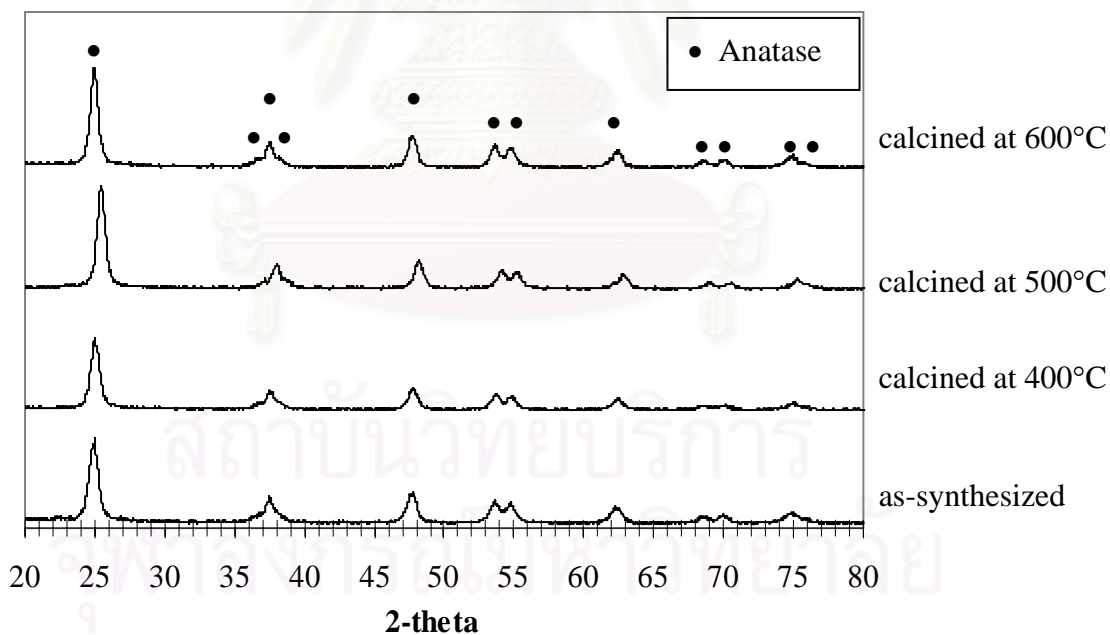
(b)

Figure 4.2 XRD patterns of titania synthesized in1,4-butanediol at: (a) 270°C and (b) 300°C.

Table 4.1 Crystallite size and surface area of titania synthesized in 1,4-butanediol.

	Crystallite size[a], d (nm)	S_{BET} (m^2/g)	S_{XRD} (m^2/g) [b]	S_{BET}/S_{XRD}
Synthesized at 270ºC				
As-synthesized	6.41	94	240	0.4
400ºC calcination	5.86	104	263	0.4
500ºC calcination	6.40	90	241	0.4
600ºC calcination	9.73	36	158	0.2
Synthesized at 300ºC				
As-synthesized	5.90	65	261	0.2
400ºC calcination	7.06	68	218	0.3
500ºC calcination	8.09	62	190	0.3
600ºC calcination	7.97	57	193	0.3

[a] Crystallite size calculated from XRD peak broadening
[b] Specific surface area calculated from $S_{XRD} = 6/d\rho$ under assumption that the crystal is spherical and the density of anatase titania is 3.9 g cm^{-3}

Considering S_{BET}/S_{XRD} values, which compared the BET surface area with the surface area calculated from crystallite size (S_{XRD}) by assuming that the particles were spherical and nonporous, it was found that the value for the obtained titania was significantly lower than one. It was therefore suggested that the primary particles were heavily agglomerated. It was shown in SEM micrographs (Figure 4.3 and 4.4) and TEM micrographs (Figure 4.5) that the synthesized powder was an irregular aggregate of nanometer particles. The agglomeration of the precipitates has been reported to be influenced by dielectric constant of reaction medium (Park 1997). The

lower the dielectric constant, the higher the degree of agglomeration. However, the dielectric constant of 1, 4-butanediol is quite high ($\varepsilon = 32$) so that the repulsive force between anatase particles formed in this reaction medium should be more pronounced than the attraction force and the resulting product should have low degree of agglomeration. This is in contrast with the observed results. Therefore, it is suggested that the formation of titania in 1,4-butanediol may note be a sole result of the crystallization process as reported earlier. Nevertheless, the electron diffraction pattern shown in Figure 4.6(b) still suggested that the as-synthesized primary particles were titania crystals with high crystalinity. The crystalinity was increased after calcinations (Figure 4.5(d)).

(a)

(b)

(c)

(d)
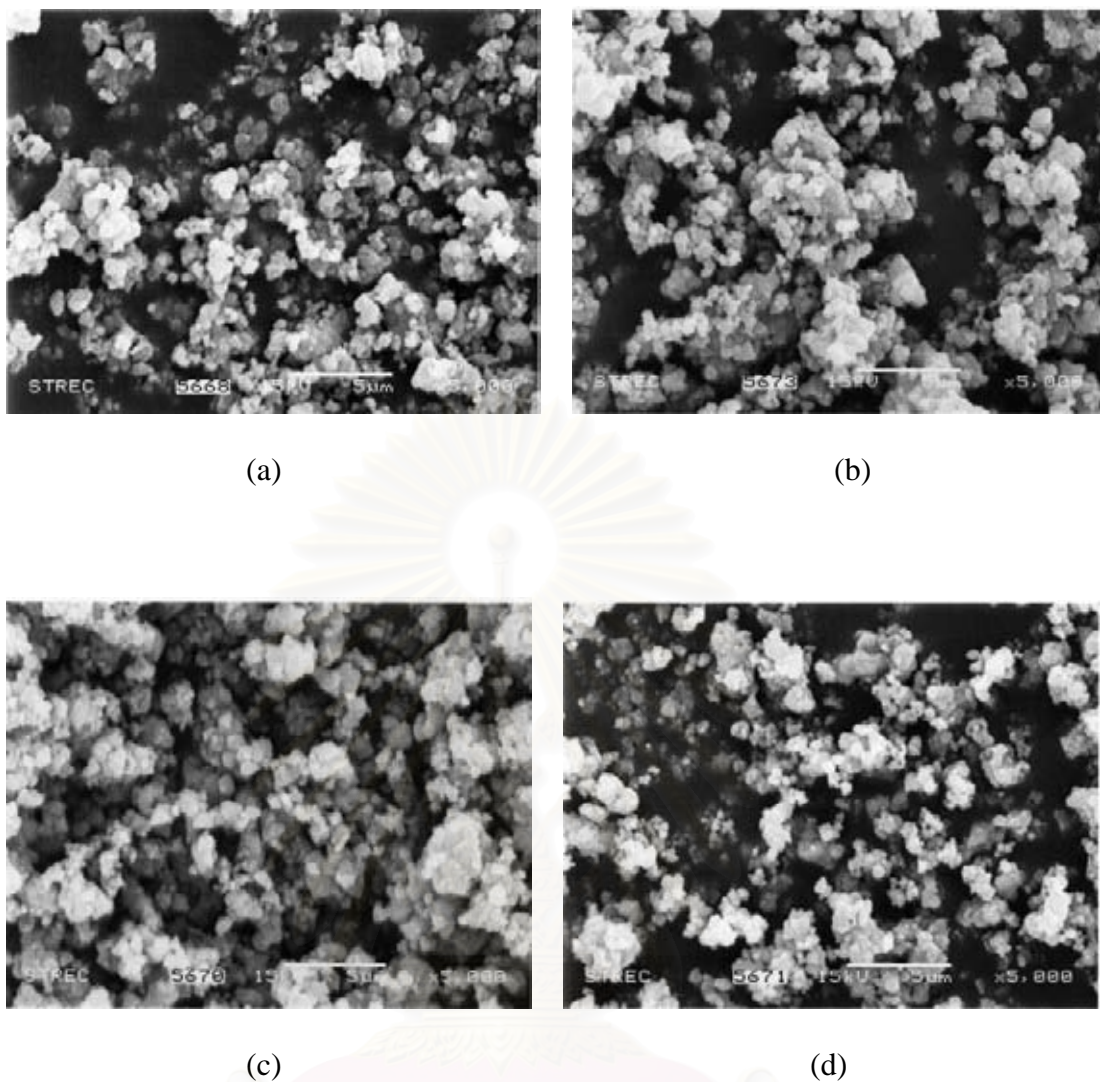
Figure 4.3 SEM micrographs of titania synthesized in 1,4-butanediol at 270ºC: (a) as-synthesized, (b) calcined at 400ºC, (c) calcined at 500ºC, (d) calcined at 600ºC.

(a)

(b)

(c)

(d)

Figure 4.4 SEM micrographs of titania synthesized in 1,4-butanediol at 300ºC: (a) as-synthesized, (b) calcined at 400ºC, (c) calcined at 500ºC, (d) calcined at 600ºC.

(a)

(b)

(c)

(d)
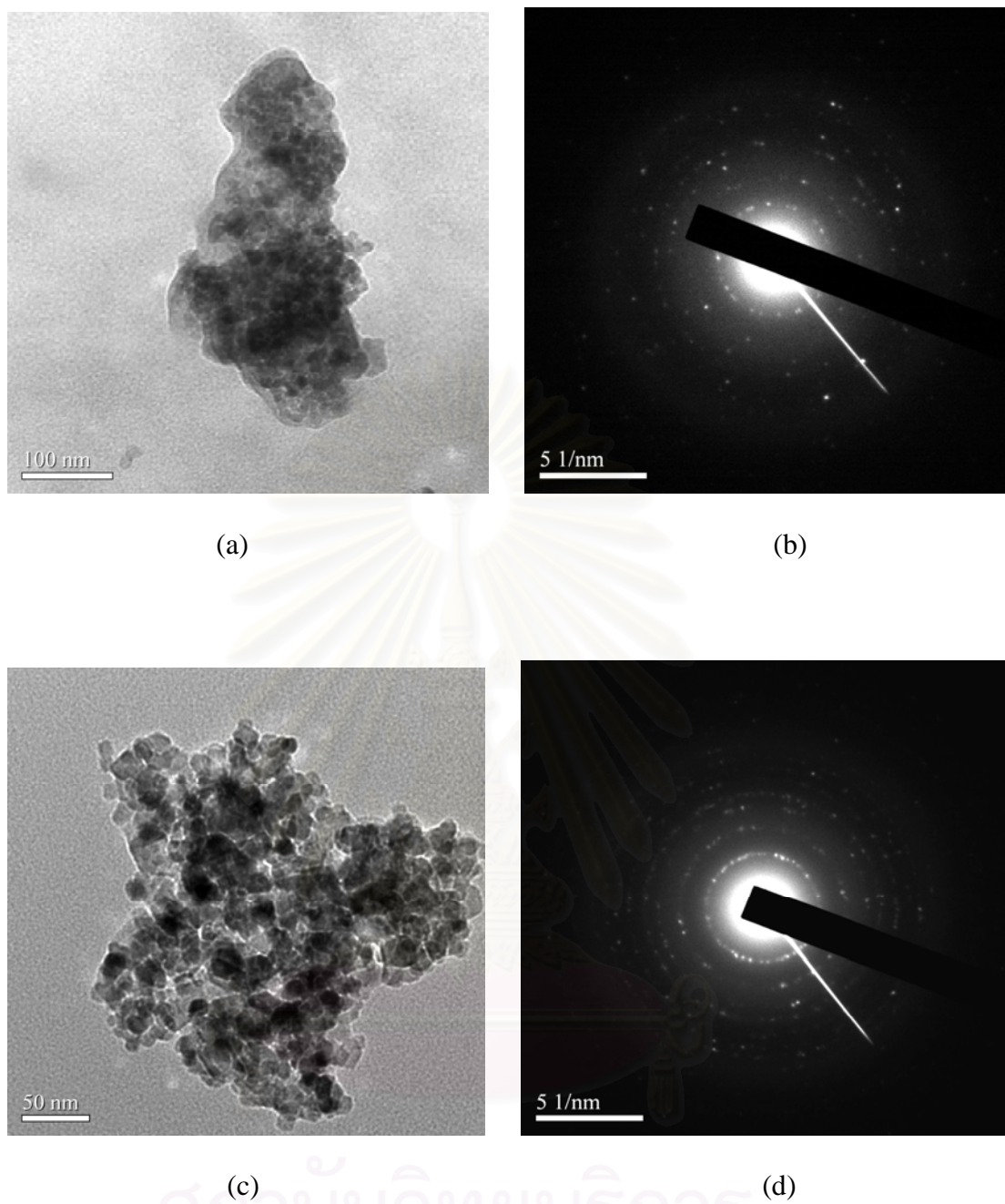
Figure 4.5 TEM micrographs and SAED patterns of titania synthesized in 1,4-butanediol at 300°C: (a)-(b) as-synthesized, (c)-(d) calcined at 500°C.

4.1.2 Synthesis in toluene

It has been reported that, at relatively high temperature, thermal decomposition of TNB in toluene could occur, yielding a $\equiv$Ti-O⁻ anion. The nucleophilic attraction among titanate ions initiated the crystallization to form titania in anatase phase (Payakgul 2002). The mechanism of TNB decomposition in toluene can be depicted as shown in Figure 4.6.

$$\overset{|}{\underset{|}{-Ti}}-O-CH_2-CH_2-CH_2-CH_3 \xrightarrow{\text{Toluene}} \overset{|}{\underset{|}{-Ti}}-O^- \;+\; \text{Organic moiety}$$

$$\downarrow$$

Crystallization

$$\downarrow$$

Anatase structure
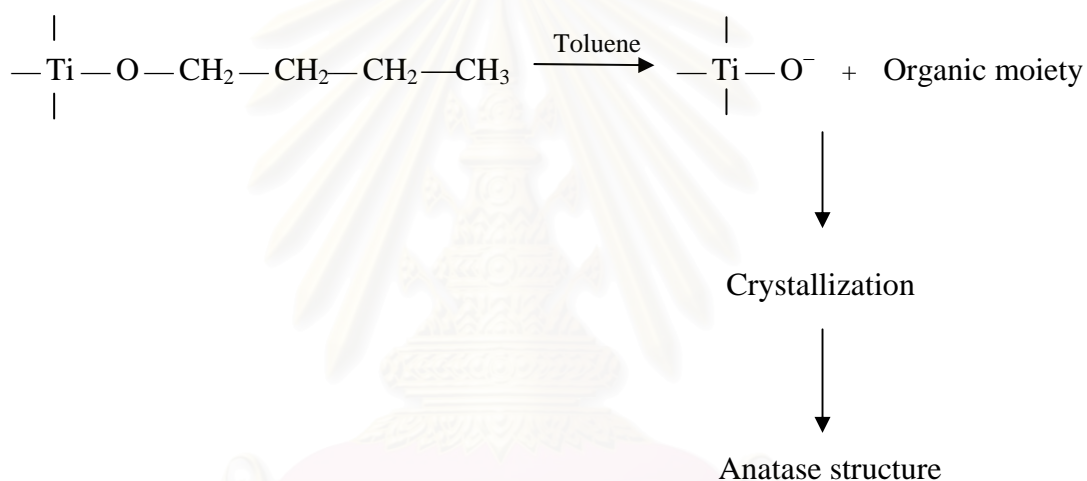
Figure 4.6 Mechanism of the reaction in toluene for anatase formation.

XRD patterns of titania products prepared in toluene at 270 and 300°C are depicted in Figure 4.7. It is shown that anatase was formed without contamination of any other phase such as rutile or brookite. XRD patterns also show that after calcinations up to 600°C remains in anatase phase.

The crystallite size and surface area of as-synthesized and calcined product are shown in Table 4.2. Titania synthesized in toluene has crystallite size, which was

calculated from XRD broadening, in the range of 5-6 nm. TEM micrographs of as-synthesized titania and its calcination products (Figure 4.8) confirmed the sized of primary crystals, which also showed high crystalinity. The crystallite size was increased after calcinations due to crystal growth. The agglomeration of titania products can be clearly seen by SEM micrographs in Figure 4.9 and 4.10. It was observed that the agglomeration patterns of the products synthesized at 270 and 300°C were different. The titania product prepared at 270°C was an irregular aggregate of nanometer particles, while titania synthesized at 300°C showed that the primary particles were highly agglomerated into micron-size spherical particles. High degree of agglomeration in the products synthesized in toluene was consistent with the effect of dielectric constant, as discussed in the prior section. Since toluene has quite low electric constant (ε = 2.4 at 68°F (Clipper Control 2006)), it was expected that the anatase particles formed in this reaction medium would have high degree of agglomeration and form spherical secondary particles. The value of ratio between S_{BET} and S_{XRD} also confirmed the degree of agglomeration of the samples. The degree of ratio from titania prepared in toluene were quite lower than 1, especially after calcinations. Investigation of the change in BET surface area with an increase calcination temperature revealed that surface area of titania synthesized at 270°C decreased more dramatically than titania synthesized at 300°C. It has been reported that titania synthesized by solvothermal process at lower temperatures was contaminated with amorphous-like hydrated phase attributed to insufficient thermal energy for dehydration and crystallization (Kominami 1997).
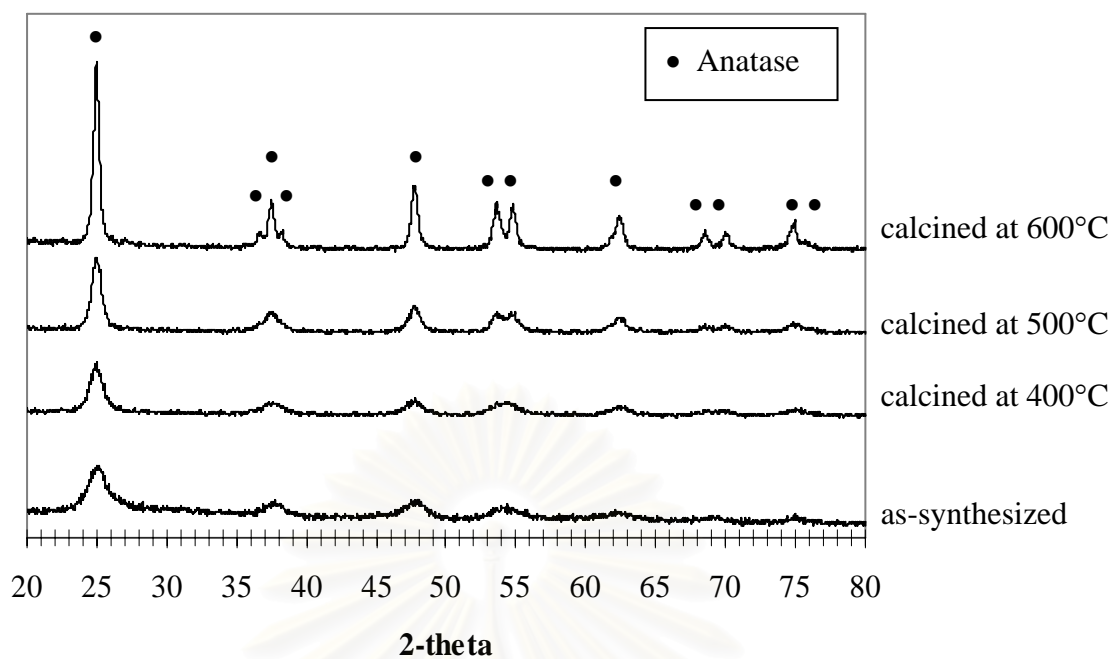
(a)
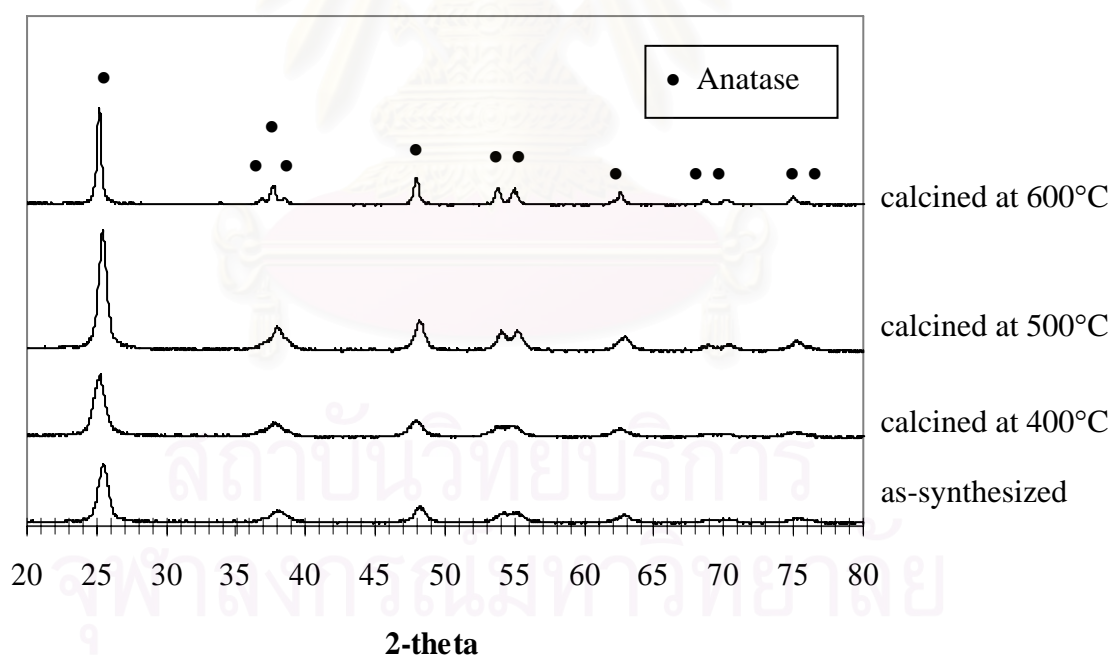
(b)

Figure 4.7 XRD patterns of titania synthesized in toluene at: (a) 270°C and (b) 300°C.

Table 4.2 Crystallite size and surface area of titania synthesized in toluene.

	Crystallite size[a], d (nm)	S_{BET} (m^2/g)	S_{XRD} (m^2/g) [b]	S_{BET}/S_{XRD}
Synthesized at 270ºC				
As-synthesized	5.17	152	297	0.5
400ºC calcination	5.36	137	287	0.5
500ºC calcination	6.16	69	250	0.3
600ºC calcination	9.37	31	164	0.2
Synthesized at 300ºC				
As-synthesized	5.88	95	262	0.4
400ºC calcination	6.57	87	234	0.4
500ºC calcination	9.73	62	158	0.4
600ºC calcination	15.71	20	98	0.2

[a] Crystallite size calculated from XRD peak broadening
[b] Specific surface area calculated from $S_{XRD} = 6/d\rho$ under assumption that the crystal is spherical and the density of anatase titania is 3.9 g cm^{-3}
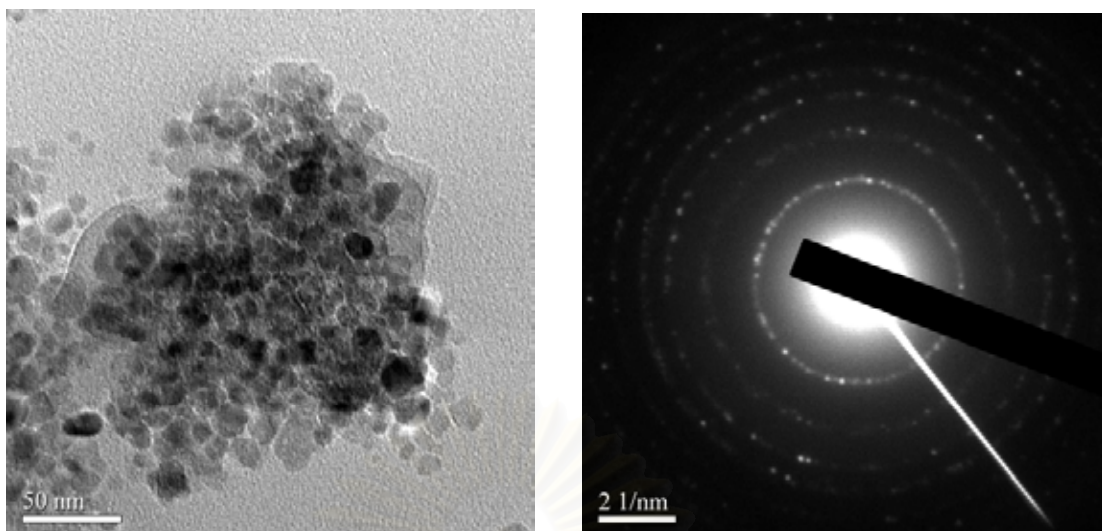
(a)

(b)
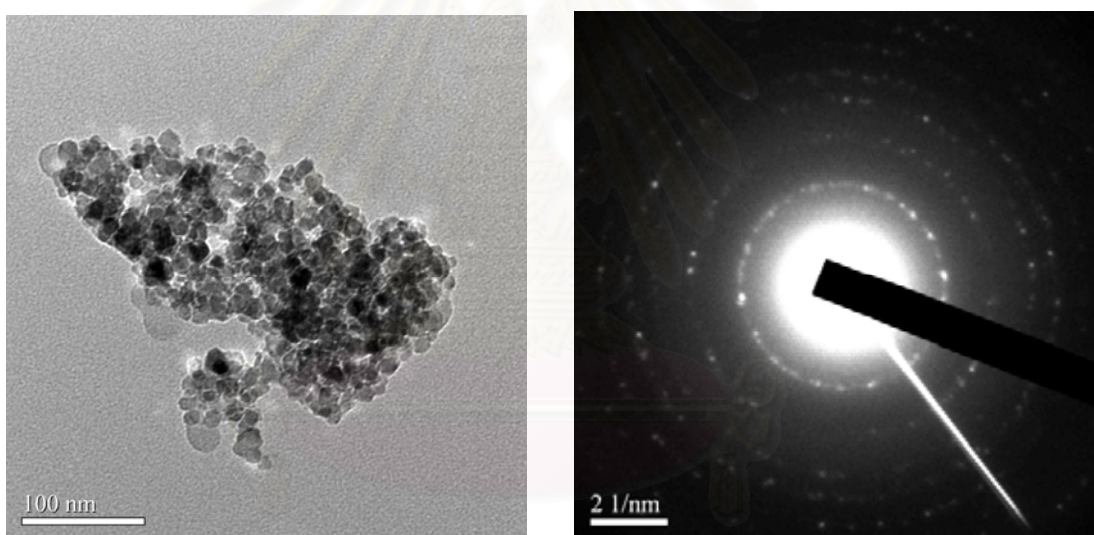
(c)

(d)

Figure 4.8 TEM micrographs and SAED patterns of titania synthesized in toluene at 300°C: (a)-(b) as-synthesized, (c)-(d) calcined at 500°C.
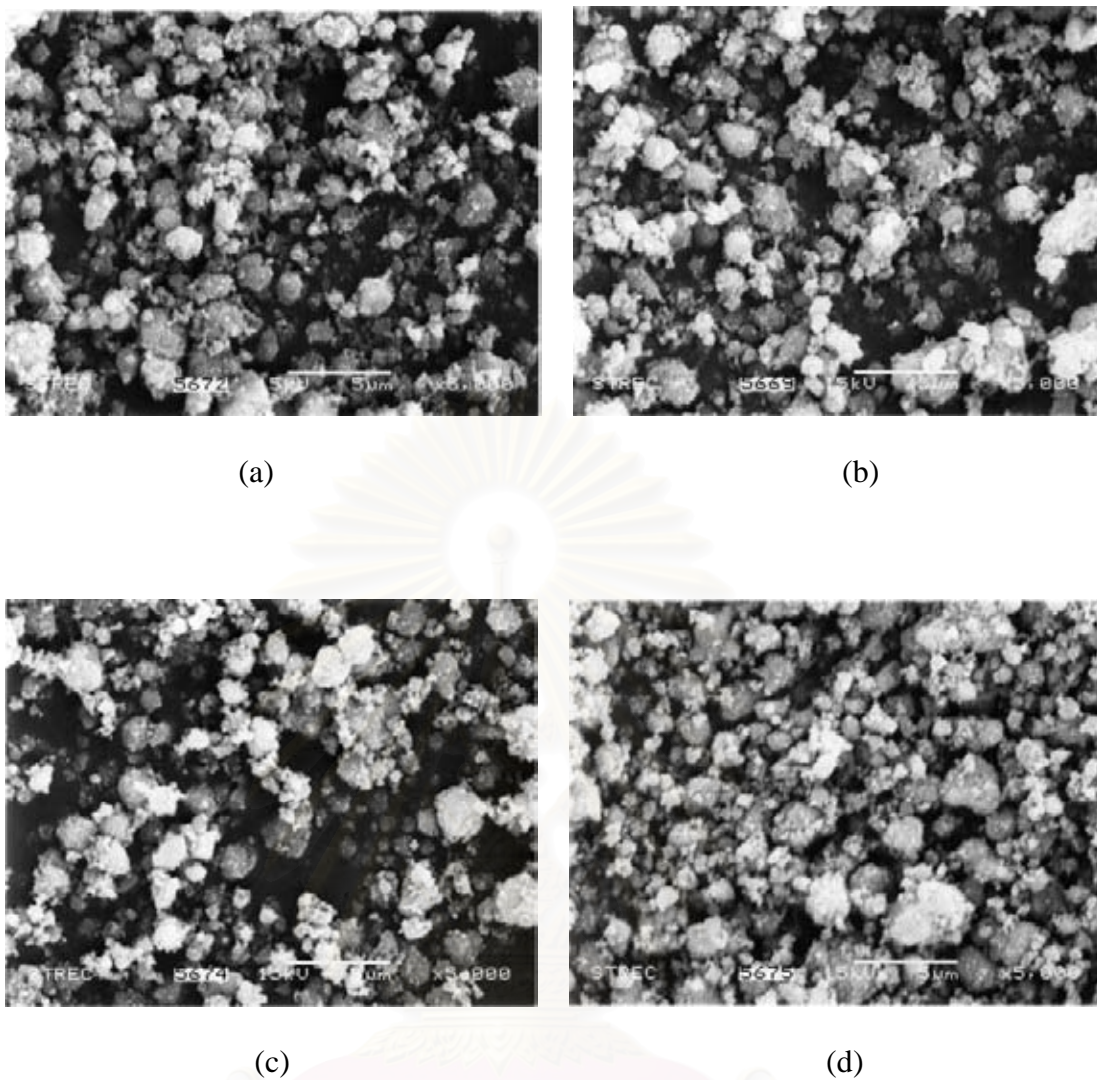
(a)

(b)

(c)

(d)

Figure 4.9 SEM micrographs of titania synthesized in toluene at 270ºC: (a) as-synthesized, (b) calcined at 400ºC, (c) calcined at 500ºC, (d) calcined at 600ºC.

(a)

(b)

(c)

(d)

Figure 4.10 SEM micrographs of titania synthesized in toluene at 300ºC: (a) as-synthesized, (b) calcined at 400ºC, (c) calcined at 500ºC, (d) calcined at 600ºC.

4.1.3 Synthesis in mineral oil

Anatase titania was synthesized at 270 and 300°C in mineral oil. Figure 4.11 shows XRD patterns confirming that the products from the decomposition of TNB in mineral oil at temperature of 270 and 300°C in autoclave contained no other crystalline phase.

The calcined products of titania synthesized at both temperatures were also anatase phase without contamination from other phases. The crystallite size and surface area of as-synthesized and calcined products are shown in Table 4.3. The crystallite size of the as-prepared titania calculated from XRD broadening was in the range of 6-7 nm, regardless of the synthesis temperature. TEM micrographs clearly showed agglomeration of primary crystals with crystallite size in the same range as the calculated values. Nevertheless, the SAED patterns (Figure 4.12) suggested that the products had lower crystalinity, comparing to those synthesized in 1,4-butanediol or toluene. It was suggested that the products were contaminated with amorphous phase. The crystalinity of titania was improved after heat treatment.

The agglomeration of titania products are shown by SEM micrographs in Figure 4.13 and 4.14. It was indicated that the primary particles were heavily agglomerated, especially in products synthesized at 300°C, in which the secondary particles was formed as micron-sized spherical particles. The ratio between S_{BET} and S_{XRD}, i.e. the degree of agglomeration, reported in Table 4.3 also indicated that primary particles in the spherical secondary particles were highly packed, since the value of S_{BET}/S_{XRD} was greatly deviated from 1. This behavior can be explained by

low dielectric constant of mineral oil (ε = 2.1 at 80 °F (Clipper Control 2006)), as previously observed from titania synthesized in toluene.

According to Table 4.3, the crystallite size of titania products were increased with an increase in calcination temperature, due to crystal growth. Morever, the BET surface area was notably decreased upon the calcination at high temperature because sintering of agglomerated primary particles that increased by increasing temperature. The decrease in BET surface area of titania synthesized at 270°C was more drastic than that prepared at 300°C. This maybe the result from the contaminated amorphous phase, which was more abundant in the product synthesized at 270°C.
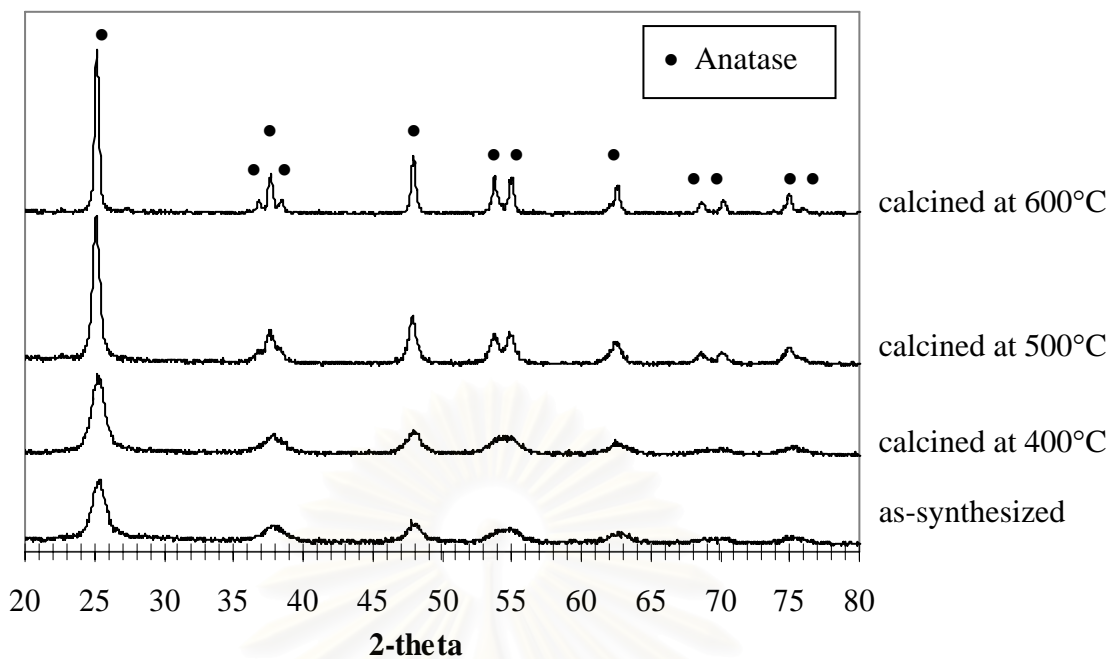
(a)
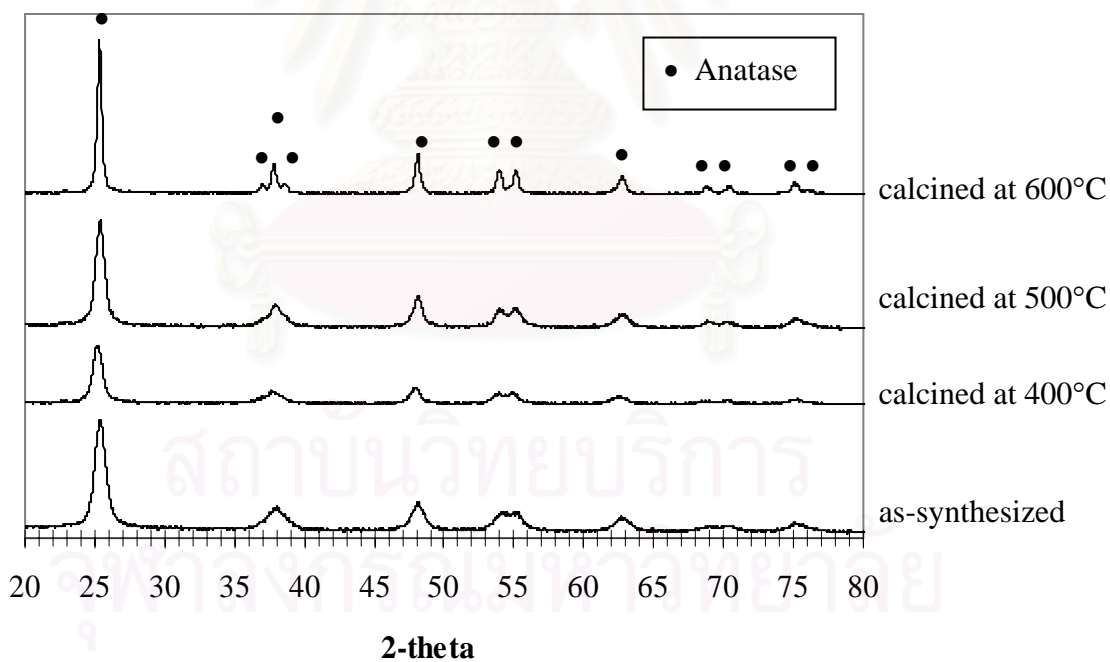
(b)

Figure 4.11 XRD patterns of titania synthesized in mineral oil at: (a) 270°C and (b) 300°C.

Table 4.3 Crystalline size and surface area of titania synthesized in mineral oil.

	Crystallite size[a], d (nm)	S_{BET} (m^2/g)	S_{XRD} (m^2/g)[b]	S_{BET}/S_{XRD}
Synthesized in 270ºC				
As-synthesized	6.66	96	231	0.4
400ºC calcination	5.55	89	280	0.3
500ºC calcination	6.53	32	236	0.1
600ºC calcination	9.23	9	167	0.1
Synthesized in 300ºC				
As-synthesized	6.15	96	250	0.4
400ºC calcination	6.98	92	233	0.4
500ºC calcination	8.57	68	180	0.4
600ºC calcination	14.60	28	105	0.3

[a] Crystallite size calculated from XRD peak broadening
[b] Specific surface area calculated from $S_{XRD} = 6/d\rho$ under assumption that the crystal is spherical and the density of anatase titania is 3.9 g cm^{-3}

(a)

(b)

(c)

(d)
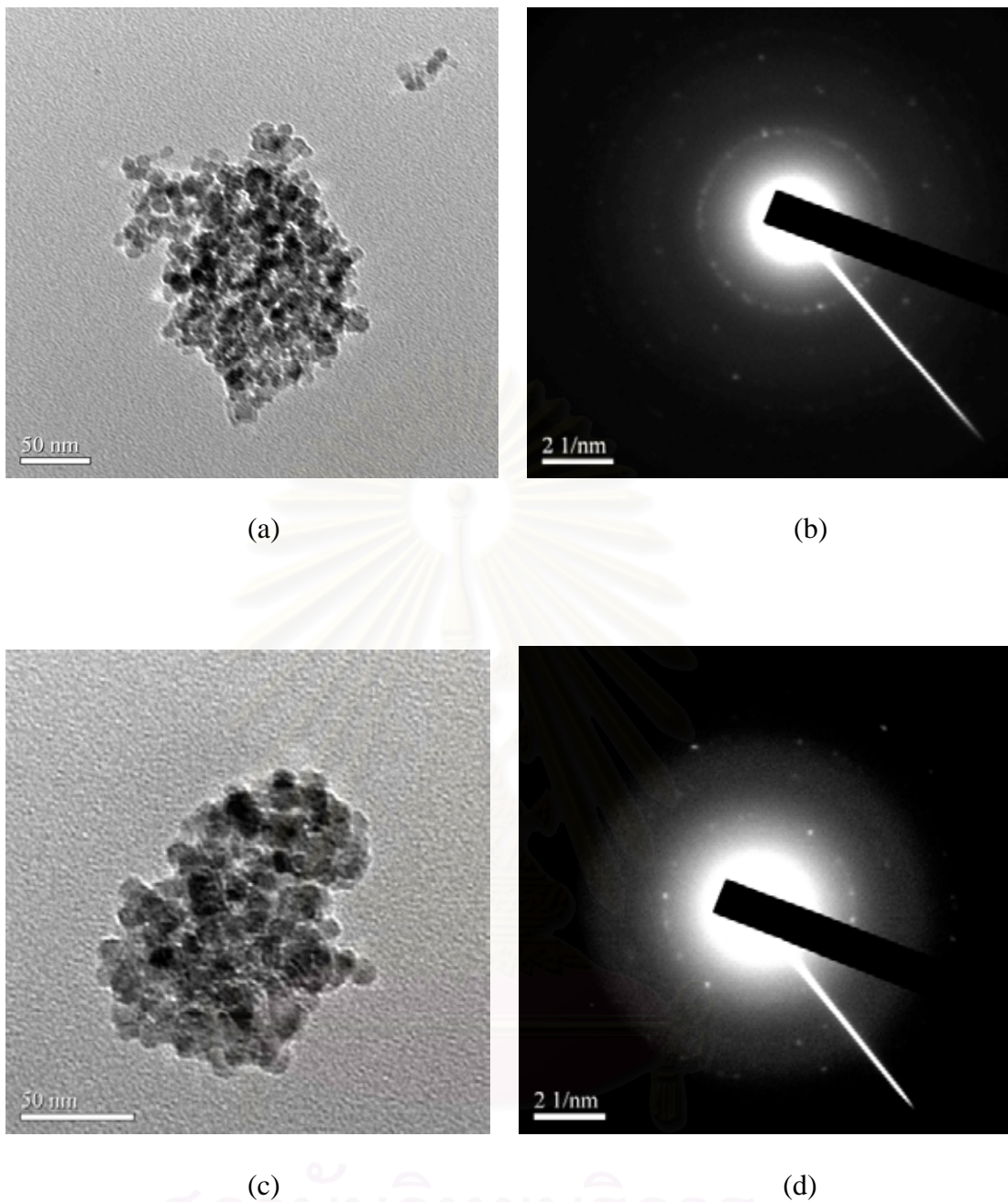
Figure 4.12 TEM micrographs and SAED patterns of titania synthesized in mineral oil at 300°C: (a)-(b) as-synthesized, (c)-(d) calcined at 500°C.
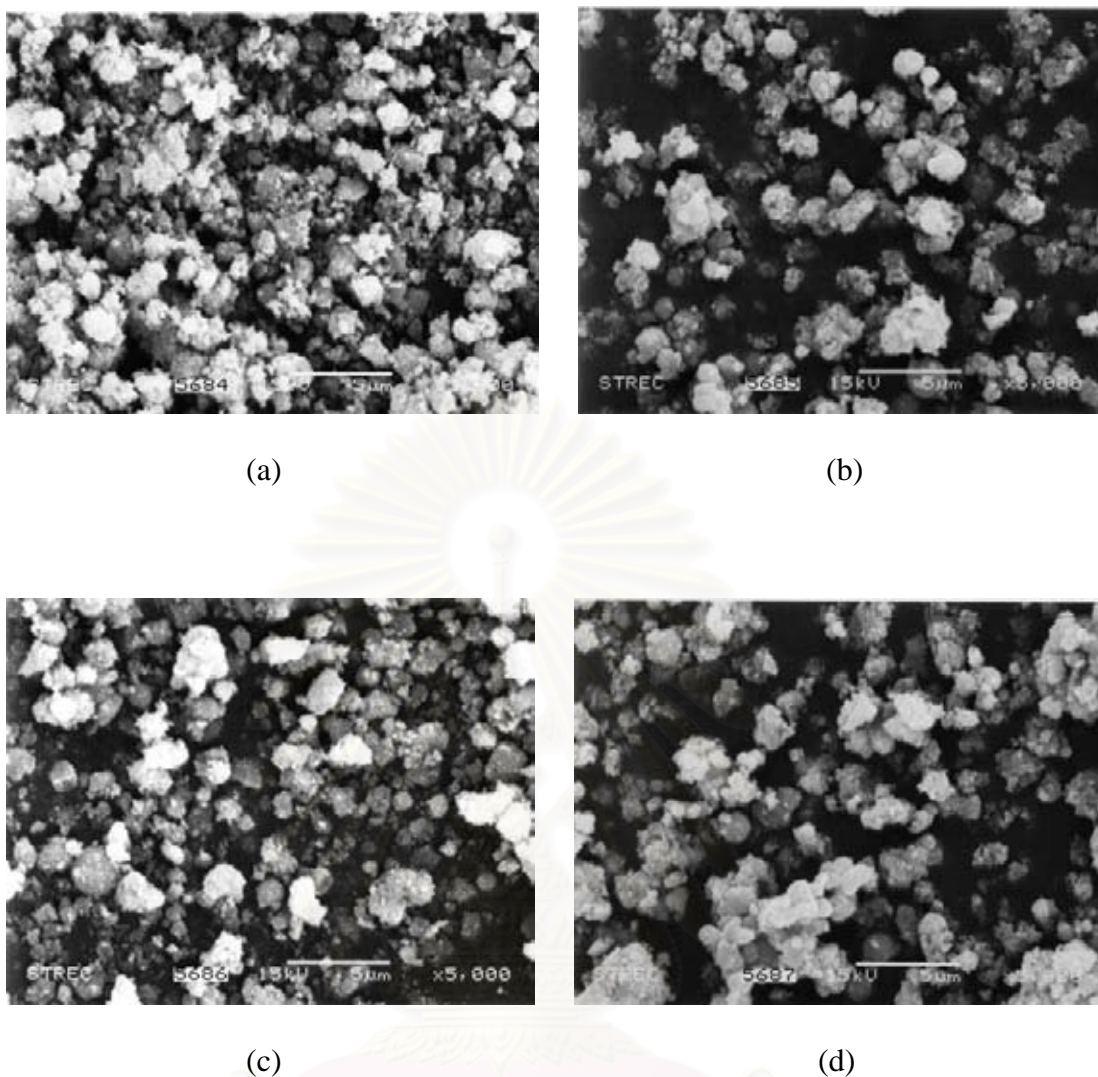
.

(a)   (b)

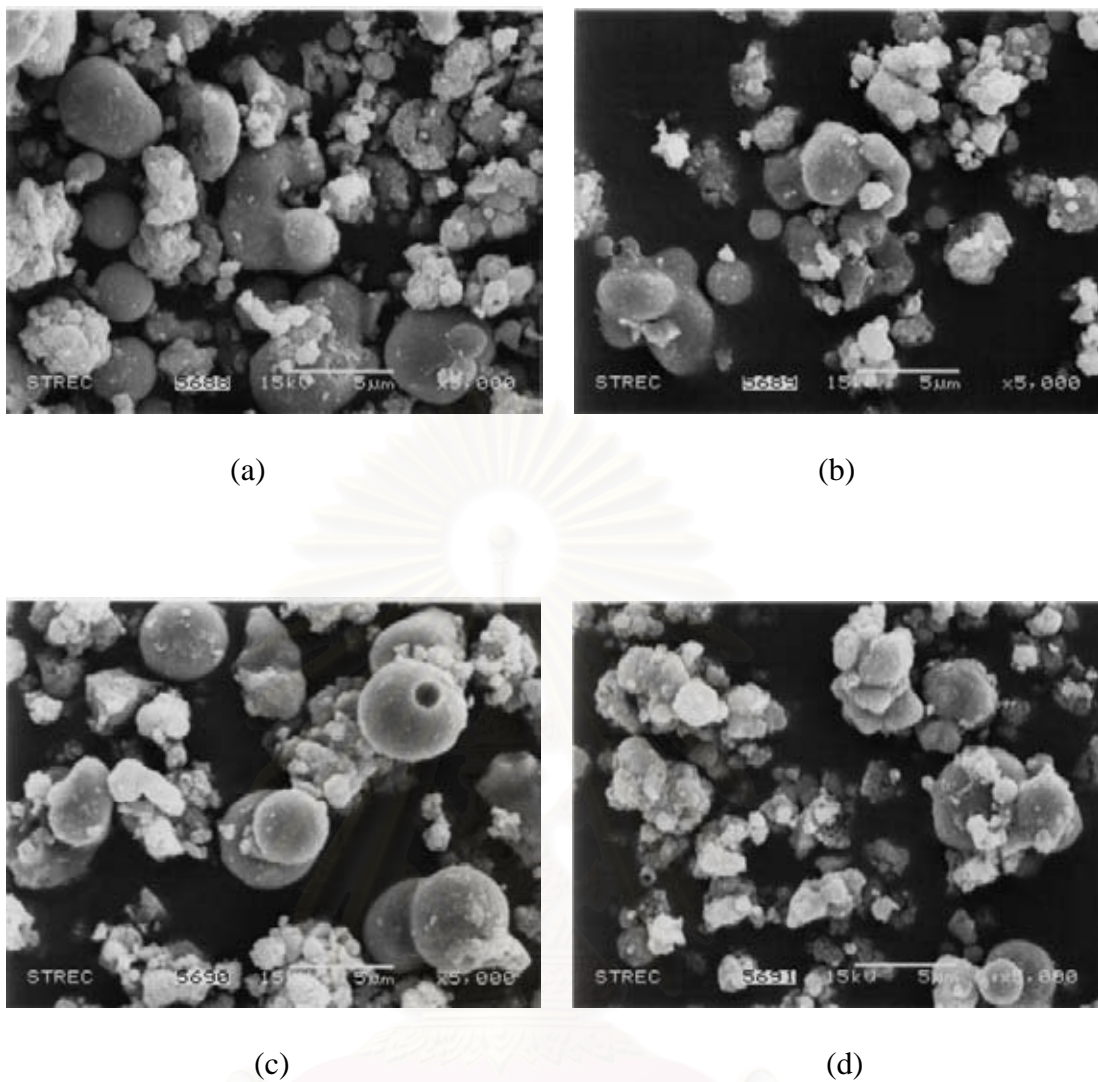(c)   (d)
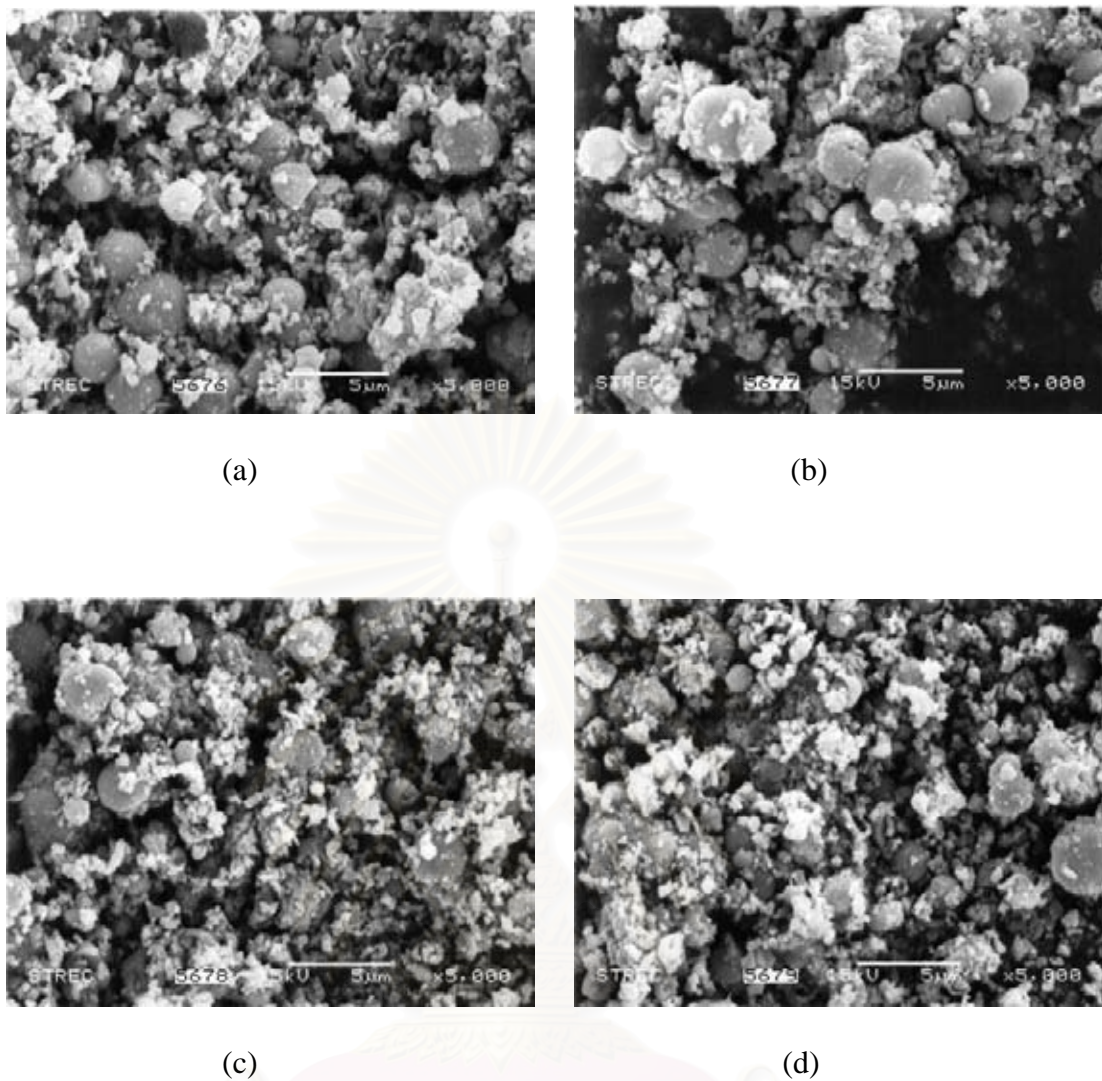
Figure 4.13 SEM micrographs of titania synthesized in mineral oil at 270ºC: (a) as-synthesized, (b) calcined at 400ºC, (c) calcined at 500ºC, (d) calcined at 600ºC.

.

(a)   (b)

(c)   (d)
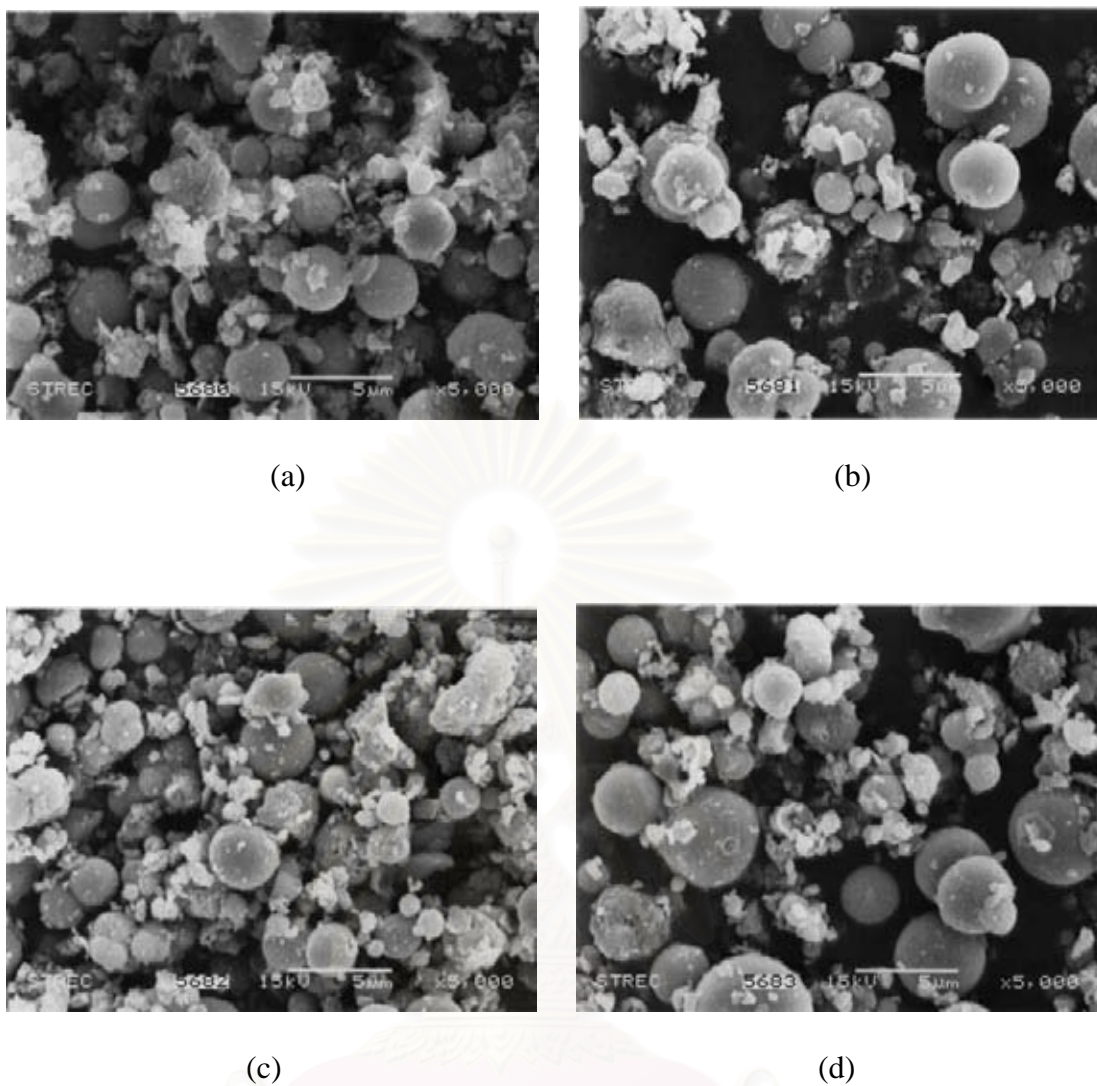
Figure 4.14 SEM micrographs of titania synthesized in mineral oil at 300ºC: (a) as-synthesized, (b) calcined at 400ºC, (c) calcined at 500ºC, (d) calcined at 600ºC.

Physical properties of titania synthesized in mineral oil were similar to titania synthesized in toluene, especially the agglomeration behavior of the product. It can be suggested that formation reaction of titania in mineral oil was similar to in that in toluene. It started from the thermal decomposition of TNB in mineral oil, yielding a $\equiv$Ti-O$^-$ anion. The nucleophilic attraction among titanate ions initiated the crystallization to form titania in anatase phase. The mechanism of TNB in mineral oil can be suggested as shown in Figure 4.15

$$—\underset{|}{\overset{|}{Ti}}—O—CH_2—CH_2—CH_2—CH_3 \xrightarrow{\text{Mineral oil}} —\underset{|}{\overset{|}{Ti}}—O^- \; + \; \text{Organic moiety}$$

Crystallization

Anatase structure
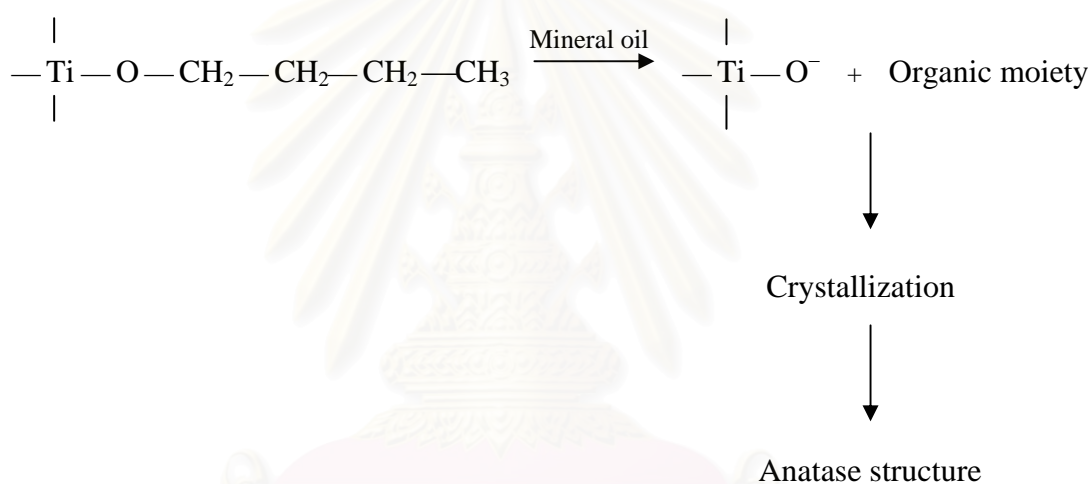
Figure 4.15 Mechanism of reaction in mineral oil for the titania product.

4.2 Photocatalytic Degradation of Phenyluea Herbicides

Titania synthesized via thermal decomposition if TNB in various organic solvents was also investigated for chemical properties, namely catalytic activity. Anatase is the most efficient phase of titania as a photocatalyst because its structure permits low electron-hole recombination rate (Tsai 1997). Catalytic activity for photodegradation of phenylurea herbicides, i.e. diuron, isoproturon and linuron, of the synthesized titania was investigated in this work.

4.2.1 Preliminary studies

4.2.1.1 Verification for effect of tube position in the system

There are many parameters that can effect the rate of photodegradation, such as light intensity, wave length of the incident light, initial concentration of organic compounds, pH and amount of titania employed. In this work, according to the experimental setup shown in Figure 3.3, location of test tubes placed in system may also affects the extent of the reaction. This was verified by testing the photodegradtion of methylene blue (MB) in 28 test tubes located at different positions in the system. Titania employed was synthesized in 1,4-butanediol at 300°C and calcined at 500°C. The results of MB disappearance after 4 h of reaction are shown in Figure 4.16. It was confirmed that conversions achieved from all test tubes were not significantly different. The % error of all data is 8.50% of the mean value and the standard deviation of data is 0.135. Nevertheless, it was noted that the conversions achieved from the middle row (row 2) were lower than those from row 1 and 3. Therefore,

during the actual experiment, rearrangement of test tubes was made after the test tubes in the outer rows had been removed for analysis. No test tube was in the middle row after about 1 h of the operation. According to the result that no significant difference in conversion was observed from different location in the system even after long period of reaction time, together with the fact that all test tubes were relocated so that no test tube was stayed in the middle row after relatively short period of operation, it could be assumed that there was no effect from the location in the system in this study.
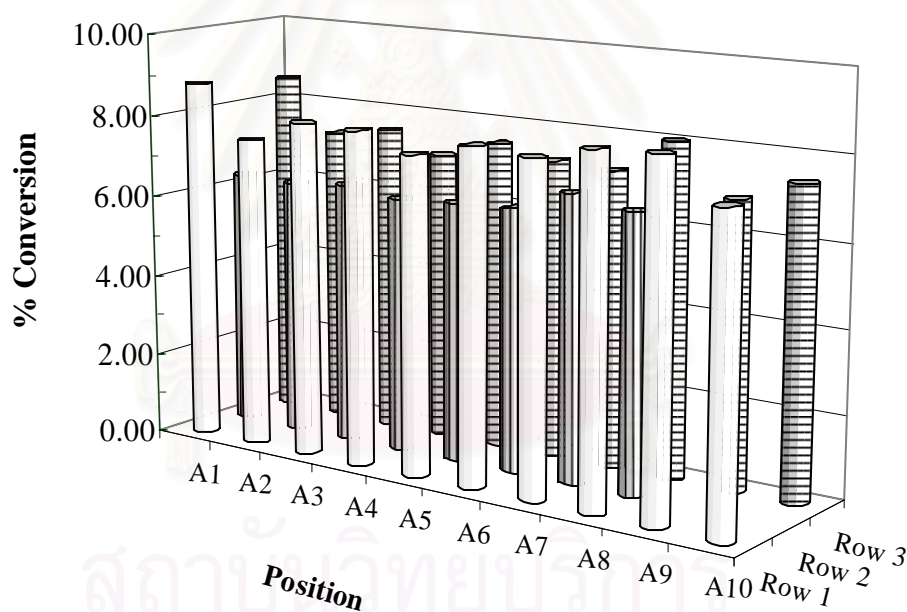
Figure 4.16 The effects of positions of test tubes in the photocatalytic experimental system to verified by methylene blue solution disappearance after 4 hours of UV irradiation.

4.2.1.2 Photocatalytic degradation of methylene blue

The photooxidation of methylene blue (MB) aqueous solution under solar irradiation was employed to preliminarily investigate the photocatalytic activity of synthesized titania. Table 4.4 summarizes physical properties of synthesized titania used for all photocatalytic experiments. Figure 4.17 illustrates the effects of the reaction medium used for titania synthesis on the photocatalytic activity of titania. It was found that the disappearance of MB, using various synthesized titania as catalyst, followed the pseudo-first-order kinetics. The transformed first order plots are given in Figure 4.18. The rate constant for each catalyst, obtained from slope of the graph in Figure 4.18, is shown in Table 4.5. The results were compared with that of the Japanese Reference Catalyst titania (JRC-TIO-1). It is shown that all titania synthesized in this work exhibited higher photocatalytic activity than the JRC-TIO-1. Moreover, it is also shown that titania, which has experienced the calcination, exhibits higher activity than the as-synthesized catalyst. This result can be explained by an increase in crystallinity of titania after heat treatment at high temperature (Ohtani 1997).

Nevertheless, it is evident that type of the solvent employed as the medium for the thermal decomposition of TNB also affects the photocatalytic activity of the obtained titania. The activity of titania synthesized in the organic solvent investigated is found to be in the following order: 1,4-butanediol > toluene > mineral oil. This difference in the activity might be the result from two possible causes, i.e. degree of agglomeration and crystallinity of crystal formed, since titania synthesized in all reaction mediums are in the same crystalline phase with relatively same crystallite

size. Moreover, all parameters for the photodegradation experiment have been controlled.

Table 4.4 Physical properties of all titania samples used in photodegradation experiments.

Titania synthesized conditions	Crystallite size[a], d (nm)	S_{BET} (m^2/g)	S_{XRD} (m^2/g) [b]	S_{BET}/S_{XRD}
Synthesized at 270ºC and calcined at 500°C				
in 1,4-butanediol	6.40	90	240	0.4
in toluene	6.16	69	250	0.3
in mineral oil	6.53	32	236	0.1
Synthesized at 300°C and calcined at 500°C				
in 1,4 butanediol	8.09	62	190	0.3
in toluene	9.73	62	158	0.4
in mineral oil	8.57	68	180	0.4
Synthesized in 1,4-butanediol at 300°C				
as-synthesized	5.90	65	261	0.2
calcined at 400°C	7.06	68	218	0.3
calcined at 500°C	8.09	62	190	0.3
calcined at 600°C	7.97	57	193	0.3
Reference titania	8.82	53	174	0.3

[a] Crystallite size calculated from XRD peak broadening
[b] Specific surface area calculated from $S_{XRD} = 6/d\rho$ under assumption that the crystal is spherical and the density of anatase titania is 3.9 g cm^{-3}
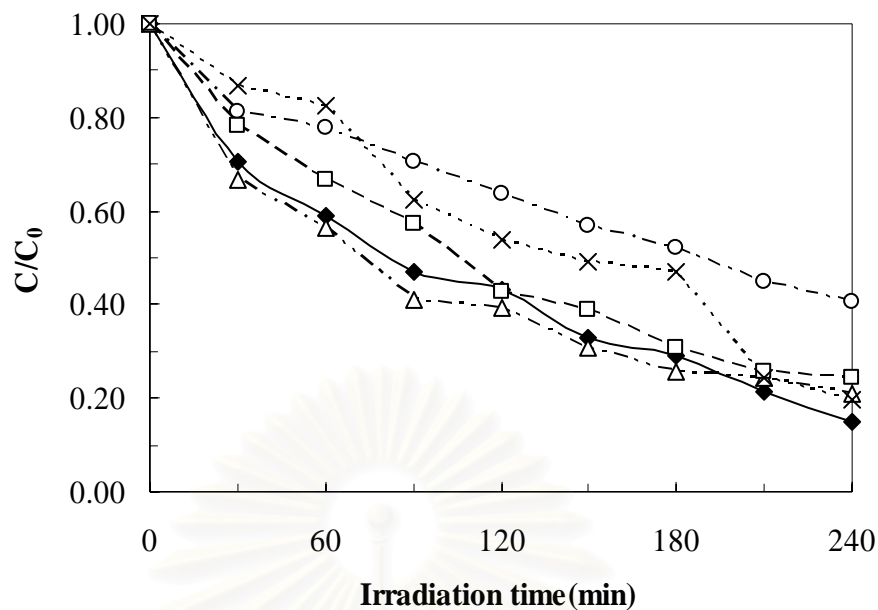
(a)
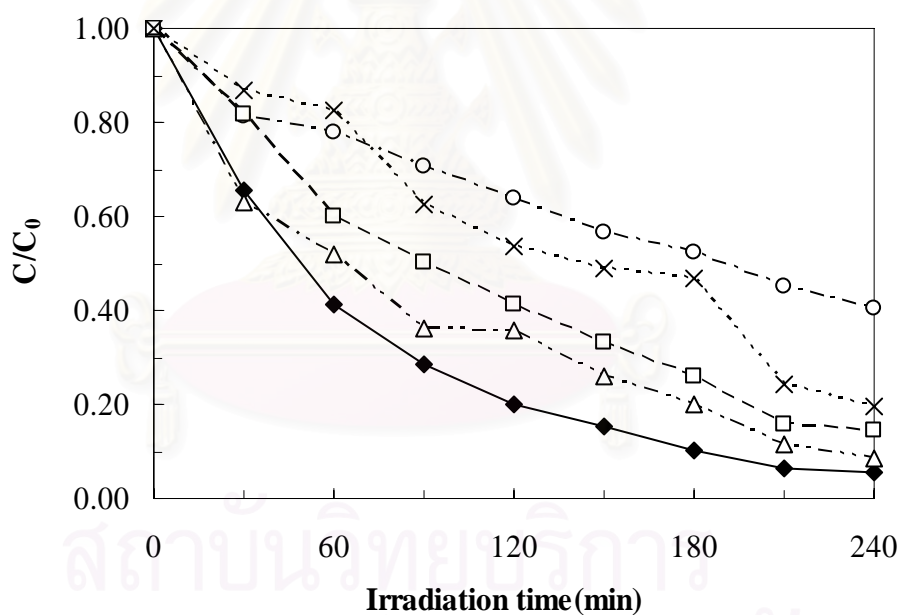
(b)

Figure 4.17 Disappearance of MB by photooxidation in solar light source using (a) as-synthesized titania, (b) titania calcined at 500°C: (◆) titania synthesized in 1,4-BG, (△) titania synthesized in toluene, (□) titania synthesized in mineral oil, (×) reference titania JRC-TIO-1, (○) no titania used.
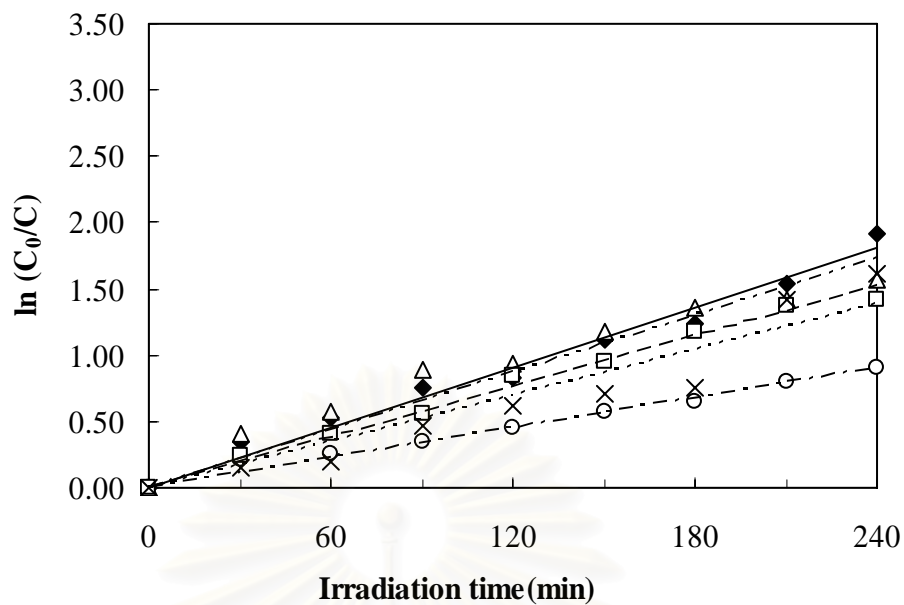
(a)
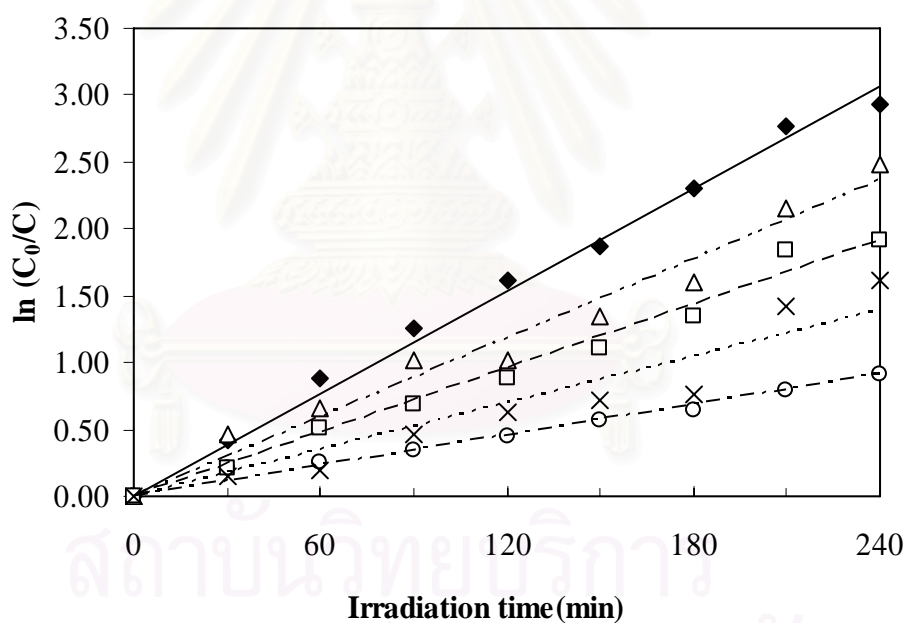
(b)

Figure 4.18 Pseudo-first-order transforms for the disappearance of MB by photooxidation using (a) as-synthesized titania, (b) titania calcined at 500°C: (–◆–) synthesized in 1,4-butanediol, (–△··-)synthesized in toluene, (–□–) synthesized in mineral oil, (-✕) reference catalyst JRC-TIO-1, (–○··-) no titania used.

Table 4.5 Rate constants of the photocatalytic degradation of MB using titania synthesized in various solvents.

Titania preparation		k_{app}
Solvent used	Condition	(min^{-1})
1,4-butandiol	as-synthesized	7.53×10^{-3}
	calcined at 500°C	1.28×10^{-2}
toluene	as-synthesized	7.26×10^{-3}
	calcined at 500°C	9.82×10^{-3}
mineral oil	as-synthesized	6.34×10^{-3}
	calcined at 500°C	7.95×10^{-3}
JRC-TIO-1		5.79×10^{-3}
no catalyst used		3.78×10^{-3}

For the effect of the agglomeration, it not only decreases the surface area of the catalyst, but also the light exposure area, which is the active area for photooxidation reaction. Therefore, titania synthesized in mineral oil, which is highly agglomerated (see Figure 4.14c and Figure 4.4c), is expected to have lower activity than more dispersed titania such as one synthesized in 1,4-butanediol.

Another factor affecting the activity of titania is the crystallinity of the crystal formed. It has been report that crystallization mechanism of titania during the thermal

decomposition of titanium alkoxide depends upon the reaction medium (Payakgul 2005). When 1,4-butanediol is employed as reaction medium, anatase crystals are formed via direct crystallization, once the temperature in the autoclave reaches approximately 250°C, which is significantly lower than the synthesizing temperature in this research. Subsequent heating only results in growth of the crystals. On the other hand, for the reaction in toluene, anatase titania is formed from the solid state transformation of amorphous intermediate, which is initially precipitated from the solution (Payakgul 2005). The difference in the formation mechanism of titania reflects the difference in crystallinity of obtained particles. Therefore, its affects the photocatalytic activity, since it has been accepted that the decrease in crystal defects generally improves the photocatalytic activity of titania (Anpo 1987; Gopidas, Bohorquez et al. 1990; Yin, Inoue et al. 1998). The photocatalytic results are in the good agreement with the results from titania characterization that titania synthesized in 1,4-butanediol has higher crystallinity than those synthesized in toluene and mineral oil.

4.2.2 Photocatalytic degradation of diuron

Diuron or 3-(3,4-dichlorophenyl)-1,1-dimethylurea is a herbicide belonging to phenylurea family. The chemical structure of diuron is quite complex. It consists of a benzene ring attached by 2 atoms of chlorines and one alkylurea group.

As the preliminary work, the photodegradation of 1 ppm diuron aqueous solution was investigated in a system with continuous flow of air bubbling through the solution. Titania synthesized in 1,4-butanediol at 300°C and subsequently calcined

at 500°C was used as photocatalyst. The reference anatase titania (JRC-TIO-1) was also used for photocatalytic activity comparison. The results in Figure 4.19a confirm the prior findings from MB decomposition experiments that titania synthesized by thermal decomposition of TNB in 1,4-butanediol has higher photocatalytic activity than reference catalyst because of the structure with high crystallinity that prevents electron-hole recombination. On the contrary, when all oxygen dissolved in the solution was purged by thoroughly bubbling with nitrogen gas, the conversion of diuron photodegradation dramatically decreased (Figure 4.19b). Only about 30% of diuron was degraded within 6 h of the reaction with either the synthesized or the reference catalyst. This is in agreement with the generally accepted mechanism of the photocatalytic reaction that the presence of dissolved oxygen in the solution as an electron scavenger is required for the course of the reaction (Kormann 1988; Houas 2001; Li 2004). Without electron scavenger, the electron-hole recombination spontaneously took place on the surface of titania. The enhanced effect from crystallinity of the synthesized titania is therefore compromised and the progress of the photocatalytic reactions from both catalysts are roughly the same. However, regardless of the depletion of dissolved oxygen in the solution, the reaction can progress slowly. This is expected to be the results from chlorine radicals produced from diuron degradation. Several studies involving photocatalytic decomposition of chlorinated organic materials have proposed that chlorine radicals may be generated during photocatalysis (Nimlos 1993) and these radicals participate in radical chain reactions (Luo 1996; d'Hennezel 1997; Lewandowski 2003).
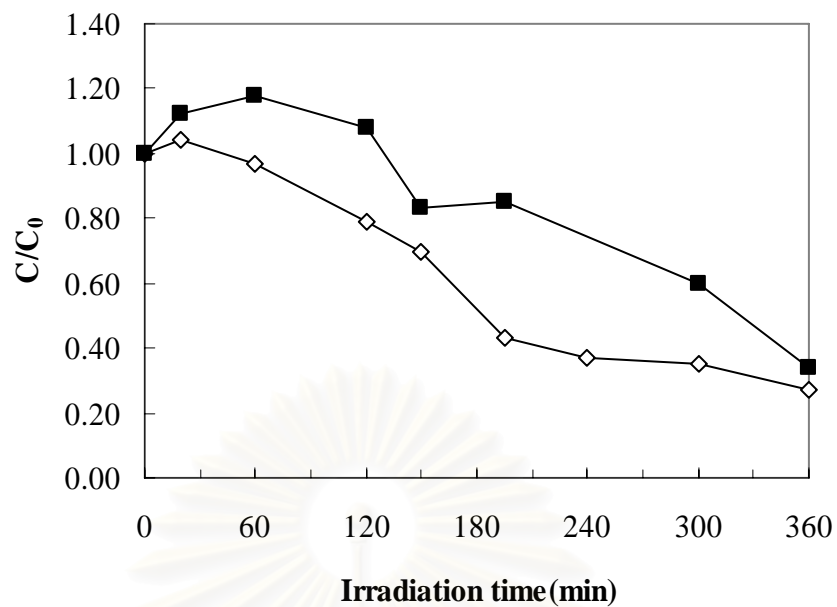
(a)
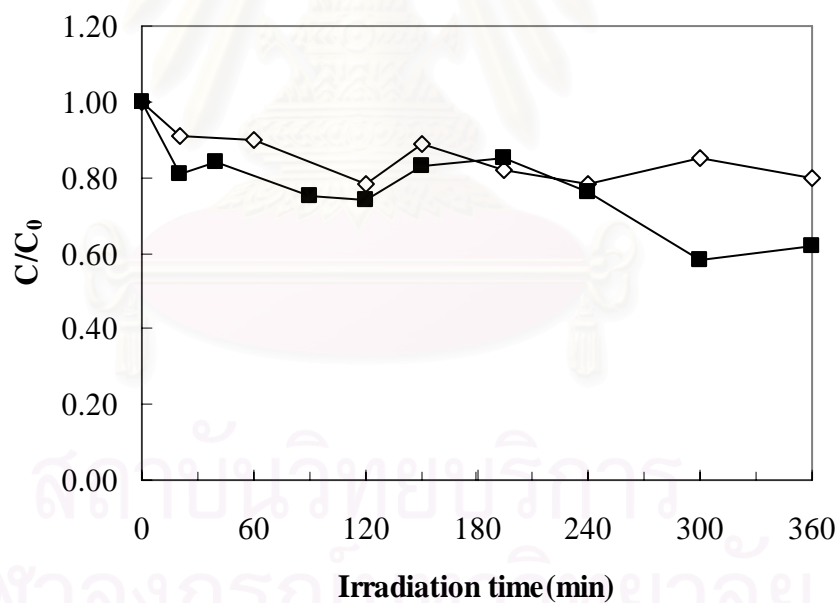
(b)

Figure 4.19 Results for photocatalytic degradation of 1 ppm diuron aqueous solution:

(a) in oxygen saturated solution, (b) in nitrogen-purged solution; ($\diamond$) synthesized

titania, (■) reference titania**.**

As mentioned earlier that the efficiency of titania in photocatalytic reaction is influenced by many factors such as crystallinity of the anatase phase (Fox 1993), particle size (Xu 1999) and surface area (Xu 1999). Since the synthesized and reference titania are both anatase with roughly same particle size and surface area, the main factor accountable for the enhanced activity of the synthesized titania is its crystallinity. Although there has been no consensus on the detailed mechanism of the photocatalytic reaction on titania, it is generally agreed that the reaction involves generation of electron-hole pairs upon illumination of UV light on titania. The photogenerated holes can be subsequently scavenged by oxidizing species such as H_2O or OH^- and result in highly reactive hydroxyl radicals, which are the key for decomposition of most organic contaminants. Therefore, the separation of the photogenerated electron-hole pairs is considered to have a predominant role in photocatalytic reaction. The longer the separation period, the higher the activity. Crystallinity, including quality and quantity of both bulk and surface crystal defects, is one factor that affects the electron-hole separation (Tsai 1997). It has been reported that negligible photocatalytic activity of amorphous titania is attributable to the facilitated recombination of photoexcited electrons and holes in the amorphous structure.

Further investigations on the enhanced activity of the synthesized titania were conducted by using solar irradiation, which had much higher light intensity than UV lamps. In this experiment, the concentration of diuron solution was increased to 10 ppm in order to heighten the effect of light intensity. The results in Figure 4.20 reveal that the activity of both synthesized and reference titania increase when the light intensity is increased, yet titania synthesized in this work still shows higher activity.
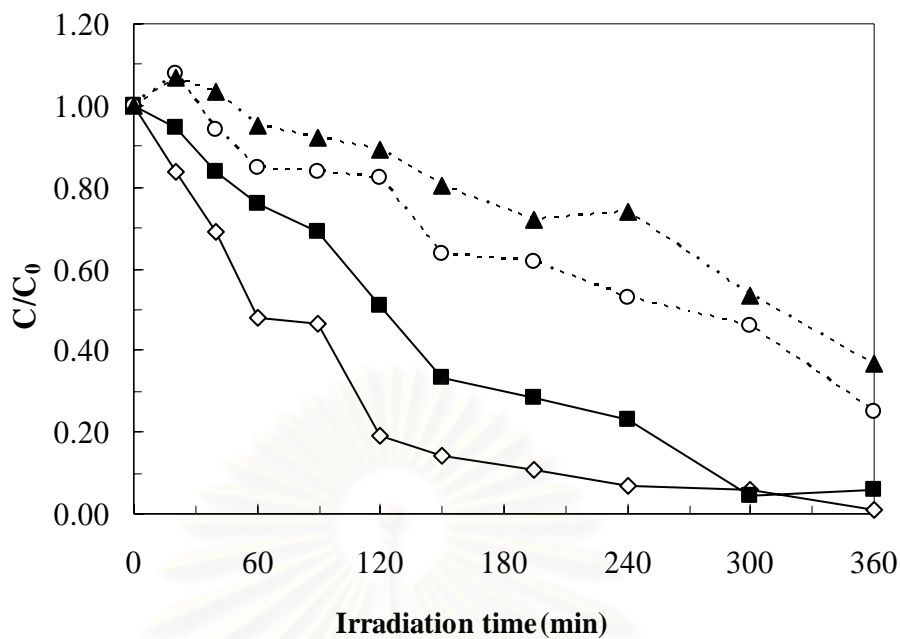
(a)
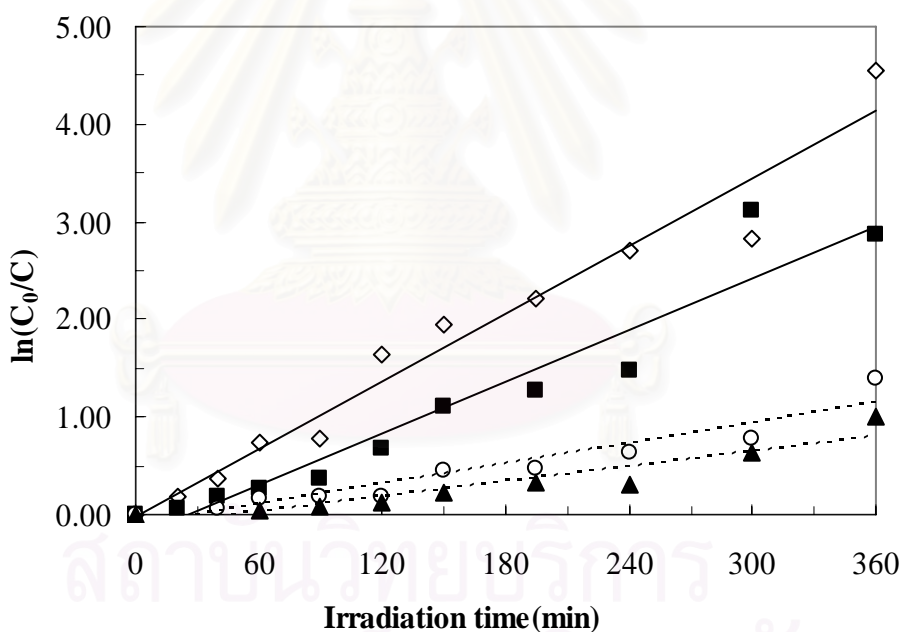
(b)

Figure 4.20 Results for photocatalytic degradation of 10 ppm diuron aqueous solution

using titania synthesized in 1,4-butanediol at 300°C and calcined at 500°C: ($--$)

using UV lamps, ($—$) using solar radiation; ($\diamondsuit$), ($\circ$) synthesized titania, ($\blacksquare$), ($\blacktriangle$)

reference titania. (a) the disappearance of diuron, (b) first-order linear transforms.

More importantly, the enhancement in the activity from the synthesized titania increases with an increase in light intensity. Although more photo-electron-hole pairs are generated under higher light intensity, it has been reported that a rate of the electron-hole recombination increases more progressively than the rate of charge transfer reaction (Hoffmann 1995). Therefore, titania with high cystallinity, which prolongs the separation lifetime of the photogenerated electron-hole pairs, would utilize these greater amount of photoexcited electrons and holes with higher efficiency. These results in such enhancement reported earlier.

Next, the photodegradation of diuron was studied as a function of initial concentration of diuron. Three initial concentrations of diuron, i.e. 1, 5 and 10 ppm were investigated and results are shown in Figure 4.21. The first-order rate constant (k_{app}) of all experiments are also listed in Table 4.6. It can be seen from Figure 4.21(b) that the degradation rate of diuron in high concentration is only slightly less than that observed in low concentration. This result confirms that the reaction is pseudo-first-order in nature and complies with the Langmuir-Hinshelwood kinetic. Nevertheless, it can be seen from the data in Table 4.6 that the first-order rate constants k_{app} decreased with an increasing initial concentration of diuron, which can be related to the faster consumption of photogenerated hydroxyl radicals by higher concentrated organic molecules. Consequently, the photostationary concentration of hydroxyl radical decreases. Then, lower concentration of hydroxyl radicals reduces a probability of the recombination of hydroxyl radicals with electrons trapped on surface of anatase titania particles (Macounova 2003). The result is contrary to degradation rate of diuron in Figure 4.20(a).
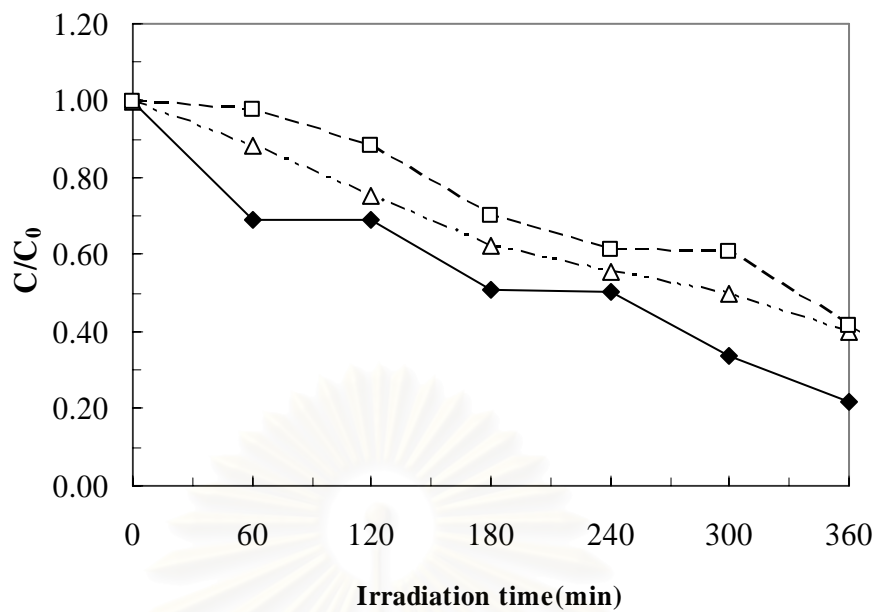
(a)
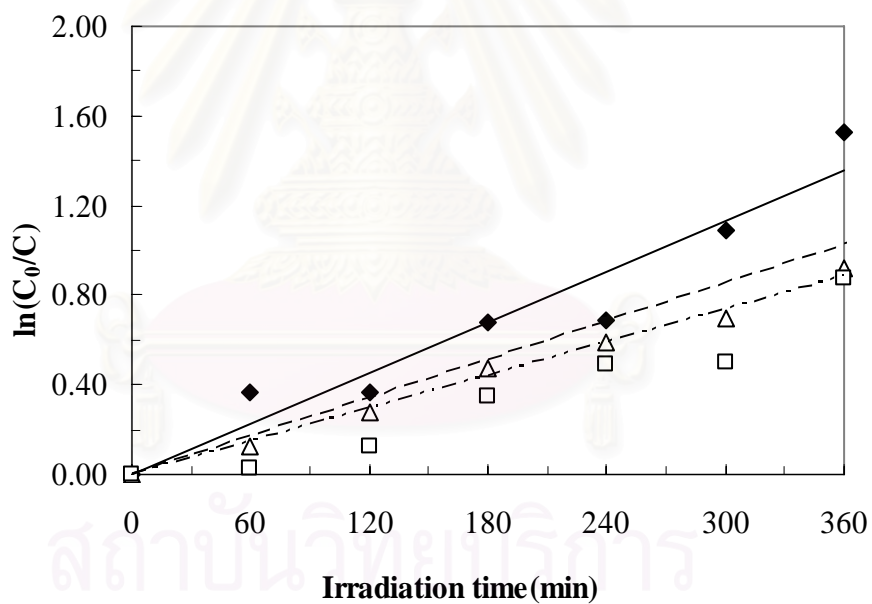
(b)

Figure 4.21 Results for photocatalytic degradation of diuron aqueous solution various concentrations of using titania synthesized in 1,4-butannediol at 300°C and calcined at 500°C: (◆)1 ppm diuron; (△··) 5 ppm diuron; (□-) 10 ppm diuron :(a) the disappearance of diuron, (b) first-order linear transforms.

Table 4.6 Rate constant and half-life of the photocatalytic degradation of diuron.

Organic medium	Syn-temp (°C)	Calcined-temp (°C)	C_0 (ppm)	k_{app} (min^{-1})	Half-life, $t_{1/2}$ (min)
Degradation using UV lamps irradiation					
1. Effect of initial concentration of diuron					
1,4-butanediol	300	500	1	3.76×10^{-3}	169.9
1,4-butanediol	300	500	5	2.47×10^{-3}	259.1
1,4-butanediol	300	500	10	2.84×10^{-3}	245.5
2. Effect of organic medium in titania synthesis					
1,4-butanediol	300	500	10	2.84×10^{-3}	245.5
Toluene	300	500	10	1.96×10^{-3}	356.1
Mineral oil	300	500	10	1.68×10^{-3}	416.2
Reference titania	-	-	10	1.28×10^{-3}	544.9
3. Effect of synthesizing and calcination temperature					
1,4-butanediol	300	-	10	9.71×10^{-4}	658.0
1,4-butanediol	300	400	10	1.72×10^{-3}	372.3
1,4-butanediol	300	500	10	2.84×10^{-3}	245.5
1,4-butanediol	300	600	10	1.43×10^{-3}	447.2
1,4-butanediol	270	500	10	1.78×10^{-3}	479.3
Toluene	270	500	10	1.33×10^{-3}	497.3
Mineral oil	270	500	10	1.09×10^{-3}	584.7
Degradation using solar irradiation					
1,4-butanediol	300	500	10	1.15×10^{-2}	60.5
Reference titania	-	-	10	7.03×10^{-3}	98.6

Since diuron is chemically stable, it is suggested that persistent intermediate compounds, which are difficult to be degraded intermediate are produced during the photocatalytic process. The degradation pathway of diuron has been reported ealier in literature (Konstantinou 2003; Macounova 2003). Ammonia, nitrate ion and carbon dioxide were released from diuron structure and produced during the photocatalytic process. The nitrogen balance in diuron degradation system was complex. The nitrogen content was converted mainly to ammonia or nitrogen (Malato 2003). HPLC analysis can not detect these moiety compounds. The degradation intermediates results will be reported in the next section.

Effects of the solvent employed during titania synthesis on the photocatalytic activity of titania toward the degradation of diuron are shown in Figure 4.22. It shows that the disappearance of diuron is in similar trend as the disappearance of methylene blue. It is found that the photodegradation of diuron, using various synthesized titania as catalyst, also follows the pseudo-first-order kinetics. The transformed first order plots are given in Figure 4.22(b), whereas the slopes are rate constants of the degradation. The rate constant for each catalysts are shown in Table 4.6. The results show that all titania synthesized according to the method in this work and subsequently calcined at 500°C, exhibits higher photocatalytic activity than the reference titania. The activity of titania synthesized in organic solvent investigated found to be is in the order: 1,4-butanediol > toluene > mineral oil, which is the same order as order as asberved in the degradation of methylene blue. The possible causes for this difference in the activity have already been discussed in the previous section.
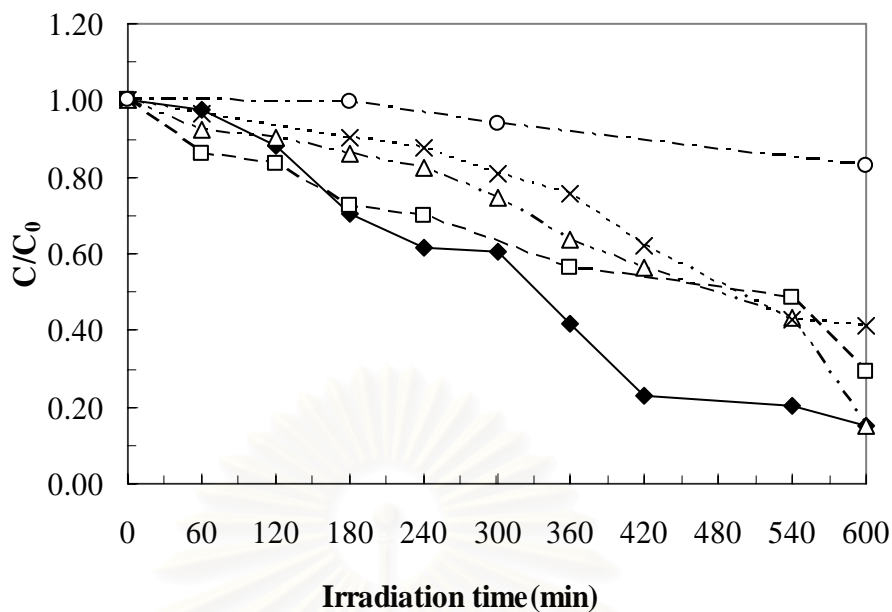
(a)
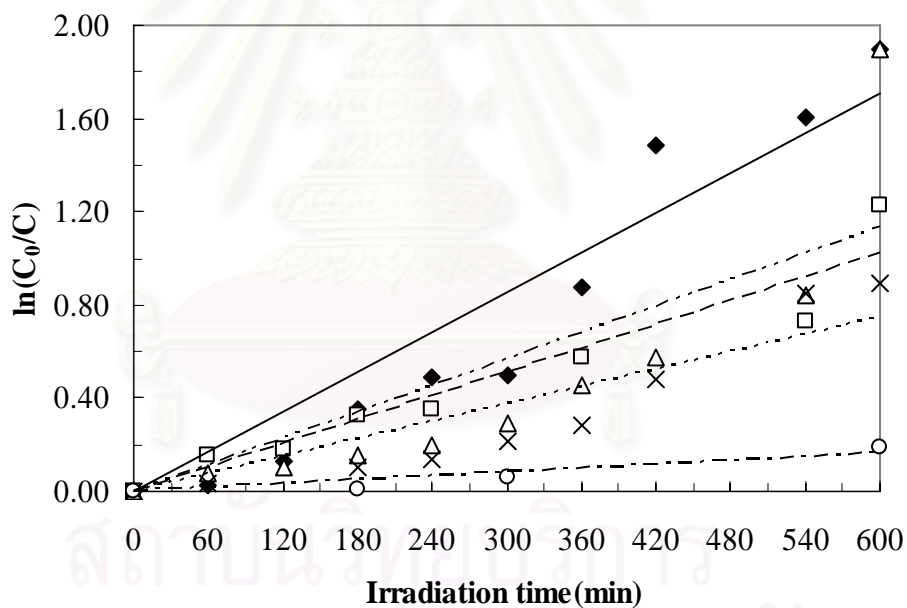
(b)

Figure 4.22 Disappearance of diuron by photooxidation using titania for 10 h and UV lamp irradiation: (a) the disappearance of diuron, (b) first-order linear transforms; (◆) synthesized in 1,4-butanediol, (–△··-) synthesized in toluene, (–□-) synthesized in mineral oil, (-✕) reference catalyst JRC-TIO-1, (–⊖··-) no titania used.

Further investigation has shown that titania, which has experienced the calcination, exhibits higher activity than as-synthesized catalyst, as shown in Figure 4.23. In this part, the photodegradtion experiments were conducted, using titania synthesized in 1,4-butanediol that was calcined at different temperature for 2 h. This enhanced activity by calcination can be explained by an increase in crystallinity of titania after heat treatment at high temperature (Ohtani 1997). Although surface area of titania is decreased with the increasing calcination temperature, the calcination reduces the number of crystal defects, which predominantly act as center for electron-hole recombination. Less defect leads to smaller probability of the recombination and enhanced photocatalytic activity. This result suggests that the crystallinity of titania predominantly influences the activity rather than surface area. It is shown that the activity increases with the calcination up to 500°C and then decreases at the higher temperature, i.e. 600°C. Upon the calcinations at high temperature, phase transformation from anatase to rutile take place and retards photocatalytic activity of titania particles, since rutile phase shows no activity. Therefore, the interpretation of the result of diuron degradation on titania calcined at 600°C is a slightly complicated. However, when titania is all in anatase form, a predominant effect of crystallinity from the calcination rather than the surface area is clearly seen (see in Table 4.4).
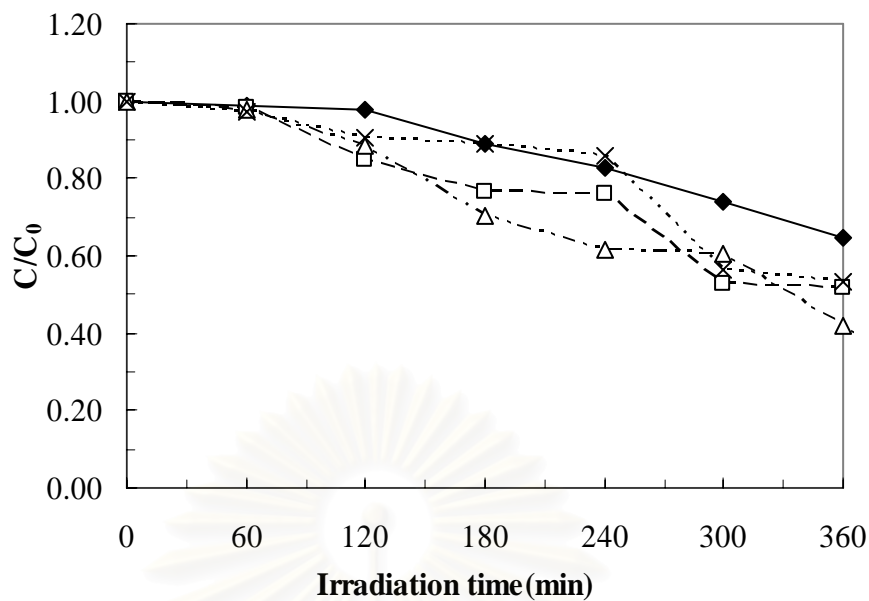
(a)
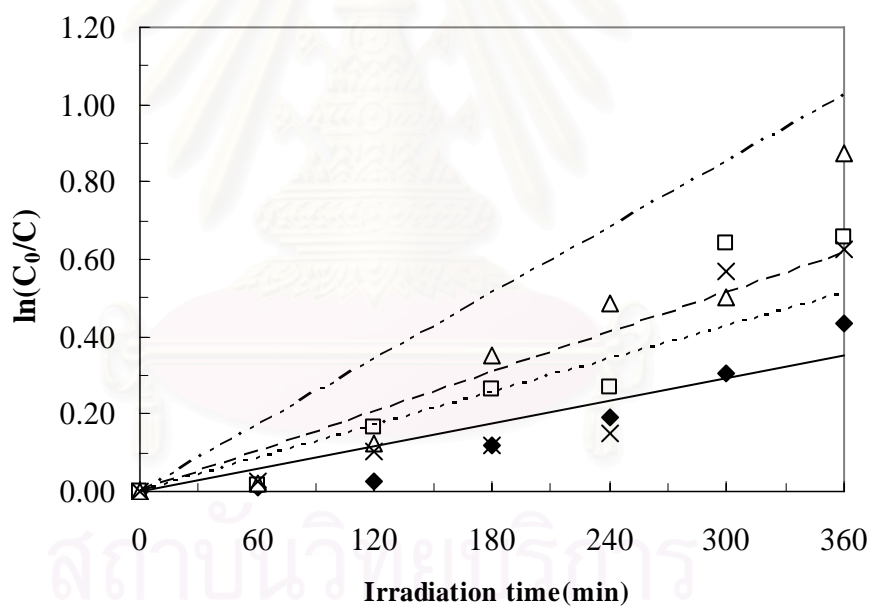
(b)

Figure 4.23 Results for photocatalytic degradation of diuron aqueous solution using titania synthesized in 1,4-butanediol (a) the disappearance of diuron, (b) first-order linear transforms; (—◆—) uncalcined titania, (–□–) titania calcined at 400°C, (–△··-) titania calcined at 500°C, (-✕) titania calcined at 600°C.

4.2.3 Photocatalytic degradation of isoproturon

Isoproturon or 3-(4-isopropylphenyl)-1,1-dimethylurea is a phenylurea herbicide and consist of an aromatic ring with an alkylic chain and uretic group (diamide). Its molecular structure allows an easy hydroxyl radical attack on different positions of the molecule, giving a rise to several chain reactions.

Figure 4.24 shows the time-dependent degradation profiles at different initial concentrations of isoproturon. It is shown that the lower concentration of isoproturon, higher rate of degradation. Nevertheless, as observed in the degradation of diuron, the rate of isoproturon degradation does not dramatically change with the initially concentration of isoproturon. The first-order kinetic transformation plot of the photodegradation reaction was evaluated and the calculated first-order rate constant (k_{app}) for all experiments are listed in Table 4.7.

It can be indicated that the degradation of isoproturon is relatively fast. Almost complete disappearance of isoproturon is observed near the end of the experiment. After 10 h of irradiation, for 10 ppm solution, the photodegradation of isoproturon reaches 63-89 %, depending on catalyst used (shown in Figure 4.25). The result is quite similar to that of diuron, although rate of but isoproturon disappearance, on average, is slightly higher than diuron.

The difference in the degradation rate between isoproturon and diuron can be discussed from the fact that an initial degradation rate is directly related to the

electron-donating or electron-withdrawing character of different functional group attaching to the aromatic ring of herbicides, which can alter the reactivity of the aromatic ring with the OH radical. This OH radical is very reactive in oxidation of organic substances and it is generated from the interaction between photoexcited electron/hole and water as previously mentioned (Blake 1999). Isoproturon is more active than diuron as withnessed from shorter half-life in nature. This is probably isoproturon due to the presence of the $CH(CH_3)_2$ group, which is benzene ring activating group (Parra 2002). On the contrary, the presence of halogen group in diuron causes the aromatic to be more stable and results in lower reactivity of diuron toward the decomposition, comparing to isoproturon.

For the effect of type of organic medium used in titania synthesis on the activity of degradation, it is slightly different than that observed in case of diuron. The activity of titania synthesized in organic solvents investigated is in the following order: 1,4-butanediol > mineral oil > toluene.
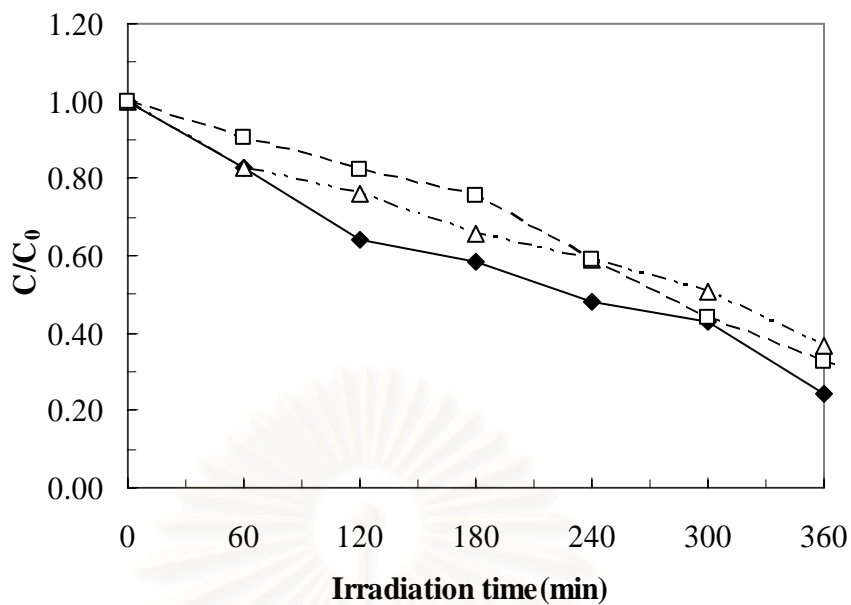
(a)
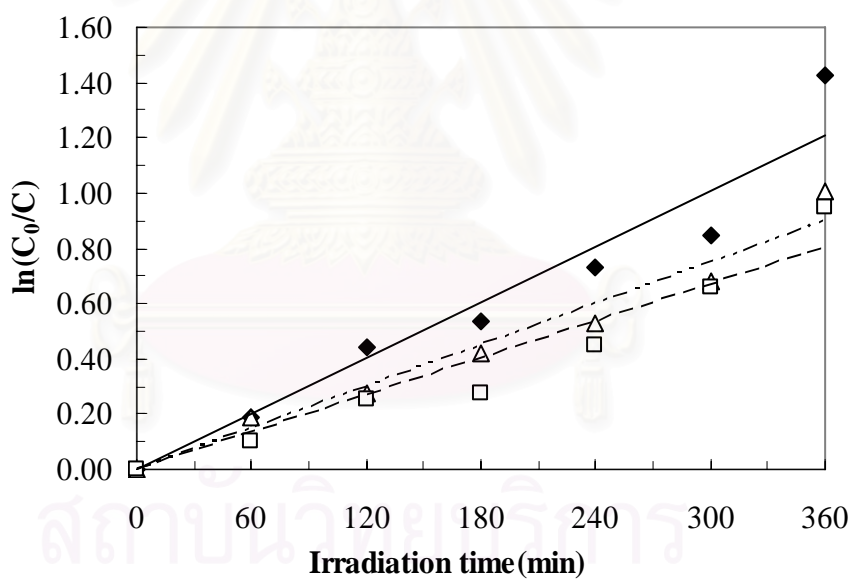
(b)

Figure 4.24 Results for photocatalytic degradation of isoproturon aqueous solution various concentrations of using titania synthesized in 1,4-butannediol at 300°C and calcined at 500°C: (◆)1 ppm isoproturon; (–△·-) 5 ppm isoproturon; (–□–) 10 ppm isoproturon : (a) the disappearance of isoproturon, (b) first-order linear transforms.
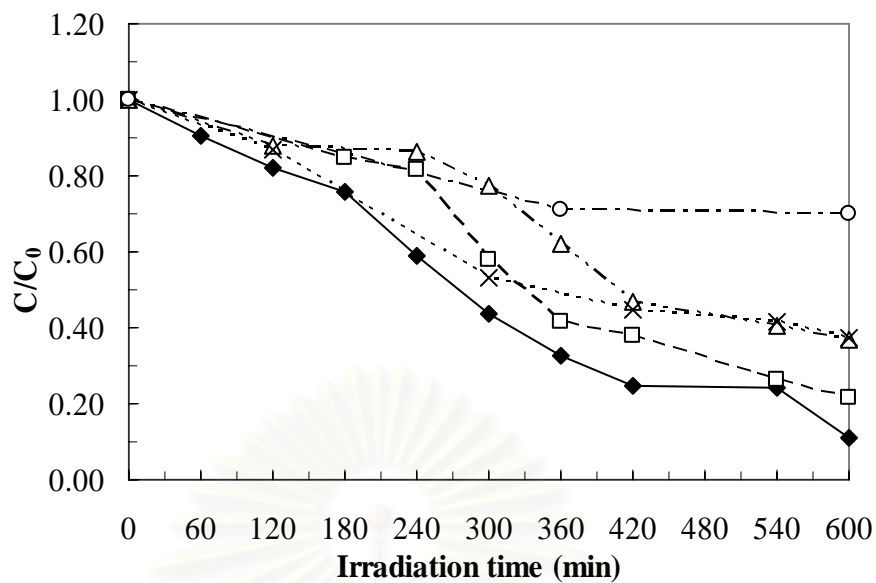
(a)
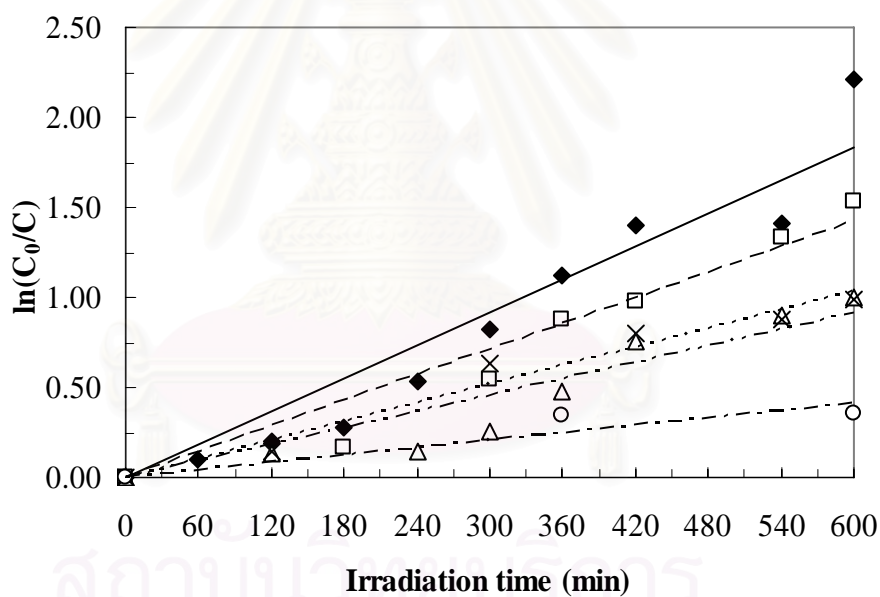
(b)

Figure 4.25 Disappearance of isoproturon by photooxidation using titania synthesized

in various organic solvents: (a) the disappearance of isoproturon, (b) first-order linear

transforms; (◆) synthesized in 1,4-butanediol, (△··) synthesized in toluene, (□)

synthesized in mineral oil, (✕) reference catalyst JRC-TIO-1, (○··) no titania

used.

Table 4.7 Rate constant and half-life of the photocatalytic degradation of isoproturon.

Organic medium	Syn-temp (°C)	Calcined-temp (°C)	C_0 (ppm)	k_{app} (min^{-1})	Half-life, $t_{1/2}$ (min)
Effect of initial concentration of isoproturon					
1,4-butanediol	300	500	1	3.37×10^{-3}	189.9
1,4-butanediol	300	500	5	2.41×10^{-3}	265.6
1,4-butanediol	300	500	10	3.06×10^{-3}	208.6
Effect of organic medium in titania synthesis					
1,4-butanediol	300	500	10	3.06×10^{-3}	208.6
Toluene	300	500	10	1.52×10^{-3}	420.9
Mineral oil	300	500	10	2.36×10^{-3}	269.7
Reference titania	-	-	10	1.73×10^{-3}	370.4

4.2.4 Photocatalytic degradation of linuron

Linuron or 3-(3,4-dichlorophenyl)-1-methoxy-1-methyl urea is another common phenylurea herbicide. Its structure consists of an aromatic ring with an alkoxy alkylurea chain and two chlorine atoms.

It can be seen from Figure 4.26 that the degradation rate of linuron increases when the initial concentration of linuron is decreased, especially when the concentration is 1 ppm. The first order kinetic transformation plot of the reaction was evaluated and the apparent first-order rate constant (k_{app}) of all experiments were calculated, as shown in Table 4.8. The 10 h degradation of linuron is in the range of 47-80 %, depending on catalyst (shown in Figure 4.26). The photodegradation result of 10 ppm linuron solution is quite similar to those of diuron and isoproturon but, linuron disappearance rate is generally lower than diuron and isoproturon. Linuron exhibits slow degradation rate because the stability of linuron is higher than diuron. Chlorine group consisting in the structure of both diuron and linuron is an aromatic ring deactivating group, which causes the benzene ring to be less reactive. Comparing to the chloride group, alkyl group attaching to an aromatic ring in isoproturon has more reactive structure and tends to release electron easier (Graham 1996). In the other words, the electrophilic attack of the OH radical to isoproturon is easier than diuron and linuron. For this reason it can be explained why the degradation rate of diuron and linuron is less than that of isoproturon. Between diuron and linuron, the -NHCON(CH$_3$)$_2$ group attaching to the aromatic ring of diuron and -NHCON(OCH$_3$)(CH$_3$) group in linuron are not so different that it can cause significantly difference in the electron-releasing habit of these groups.

Instead, the steric effect of organic substance is employed to explain the difference in the degradation of these two compounds. The $-NHCON(OCH_3)(CH_3)$ group in linuron is more difficult to be attacked by OH radical. Nevertheless, further investigation is need.

The effect of organic medium for synthesized titania to photodegradation of linuron were similar to in case of diuron in the following order; 1,4-butanediol > toluene > mineral oil.
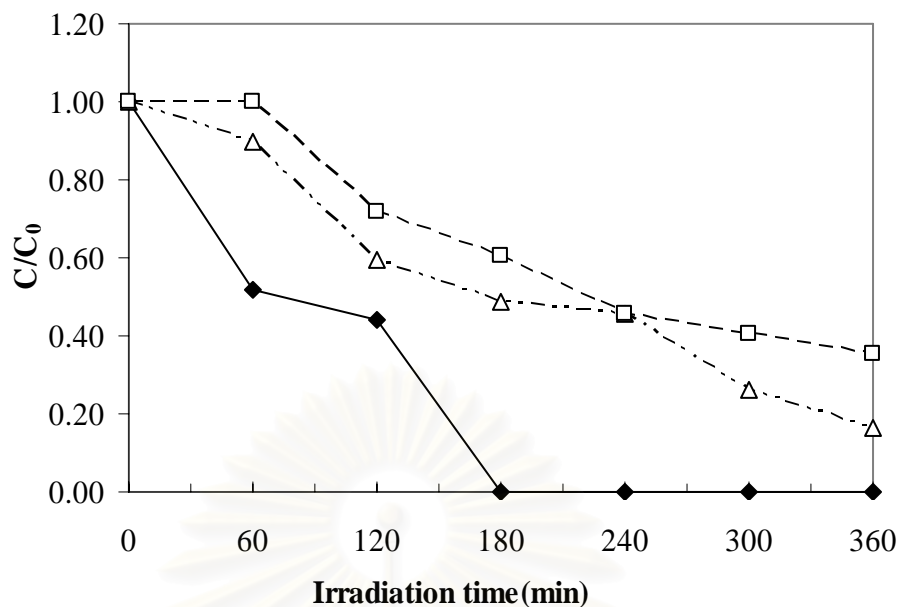
(a)
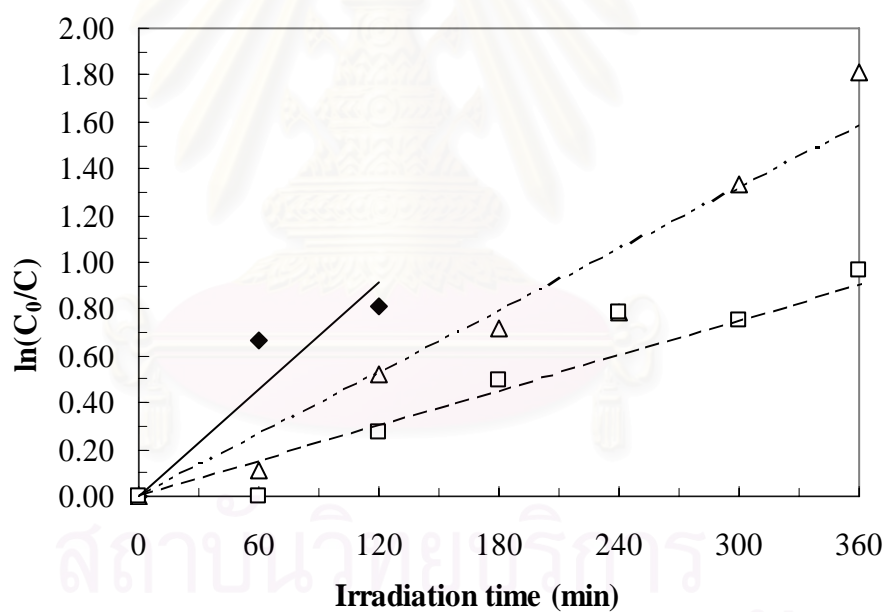
(b)

Figure 4.26 Results for photocatalytic degradation of linuron aqueous solution various concentrations of using titania synthesized in 1,4-butannediol at 300°C and calcined at 500°C:(–◆–) 1 ppm linuron; (–△··–) 5 ppm linuron; (–□–) 10 ppm isoproturon: (a) the disappearance of linuron, (b) first-order linear transforms.
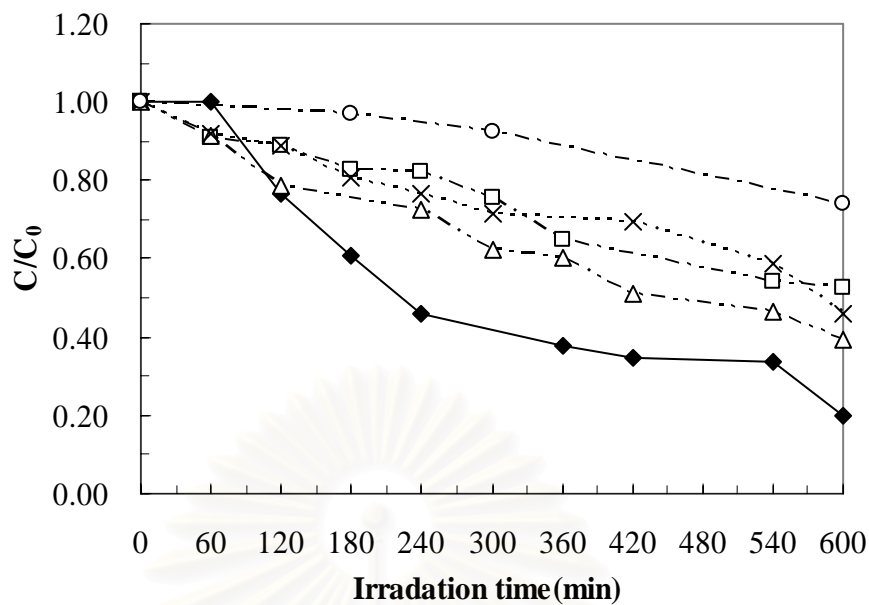
(a)
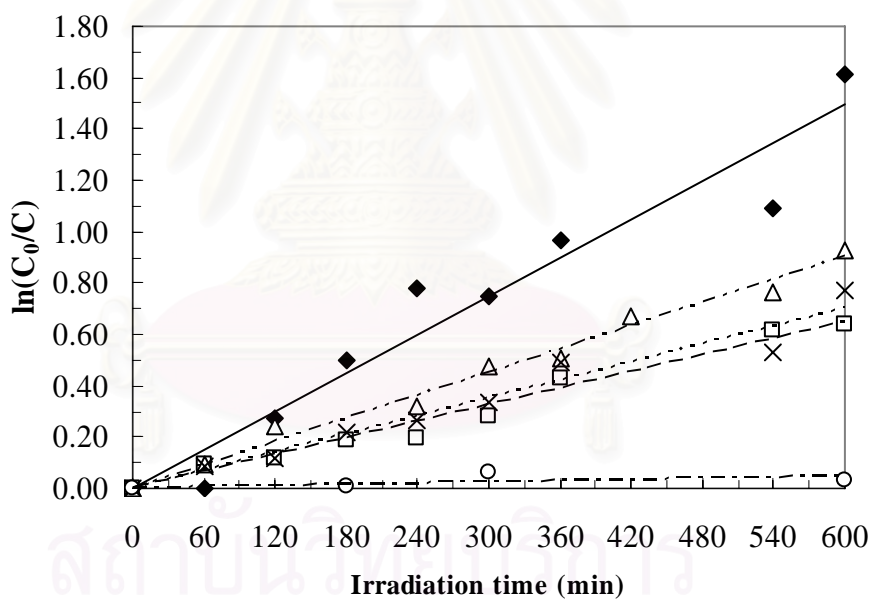
(b)

Figure 4.27 Disappearance of linuron by photooxidation using titania synthesized in various organic solvents: (a) the disappearance of linuron, (b) first-order linear transforms; (—◆—) synthesized in 1,4-butanediol, (—△··-) synthesized in toluene, (—□-) synthesized in mineral oil, (-✕-) reference catalyst JRC-TIO-1,(—⊖··-) no titania used.

Table 4.8 Rate constant and half-life of the photocatalytic degradation of linuron

Organic medium	Syn-temp (°C)	Calcined-temp (°C)	C_0 (ppm)	k_{app} (min^{-1})	Half-life, $t_{1/2}$ (min)
Effect of initial concentration of linuron					
1,4-butanediol	300	500	1	7.65×10^{-3}	83.6
1,4-butanediol	300	500	5	4.39×10^{-3}	145.6
1,4-butanediol	300	500	10	2.49×10^{-3}	256.3
Effect of organic medium in titania synthesis					
1,4-butanediol	300	500	10	2.49×10^{-3}	256.3
Toluene	300	500	10	1.50×10^{-3}	425.7
Mineral oil	300	500	10	1.08×10^{-3}	593.2
Reference titania	-	-	10	1.18×10^{-3}	543.9

4.2.5 Summaries of observation

The effect of type of phenylurea herbicides can be observed as following (Table 4.9):

1. The degradation of isoproturon generally has the largest of rate constant and the shortest of half-life, regardless of catalyst. This indicates that the chemical activity and uncomplicated chemical structure of the herbicide allows an easy electrophilic attack from the OH radical for its degradation.

2. The R^2 value indicates how well first order kinetics represent the degradation data. The degradation behavior of linuron is closest to the first order kinetics, comparing to the degradation behavior of diuron and isoproturon. It can also see that reaction kinetics is affected by the solvent used to prepare titania.

Table 4.9 Rate constant, half-life time and R^2 of photocatalytic degradation reaction of phenylurea herbicides

Type of solvent used for titania synthesis	k_{app}(min^{-1})			$t_{1/2}$ (min)			R^2		
	Diuron	Isoproturon	Linuron	Diuron	Isoproturon	Linuron	Diuron	Isoproturon	Linuron
1,4-butanediol	2.843×10^{-3}	3.063×10^{-3}	2.493×10^{-3}	245.6	208.6	256.3	0.9077	0.9208	0.9402
Toluene	1.960×10^{-3}	1.518×10^{-3}	1.501×10^{-3}	356.1	420.9	425.7	0.7126	0.8792	0.9851
Mineral oil	1.677×10^{-3}	2.369×10^{-3}	1.077×10^{-3}	416.2	269.7	593.2	0.9142	0.9422	0.9772
Reference titania	1.281×10^{-3}	1.725×10^{-3}	1.175×10^{-3}	544.9	370.4	596.2	0.8717	0.9650	0.9543

4.3 Evaluation of Degradation Intermediates

4.3.1 Degradation of diuron

Diuron has the chemical structure which is consisted of an aromatic ring attached by one urea group and two chlorine atoms. During the photocatalytic degradation, active radicals generated from titania react with diuron, resulting in intermediate products. Structure of the functional groups attaching to aromatic ring of diuron is the mainly responsible for the structure of the intermediates formed. Diuron clearly offers two sites for the reaction, i.e. the aromatic ring and the aliphatic side chain (Hincapie 2005). Figure 4.28 shows relative amount of various intermediates generated, as the photocatalytic treatment of diuron proceeds, using titania synthesized in different solvents. Each fraction of intermediate, separated from each other by HPLC, was analyzed by using GC-MS in order to identify the intermediate products. The results are summarized in Table 4.10, while the detailed mass spectra are shown in Appendix B. Figure 4.28 (a)-(d) illustrate seven HPLC fractions representing the intermediates generated during photodegradation. Concentrations of most intermediate increase with irradiation time, although the data show some fluctuation. It can be observed that each unknown intermediates are presented at very low concentration. This result is contrary with mass balance of diuron in the process. It can be suggested that nitrogen containing in diuron forms ammonia, urea and nitrate. Carbon dioxide is also the main product of oxidation reaction (Malato 2003). However these small molecules are not detectable by HPLC analysis.
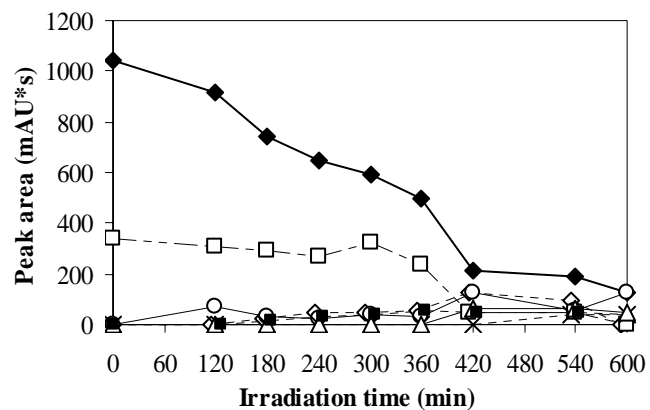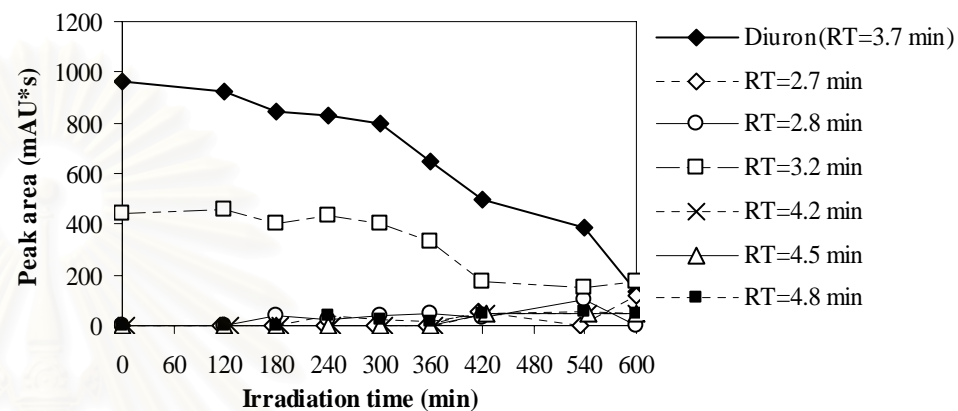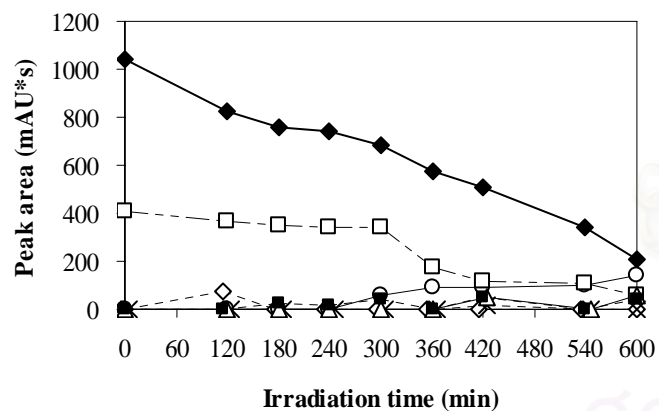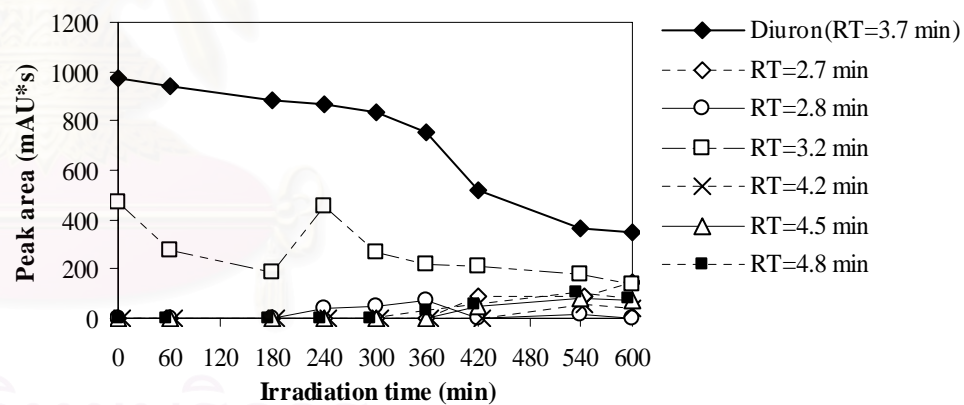
Figure 4.28 Intermediates generated during photocatalytic treatment of diuron, using titania synthesized at 300°C and calcined at 500°C, where

the synthesis medium is: (a) 1,4-butanediol, (b) toluene, (c) mineral oil, (d) Reference titania JRC-TIO1.

Table 4.10 Molecular ion (m/z), molecular weight (MW), and chemical formula of intermediates generated from photodegradation of diuron.

Compound	m/z	MW	Chemical substance identified
1	133, 281, 282	281	$C_9H_{10}N_2O_4Cl_2$
2	133, 135, 151	151	unidentifiable
3	73, 147, 249	249	$C_9H_{10}N_2Cl_2O_2$
4	68, 77, 121, 133, 152	133	unidentifiable
5	73, 267	267	unidentifiable
6	103, 105, 117, 119, 133, 134, 135, 151, 152	151	unidentifiable
7	59, 60, 77, 133, 191, 207, 208, 209	144	C_6H_6NClO

The effect of titania synthesized in different organic medium on the activity and behavior of intermediates are also compared in Figure 4.28. It shows that most photodegradation intermediates are formed after 120 min of irradiation time. It should be noted that an intermediate at retention time of 3.2 min is already presented even before the degradation. This species should be the result from the reaction between diuron and water and it is not the product from photodegradation. According to Figures 4.28, titania synthesized in 1,4-butanediol can activate diuron degradation more aggressively than other, since several intermediates are formed within short time and the concentrations of intermediates are high. This result indicates high activity of titania synthesized in 1,4-butanediol. Nevertheless, the difference in catalytic activity

can not be clearly observed from diuron degradation. It will be discussed in more details from the degradation of isoproturon and linuron.

As mentioned earlier, each intermediate was fractionated by HPLC and then identified by GC-MS. Table 4.10 shows representative of all intermediates appeared in GC-MS spectrum for each HPLC fractions, which includes molecular weight, chemical formula and structure of each unknown intermediates evaluated. Appendix C shows details of MS spectra for all HPLC fractions. Seven products were identified based on the molecular ion and mass spectrometric fragmentation peaks, as followed. Compound 1 has molecular weight of 281 and it is suggested that the chemical formula is $C_9H_{10}N_2O_4Cl_2$. This compound is formed by oxidation of methyl group and hydroxylation of diuron. Compound 2 has molecular weight of 151, but it was unidentifiable. Compound 3 has molecular weight of 249 and it is suggested that the chemical formula is $C_9H_{10}O_2N_2Cl_2$, which is the result from hydroxylation of one methyl group of diuron. Compound 4 has molecular weight of 133. It should be noted that this compound was detected from the HPLC fraction at retention time of diuron. However, the result from GC-MS did not show the m/z of 233, instead the m/z 133. It indicates that diuron was decomposed at high temperature of GC-MS characterization and compound with m/z of 133 is detected. Compound 5 has molecular weight of 267. This compound was unidentifiable. Compound 6 has molecular weight of 151. This compound has m/z similar to compound 2 and it was unidentifiable. These results indicated that both compounds may be the resulting compounds from thermal decomposition during GC-MS analysis. Compound 7 has molecular weight of 147. It is suggested that the formula is C_6H_6ClNO. This compound is formed by oxidation of methyl group of the side chain, decarboxylation, dealkylation of uretic group,

hydroxylation and dechlorination of the aromatic ring of diuron (Amine-Khodja 2004). The chemical structures of the identified intermediates of diuron are sketched in Figure 4.29.

Diuron

(MW=233)

Compound 1

(MW=281)

Compound 3

3-(3,4-dichlorophenyl)1-hydroxymethyl-1-methylurea (MW=249)

Compound 7

3-chloro-4-hydroxylaniline (MW=144)
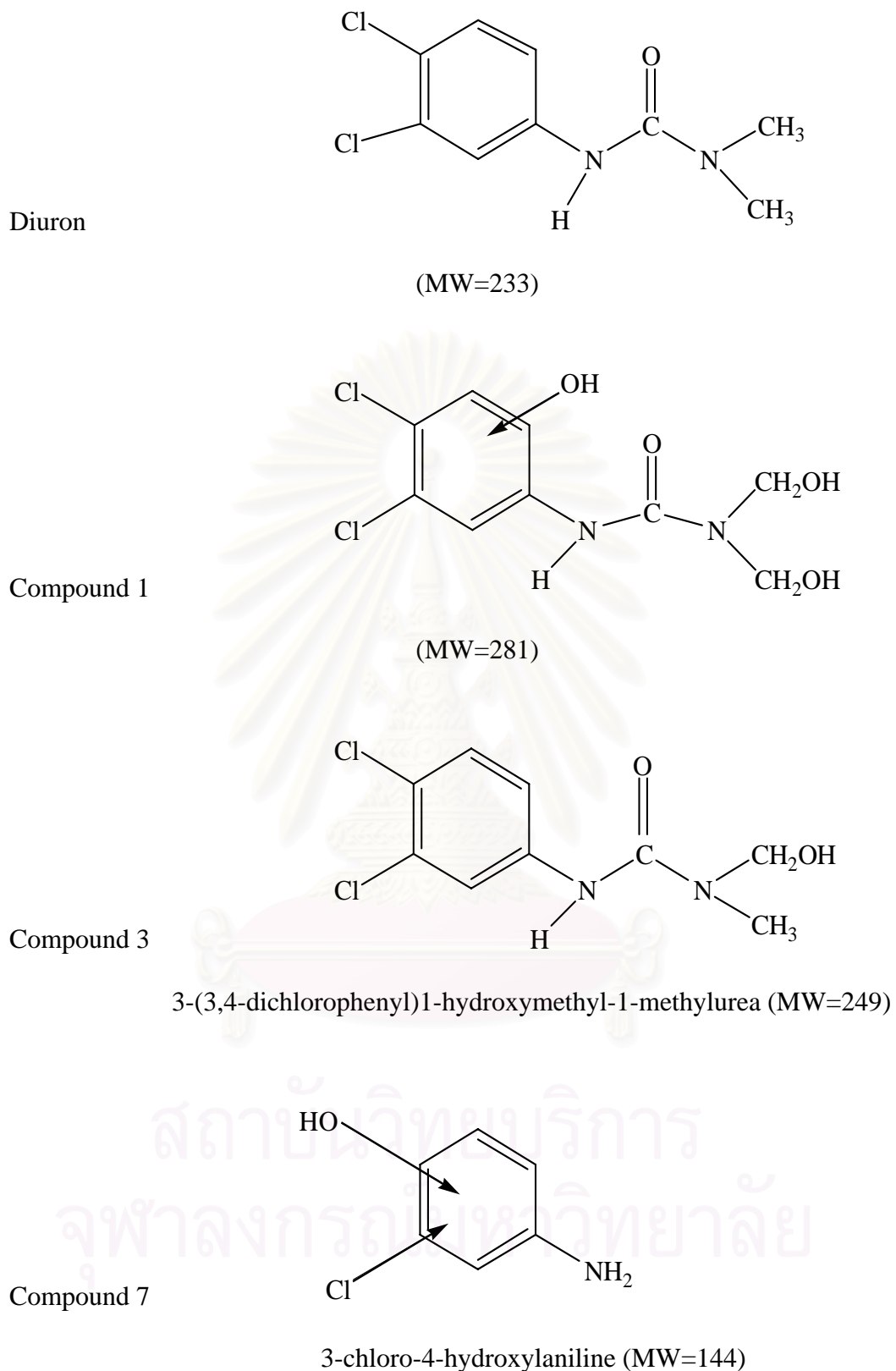
Figure 4.29 The chemical structure of intermediates generated from photodegradation of diuron.

4.3.2 Degradation of isoproturon

Isoproturon is a phenylurea herbicide consisting of an aromatic ring with an alkyl chain and one uretic group. The molecular structure of isoproturon allows OH radical attack at different sites, following by several chain reactions. The first hydroxylation can occur at the aromatic ring, at the alkyl groups and at the secondary nitrogen of the uretic group, leading to monohydroxylated products. Subsequent hydroxylation at the remaining sites results in di-hydroxylated and tri-hydroxylated products (Gora 2006). Figure 4.30 shows intermediates generated during photocatalytic treatment of isoproturon. Intermediate products formed by the photocatalytic degradation were then identified by GC-MS analysis. The GC-MS analysis confirmed the formation of several intermediates, as shown in Table 4.11. It should be noted that isoproturon has molecular structure that is more reactive than diuron, due to the presence of the $CH(CH_3)_2$ group, instead of halogen substituents, as previously discussed. Therefore several substances have already appeared in the solution before the degradation proceeds at irradiation time of 0 min. HPLC analysis gave eight intermediated fractions as shown in Figure 4.30 (a)-(d). Intermediates generated in the process are high in concentration and fluctuated with irradiation time.
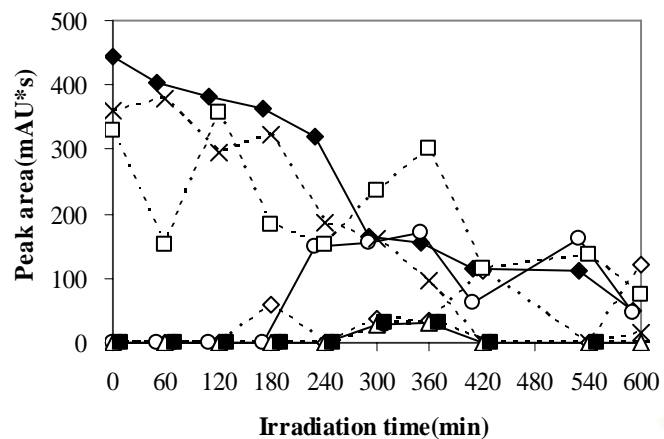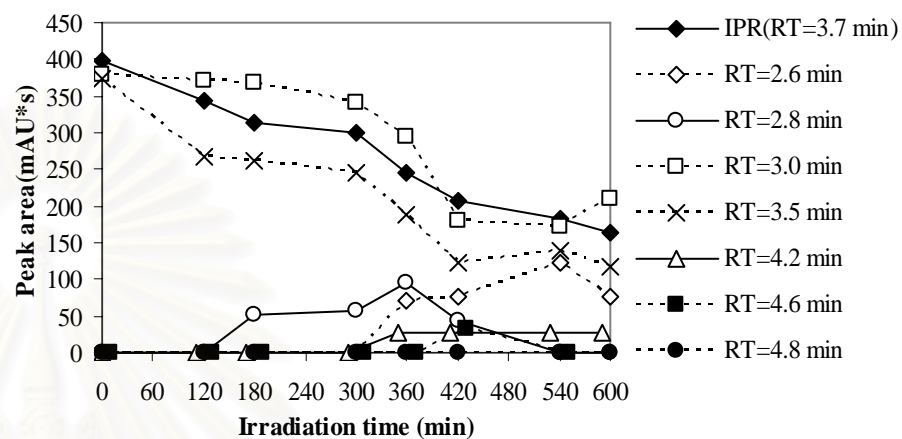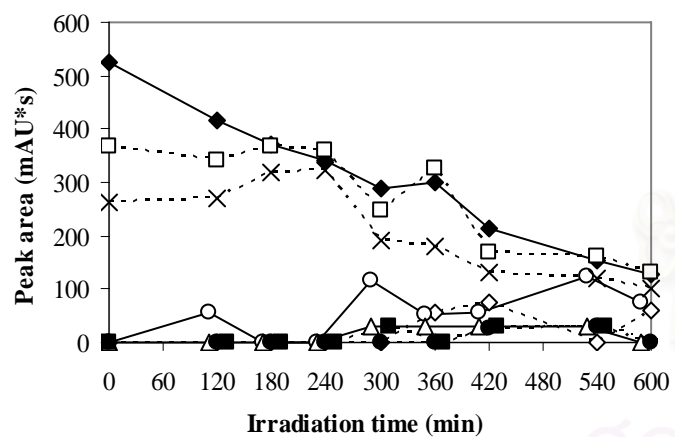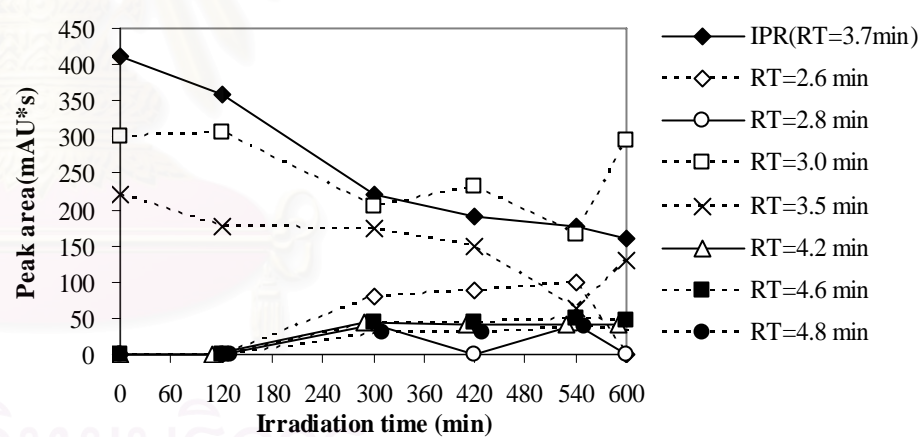
Figure 4.30 Intermediates generated during photocatalytic treatment of isoproturon (IPR), using titania synthesized at 300°C and calcined at 500°C, where the synthesis medium is: (a) 1,4-butanediol, (b) toluene, (c) mineral oil, (d) Reference titania JRC-TIO1.

The difference in catalytic activity of each titania are also observed. Figure 4.30 shows that titania synthesized in 1,4-butanediol (Figure 4.30(a)) give high concentration of intermediates within a short time period of experiment, while titania synthesized in toluene, mineral oil and reference titania (Figure 4.30(b)-(d)) results in lower concentration of intermediates. This result confirms that photocatalytic activity of titania synthesized in 1,4-butanediol is higher than titania synthesized in toluene and mineral oil as well as reference titania.

The HPLC intermediates fractions from photodegradation of isoproturon were identified by using GC-MS characterization. Table 4.11 shows eight products represented to all compounds appeared in GC-MS for each HPLC fraction, which identified based on the molecular ion and mass spectrometric fragmentation peaks. The results indicated the followings. Compound 1 has molecular weight of 135 and it is suggested to have chemical formula of $C_9H_{13}N$. This compound is formed by hydroxylation at the aromatic ring and cleavage of N-C bond in the uretic group. Compound 2 has molecular weight of 133. This compound was unidentifiable. The unidentifiable compound 3 and compound 4 both have molecular weight of 116, although they were presented in different HPLC fraction. The result indicated that these compounds may be degraded fracments generated by thermal decomposition GC-MS column. Compound 5 is molecular weight of 206 which is indicated as isoproturon. Compound 6 has molecular weight of 151 and it is suggested to be $C_9H_{13}NO$. It was formed in similar manner as compound 8. Compound 7 has molecular weight of 133, similar to compound 2. Thermal decomposition behavior in GC-MS column is also expected for this result. The chemical structures of all identified intermediates of isoproturon decomposition are sketched in Figure 4.30.

Table 4.11 Molecular ion (m/z), molecular weight (MW), and chemical formula of intermediates generated from photodegradation of isoproturon.

Compound	m/z	MW	Chemical substance identified
1	55, 77, 89, 105, 115, 119, 121, 134, 135	135	$C_9H_{13}N$
2	59, 133, 135, 151	133	unidentifiable
3	59, 83, 98, 101	116	unidentifiable
4	59, 83, 98, 101	116	unidentifiable
5	55, 101, 207	206	$C_{12}H_{18}N_2O$ (isoproturon)
6	59, 88, 133, 150, 151	151	$C_9H_{13}NO$
7	59, 133, 135, 151	133	unidentifiable
8	58, 59, 98, 101, 133, 135,151	151	$C_9H_{13}NO$

Isoproturon

(MW=206)

Compound 1

(MW=135)

Compound 6 or 8

(MW=151)
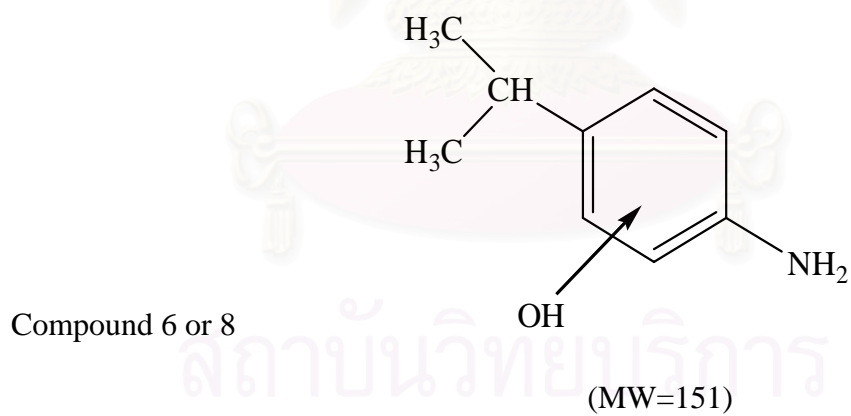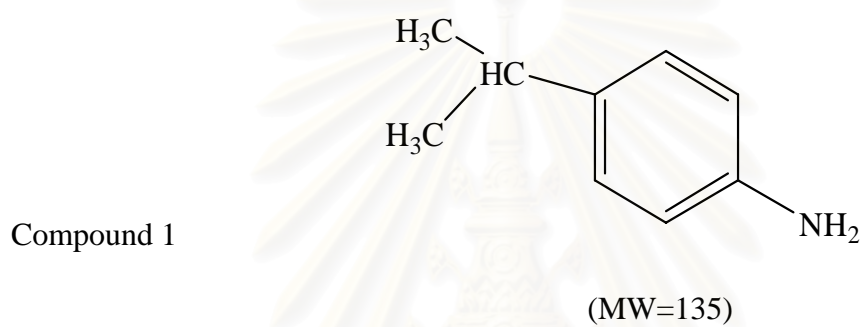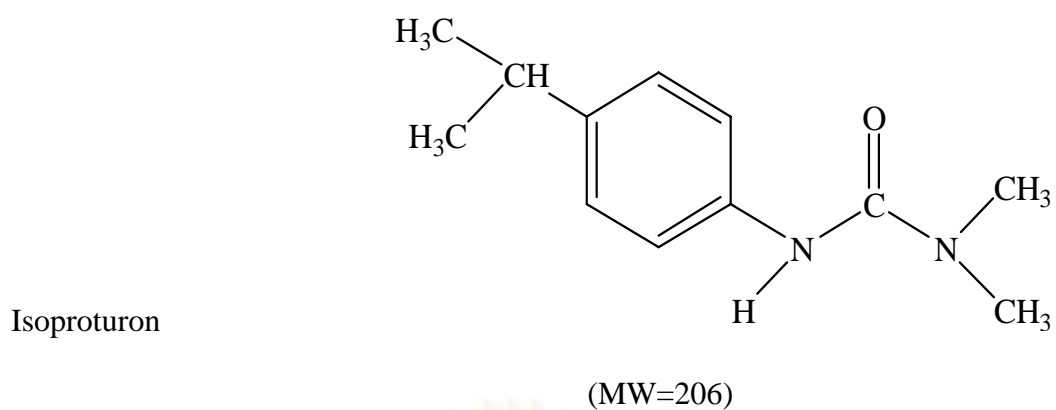
Figure 4.31 The chemical structure of intermediates generated from photodegradation of isoproturon.

4.3.3 Degradation of linuron

Linuron consists of an aromatic ring attaching to two chlorine groups and one uretic group with methoxyl group substituted in urea moiety. Photochemical behavior of linuron involves photohydrolysis as the main transformation pathway. The urea moiety is substituted by methoxyl group and demethoxylation is a competition between N-demethoxylation reaction or oxidation of methyl group (Amine-Khodja 2004). The possible degradation pathway for linuron is proposed in these steps (Katsumata 2005);

(a) The attack on the aromatic ring by OH$^\bullet$ radical without dechlorination or alkyl chain.

(b) A series of oxidation processes that eliminated alkyl groups and chlorine atom.

(c) The oxidative opening of aromatic ring, leading to small organic ion and inorganic species.

It should be noted that linuron has molecular structure that is less reactive. Therefore, the less substances are appeared in the solution before and during the degradation proceeds. It is confirmed that the stability of linuron is higher than diuron and isoproturon. HPLC analysis gives five intermediate fractions as shown in Figure 4.32(a)-(d). Intermediates generated in the process are high concentration and fluctuated with irradiation time.

The differences in catalytic activity of titania synthesized in different organic mediums are also observed. The result is similar to the photodegradation experiment of diuron and isoproturon.
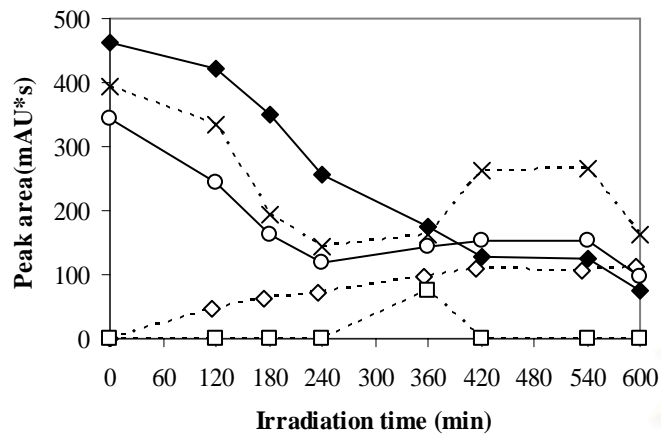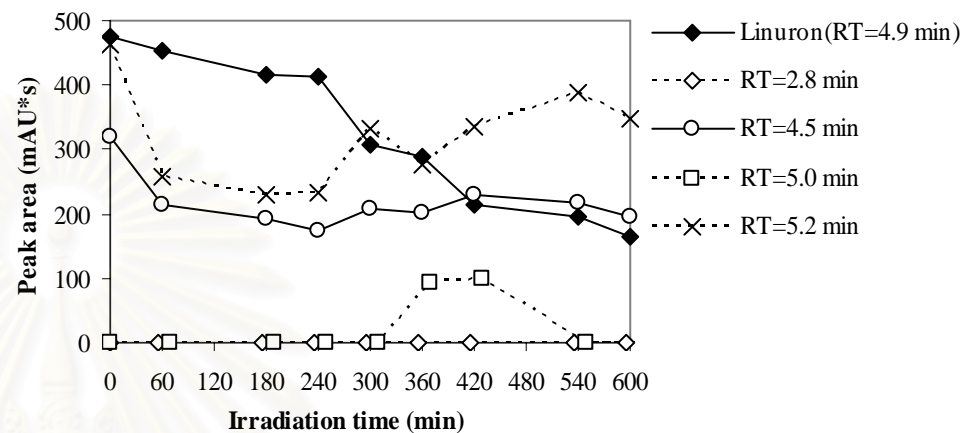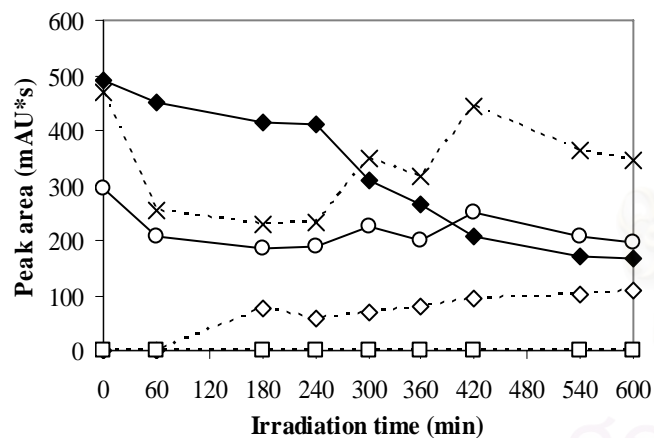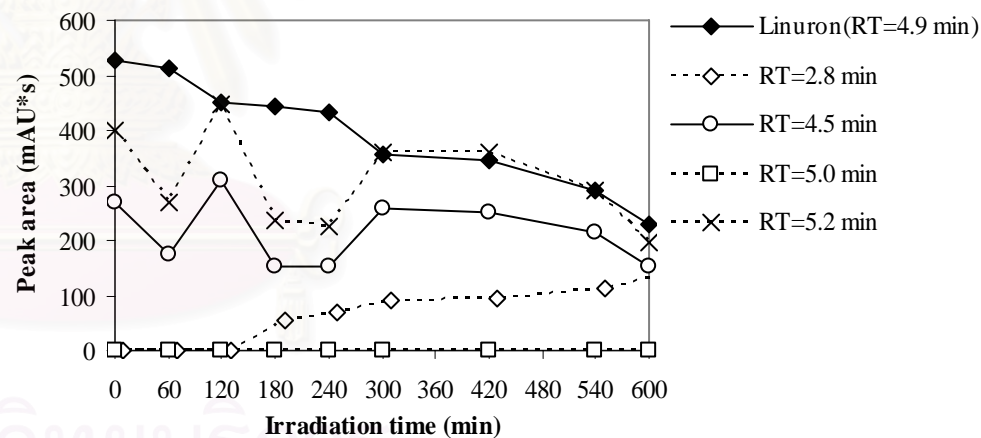
Figure 4.32 Intermediates generated during photocatalytic treatment of linuron, using titania synthesized at 300°C and calcined at 500°C, where the synthesis medium is: (a) 1,4-butanediol, (b) toluene, (c) mineral oil, (d) Reference titania JRC-TIO1.

The HPLC fractions from photodegradation of linuron are identified by using GC-MS. The five products were identified based on the molecular ion and mass spectrometric fragmentation peaks, as shown in Table 4.13. However, most of the intermediates were unidentifiable from the current mass spectra database. Only compound 4, which has molecular weight of 206, was identified to have chemical formula of $C_7H_6N_2Cl_2O_2$. It is formed by oxidation of methyl group and N-demethoxylation reaction. It should be noted that linuron itself was not detected from GC-MS analysis. It is suggested that linuron was decomposed by during GC-MS analysis, in the same manner as diuron. Compound 5 of intermediate of linuron has molecular weight of 144. It is suggested to have chemical formula is C_6H_6NCl. It is the result from oxidation of methyl and methoxyl group, dechlorination and hydroxylation of benzene ring. The evaluated chemical structure of intermediate of linuron is sketched in Figure 4.33.

Table 4.12 Molecular ion (m/z), molecular weight (MW), and chemical formula of intermediates generated from photodegradation of linuron

Compound	m/z	MW	Chemical substance identified
1	58, 59, 83, 98, 101	116	unidentifiable
2	68, 105, 133, 135, 151	151	unidentifiable
3	55, 67, 81, 91, 149	224	unidentifiable
4	59, 96, 207	206	$C_7H_5NCl_2O_2$
5	58,59,83,102,207	144	C_6H_6NCl

Linuron

(MW=249)

Compound 4

(MW=206)

Compound 5

(MW=144)
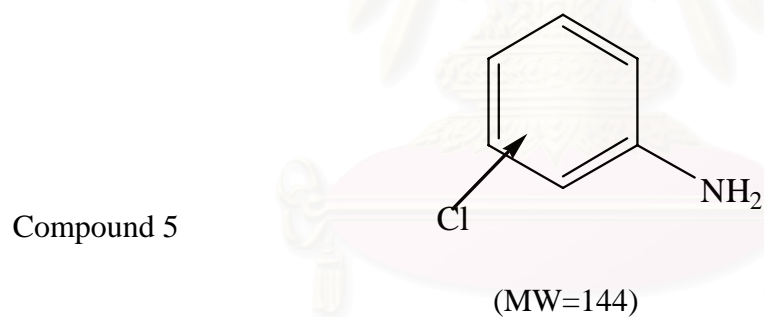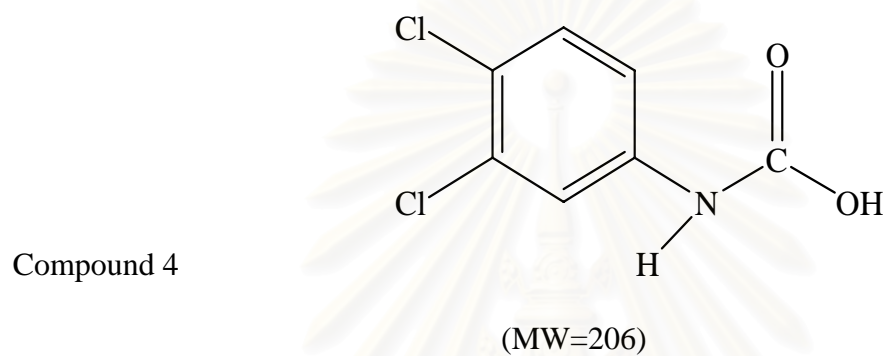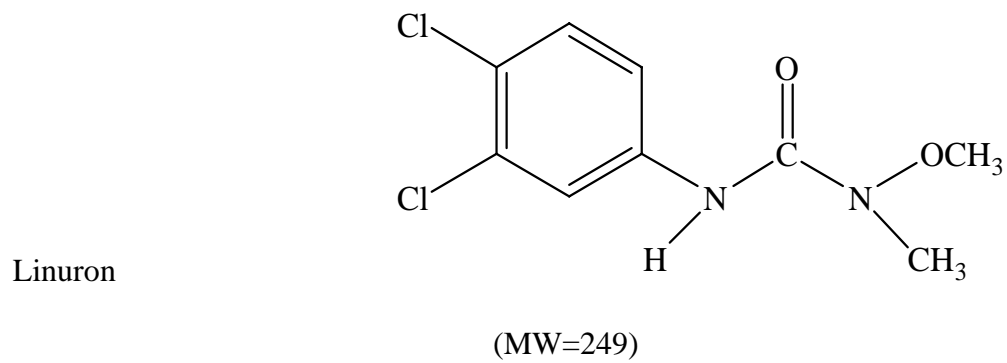
Figure 4.33 The chemical structure of intermediates generated from photodegradation of linuron.

CHAPTER V

CONCLUSIONS AND RECOMMENDATIONS

5.1 Conclusions

The conclusions of the present research are the following:

1. Titania synthesized in 1,4-butanediol has a physical and chemical properties better than titania synthesized in toluene and in mineral oil.

2. Crystallinity of the synthesized titania can be improved by heat treatment, but surface area is decrease with increased calcination temperature.

3. Photodegradation rate of phenylurea herbicide depends upon chemical structure of the herbicide, for the herbicides investigated in this study, in the following order: isoproturon > diuron > linuron.

4. Photodegradation generates several intermediates. The degradation pathway mainly consist of oxidation, demethoxylation, hydroxylation and dechlorination at phenylurea herbicide structure.

5.2 Recommendations for the Future Studies

Recommendations for the future work, based on the results of this work, are the following.

1. Study the effect of dielectric constant of the synthesis medium on physical and chemical properties of the synthesized titania.

2. Investigate the enhancement of efficiency of photocatalytic activity of synthesized titania by modified structure of titania with the second element doping.

3. Study of the effect of calcined time on physical and chemical properties of the synthesized titania.

4. Investigate photodegradation of phenylurea herbicides in solution containing organic solvents.

5. Further identification of the degradation intermediates by using LC-MS analysis, IR spectrometry and NMR analysis.

6. Evaluate total organic compound (TOC) generated during photodegradation process.

7. Study the effect of pH and catalyst concentration on the degradation kinetics of phenylurea herbicides.

8. Investigate long period of irradiation time for photocatalytic degradation of phenylurea herbicide, to achieve 100% conversion.

9. Study the regeneration of used titania.

10. Apply the photocatalytic process in continuous system.

11. Investigate photocatalytic degradation of other types of organic compound using titania synthesized by method proposed in this work.

REFERENCES

Amine-Khodja, A., Boulkamh, A. and Boule, P. (2004). "Photochemical Behavior of Phenylurea Herbicides." Photochemical & Photobiological Sciences 3: 145 - 156.

Anpo, M., Shima, T., Kodama, S. and Kubokawa, Y. (1987). "Photocatalytic Hydrogenation of CH_3CCH with H_2O on Small-Particle TiO_2: Size Quantization Effects and Reaction Intermediates." Journal of Physical Chemistry 91: 4305-4310.

Awati, P., Awate, S., Shah, P. and Ramaswamy, S. (2003). "Synthesis of Nanocrystalline Titania Using Ultrasonication Technique and its Photocatalytic Activity for the Decomposition of Monochlorobenzene." Catalysis Communication 4: 393.

Bibby, D. C., Mehrotra, R.C. and Gaur, D.P. (1978). Metal Oxide. London, Academy Press.

Blake, D. M. (1999). Bibliography of Work on the Heterogeneous Photocatalytic Removal of Hazardous Compounds from Water and Air. Department of Energy Laboratory, Midwest Research Institute: 1-167.

Bouquet-Somrani, C., Fajula, F., Finiels, A., Graffin, P., Geneste, P. and Olive, J. (2000). "Photocatalytic Degradative Oxidation of Diuron in Organic and Semi-Aqueous Systems over Titanium Dioxide Catalyst." New Journal of Chemistry 24: 999-1002.

Cawse, J. N. (1980). Kirk-Othmer Encyclopedia of Chemical Technology. New York, NY.

Clipper Control Inc. (2006). Dielectric Constant Reference Guide. http://www.clippercontrols.com/info/dielectric_constants.html.

Coulter, K.E . and Sault, A.G. (1995). "Effects of Activation on the Surface-Properties of Silica-Supported Cobalt Catalysts." Journal of Catalysis 154: 56-64.

Cruickshack, M. and Dale, M.P. (1985). "Synthesis of Silica-Sodalite form Non-aqueous Synthesis." Nature (London) **317**: 157-158.

Depero, L. E., Bonzi, P. and Zocchi, M (1993). "Study of the anatase-rutile transformation in TiO2 powders obtained by laser-induced synthesis." Journal of MATERIALS RESEARCH **Vol. 8**(10): 2709.

d'Hennezel, O. and Ollis, D. F. (1997). "Trichloroethylene-promoted Photocatalytic Oxidation of Air Contaminants." Journal of Catalysis 167(1): 118-126.

Farre, M., Franch, M.I., Malato, S., Ayllon, J.A., Peral, J.P. and Domenech, X. (2005). "Degradation of Some Biorecalcitrant Pesticides by Homogeneous and Heterogeneous Photocatalytic Ozonation " Chemosphere 58(8): 1127-1133.

Fox, M.A. and Dulay M.T (1993). "Heterogeneous Photocatalysis." Chemical Reviews 93: 341-57.

Gopidas, K. R. and Bohorquez, M. (1990). "Photophysical and Photochemical Aspects of Coupled Semiconductors: Charge-Transfer Processes in Colloidal $CdS-TiO_2$ and CdS-AgI Systems." Journal of Physical Chemistry 94: 6435-6440.

Gora, A., Toepfer, B,. Puddu, Valeria, A. and Puma, G.L (2006). "Photocatalytic Oxidation of Herbicides in Single-Component and Multicomponent Systems: Reaction Kinetics Analysis." Applied Catalysis B: Environmental 65: 1-10.

Graham, T. W. (1996). Organic Chemistry. New York, John Wiley&Sons.Inc.

Hance, R. J. (1965). "Weed Research" 5: 98.

Haque, M.M and Muneer, M. (2003). "Heterogeneous Photocatalysed Deradation of Herbicide Derivative, Isoproturon in Aqueous Suspension of Titanium Dioxide." Journal of Environmental Management 69: 169-176.

Herrmann, J.-M. (1999). "Heterogeneous Photocatalysis : Fundamentals and Applications to the Removal of Various Type of Aqueous Pollutants." Catalysis Today 53: 115-129.

Hincapie, M., Maldonado, M.I., Oller, I., Gernjak, W., Sanchez-Perez, J.A., Ballesteros, M.M. and Malato, S. (2005). "Solar Photocatalytic Degradation and Detoxification of EU Priority Substances." Catalysis Today 101: 203-210.

Hoffmann, M. R., Martin, S.T., Choi, W.Y. and Bahnemann, D.W. (1995). "Environmental Applications of Semiconductor Photocatalysis." Chemical Reviews **95**: 69-96.

Houas, A., Lachheb, H., Ksibi, M., Elaloui, E.,Guillard,G. and Herrmann, J. (2001). "Photocatalytic Degradation Pathway of Methylene Blue in Water " Applied Catalysis B ; Environmental 31: 145-157.

Inagaki, M., Imai, T., Yoshikawa, T. and Tryba, B. (2004). "Photocatalytic Activity of Anatase Powders for Oxidation of Methylene Blue in Water and Diluted NO Gas." Applied Catalysis B:Environment: 247-254.

Inoue, M., . Kominami, H and Inui, T. (1991). "Reaction of Aluminium Alkoxideswith Various Glycols and the Layer Structure of Their Product." Journal of The Chemical Society - Dalton Transactions: 3331-3336.

Inoue, M., . Kominami, H and Inui, T. (1993). "Novel Synthetic Method for the Catalytic Use of Thermally Stable Zirconia - Thermal Decomposition of

Zirconium Alkoxides in Organic Media." Applied Catalysis A - General 97: L25-L30.

Inoue, M., Kondo, Y. and Inui, T. (1988). "An Ethylene Glycol Derivative of Boehmite." Inorganic Chemistry 27 215-21.

Jung, K. Y. and Park, S.B. (1999). "Anatase-Phase Titania: Preparation by Embedding Silica and Photocatalytic Activity for the Decomposition of Trichloroethylene." Journal of Photochemistry and Photobiology A: Chemistry 127: 117–122.

Katsumata, H., Kaneco, S., Suzuki, T. and Yobiko, Y. (2005). "Degradation of Linuron in Aqueous Solution by the Photo-Fenton Reaction." Chemical Engineering Journal 108: 269-276.

Kominami, H., Kato, J., Murakami, S., Kera, Y., Inoue, M., Inui, T. and Ohtani, B. (1999). "Synthesis of Titanium (IV) Oxide of Ultra-High Photocatalytic Activity: High-Temperature Hydrolysis of Titanium Alkoxides with Water Liberated Homogeneously from Solvent Alcohols." Journal of Molecular Catalysis A-Chemical 144: 165-71.

Kominami, H., Kato, J., Takada, Y., Doushi, Y., Ohtani, B., Nishimoto, S., Inoue, M., Inui, T. and Kera, Y (1997). "Novel Synthesis of Microcrystalline Titanium(IV) Oxide Having High Thermal Stability and Ultra-High Photocatalytic Activity: Thermal Decomposition of Titanium(IV) Alkoxide in Organic Solvents." Catalysis Letters 46: 235-40.

Kongwudthiti, S., Praserthdam, P., Silveston, P. and Inoue, M (2003). "Influence of Synthesis Conditions on the Preparation of Zirconia Powder by the Glycothermal Method." Ceramics International 29: 807-14.

Konstantinou, I. K. and Albanis, T.A. (2003). "Photocatalytic Transformation of Pesticides in Aqueous Titanium Dioxide Suspensions using Artificial and Solar light: Intermediateds and Degradation Pathways." Applied Catalysis B - Environmental 42: 319-335.

Kormann, C., Bahnemann, D.W. and Hoffmann, M.R. (1988). "Photocatalytic Production of Hydrogen Peroxides and Organic Peroxides in Aqueous Suspensions of Titanium Dioxide, Zinc Oxide, and Desert Sand." Environmental Science & Technology 22(7): 798-806.

Lewandowski, M. and D. F. Ollis (2003). "Halide Acid Pretreatments of Photocatalysts for Oxidation of Aromatic Air Contaminants: Rate Enhancement, Rate Inhibition, and a Thermodynamic Rationale." Journal of Catalysis 217(1): 38-46.

Li, Y., Lee, N., Song, J.S., Lee, E.L. and Kim, S. (2004). "Synthesis and Photocatalytic Properties of Nano bi-Crystalline Titania of Anatase and Brookite by Hydrolyzing TiOCl$_2$ Aqueous Solution at Low Temperatures." Research on Chemical Intermediates **31**(4-6): 309-318.

Liska, I., and Slobodnik, J. (1996). "Comparison of Gas and Liquid Chromatography for Analyzing Polar Pesticides in Water Samples." Journal of Chromatrograph. A 733: 235.

Liu, Y.J. and Claus (1997). "Blue Light Emitting Nanosized TiO$_2$ Colloids." Journal of the American Chemical Society 119: 5273-4.

Lopez, M., Fernandez, MI., Rodriguez, S., Santabella, JA., Steenken, S. and Vulliet, E., (2005). "Mechanisms of Direct and TiO$_2$-Photocatalysed UV Degradation of Phenylurea Herbicides." CHEMPHYSCHEM 6(10): 2064-2074.

Luo, Y. and D. F. Ollis (1996). "Heterogeneous Photocatalytic Oxidation of Trichloroethylene and Toluene Mixtures in Air: Kinetic Promotion and Inhibition, Time-Dependent Catalyst Activity." Journal of Catalysis 163(1): 1-11.

Macounova, K., Krysova, H., Luduik. and Jirnousky, J. (2003). "Kinetics of Photocatalytic Degradation of Diuron in Aqueous Colloidal Solutions of Q-TiO_2 Particles." Journal of Photochemistry and Photobiology A Chemistry 156(273-282).

Madani, M. E., Guillard, C., Perol, N., Chovelon, J.M., Azzouzi, M.E., Zrineh, A. and Herrmann, J.M. (2006). "Photocatalytic Degradation of Diuron in Aqueous Solution in Presence of Two Industrial Titania Catalysts, Either as Suspended Powders or Deposited on Flexible Industrial Photoresistant Papers." Applied Catalysis B: Environmental 65: 70-76.

Malato, S., Caceres, J., Fernandez-Alba, A.R.,Piedra, L., Hernando, M.D., Aguera, A. and Vial, J. (2003). "Photocatalytic Treatment of Diuron by Solar Photocatalysis: Evaluation of Main Intermediates and Toxicity." Environmental Science & Technology 37(11): 2516-2524.

Mekasuwandumrong, O., Silveston, P.L., Praserthdam, P., Inoue, M., Pavarajarn, V. and Tanakulrungsank, W (2003). "Synthesis of Thermally Stable Micro Spherical Chi-Alumina by Thermal Decomposition of Aluminum Isopropoxide in Mineral Oil." Inorganic Chemistry Communications 6: 930-4.

Nam, H.-D., Lee, B.-H., Kim, S.-J., Jung, Ch.-H., Lee, J.-H. and Park, S. (1998). "Preparation of Ultrafine Crystalline TiO_2 Powders from Aqueous $TiCl_4$ Solution by Precipitation." Japanese Journal of Applied Physics Part 1 37: 4603-4608.

Nimlos, M.R., Jacoby, W.A., Blake, D.M. and Milne, T.A. (1993). "Direct Mass Spectrometric Studies of the Destruction of Hazardous Wastes. 2 Gas-Phase Photocatalytic Oxidation of Trichloroethylene over TiO_2: Products and Mechanisms." Environmental Science & Technology 27(4): 732-740.

Nishimoto, S., Ohtani, B., Kajiwara, H. and Kagiya, T. (1985). "Correlation of the Crystal Structure of Titanium Dioxide Prepared from Titanium Tetra-2-Propoxide with the Photocatalytic Activity for Redox Reactions in Aqueous Propan-2-ol and Silver Salt Solutions." Journal of the Chemical Society - Faraday Transactions 1 81: 61-8.

O'Regan, B. and Gratzel, M (1991). "A Low-Cost, High-Efficiency Solar Cell Based on Dye-Sensitized Colloidal TiO_2 Films." Nature 353(737).

Ohtani, B. and Nishimoto, S (1993). "Effect of Surface Adsorptions of Aliphatic-Alcohols and Silver Ion on the Photocatalytic Activity of TiO2 Suspended in Aqueous-Solutions." Journal of Physical Chemistry 97: 920-926.

Ohtani, B., Ogawa, Y. and Nishimoto, S. (1997). "Photocatalytic Activity of Amorphous-Anatase Mixture of Titanium(IV) Oxide Particles Suspended in Aqueous Solutions." Journal of Physical Chemistry B 101(19): 3746-3752.

Park, H. K., Kim, D. K. and Kim, C. H. (1997). "Effect of Solvent on Titania Particle Formation and Morphology in Thermal Hydrolysis of $TiCl_4$." Journal of the American Ceramic Society 80(3): 743-749.

Parra, S., Olivero, J. and Pulgarin, C. (2002). "Relationships between Physicochemical Properties and Photoreactivity of Four Biorecalcitrant Phenylurea Herbicides in aqueous TiO_2 suspension." Applied Catalysis B : Environmental 36: 75-85.

Payakgul, W. (2002). Crystallization and Precipitation Mechanism of Titanium (IV) Oxide under the Solvothermal Condition and the Effect of Second Element on Titanium (IV) Oxide Products Master degree in chemical engneering. Bangkok, Chulalongkorn University: 145.

Payakgul, W., Mekasuwandumrong, O., Pavarajarn, V. and Praserthdam, P (2005). "Effects of Reaction Medium on the Synthesis of TiO_2 Nanocrystals by Thermal Decomposition of Titanium (IV) n-Butoxide." Ceramics International 31: 391–397.

Pena, F., Cardenas, S. and Gallego, M (2002). "Analysis of Phenylurea Herbicides from Plant by GC/MS." Talanta 56: 727-734.

Popielarski, S. (1998). Photocatalysis on Nano-Sized Semiconductors. www.rpi.edu/dept/materials/COURSE/NANO/popielarski.html

Royal Society of Chemistry (1991). The Agrochemicals Handbook. Cambridge.

Sanchez-Martin, M. J., Delgado-Pasual, R., Iglesias-Jimenez, E.I. and Chamazano, M.S. (1996). "Determination of Linuron in Aqueous Soil Extract by High Performance Liquid Chromatography." Journal of Chromatography A 754(295-299).

Sato, T., Yamamoto, Y., Fujishiro, Y. and Uchida, S. (1996). "Intercalation of Iron Oxide in Layered $H_2Ti_4O_9$ and $H_4Nb_6O_{17}$: Visible-Light Induced Photocatalytic Properties." Journal of the Chemical Society-Faraday Transactions 92: 5089-92.

Simon, D., Helliwell, S. and Chistians, N. (1998). "Analytical Chemistry of Choropyrifos and Diuron in Aquatic Ecosystem." Analytica. Chimica. Acta 360: 1.

Tanaka, K., Hisanaga T. and Rivera, D. F. and H. Al-Ekabi (1993). "Photocatalytic Purification and Treatment of Water and Air." Elsevier A.P., Amsterdam: 169.

Tomlin, C. (1994). The Pesticide Manual, The Bath Press.

Tomlin, C. (2000). The Pesticide Manual, British Crop Protection Council.

Tonejc, A. M., Goti, M., Grzeta, B., Music S., Popovi, S., Trojko, R., Turkovi, A. and MuSevic, I. (1996). "Transmission Electron Microscopy Studies of Nanophase TiO_2." Materials Science and Engineering B-Solid State Materials for Advanced Technology 40: 177-84.

Traversa, E., Gnappi, G., Montenero, A.and Gusmano, G. (1996). "Ceramic Thin Films by Sol-Gel Processing as Novel Materials for Integrated Humidity Sensors." Sensors and Actuators B-Chemical 31: 59-70.

Tsai, S. J., Cheng, S. (1997). "Effect of TiO_2 Crystalline Structure in Photocatalytic Degradation of Phenolic Contaminants." Catalysis Today 33: 227-237.

Uchida, S., Yamamoto, Y., Fujishiro, Y., Watanabe, A., Ito, O. and Sato, T. (1997). "Intercalation of Titanium Oxide in Layered $H_2Ti_4O_9$ and $H_4Nb_6O_{17}$ and Photocatalytic Water Cleavage with $H_2Ti_4O_9/(TiO_2, Pt)$ and $H_4Nb_6O_{17}/(TiO_2, Pt)$ Nanocomposites." Journal of the Chemical Society-Faraday Transactions 93: 3229-34.

Wakanabe, T., Kitamura, A., Kojima, E., Nakayama, C., Hashimoto, K. and Fujishima, A. (1993). Photocatalytic Purification and Treatment of Water and Air, Elsevier, Amsterdam.

Watson, S. S., Beydoun, D., Scott.J.A. and Amal, R. (2003). "The Effect of Preparation Method on the Photoactivity of Crystalline Titanium Dioxide Particles." Chemical Engineering Journal 95: 213-220.

World Health Organization (1996). Guidelines for Drinking-Water Quality. Geneva, Health criteria and other supporting information

Worthing (1991). The Pesticide Manual, Farnham, British Crop Protection Council.

Xu, N. P., . Shi, Z.F., Fan, Y.Q., Dong, J.H., Shi, J. and Hu, M.Z.C. (1999). "Effects of Particle Size of TiO_2 on Photocatalytic Degradation of Methylene Blue in Aqueous Suspensions." Industrial & Engineering Chemistry Research 38: 373-9.

Yin, S., Inoue, Y., Uchida, S., Fujishiro, Y. and Sato, T. (1998). "Crystallization of Titania in Liquid Media and Photochemical Properties of Crystallized Titania." Journal of Materials Research 13(4): 844-847.

Zeman, P. and Takabayashi, S. (2003). "Nano-Scaled Photocatalytic TiO_2 Thin Film Prepared by Magnetron Sputtering." Thin Solid Films 433: 57-62.

APPENDICES

APPENDIX A

CALCULATION OF THE CRYSTALLITE SIZE

Calculation of the crystallite sized by Debye-Scherrer equation

The crystallite size was calculated from the half-height width of the diffraction peak of XRD patter using the Debye-Scherrer equation.

From Scherrer equation:

$$D = \frac{K\lambda}{\beta \cos\theta} \qquad (B.1)$$

Where   D   =   Crystallite size, $\overset{o}{A}$

K   =   Crystallite-shape factor = 0.9

λ =   X-ray wavelength, 1.5418 $\overset{o}{A}$ for CuKα

The X-ray diffraction broadening (β) is the pure width of a power diffraction free of all broadening due to the experiment equipment. Standard α-alimina is used to observe the instrumental broadening since its crystallite size is larger than $200\,\overset{o}{A}$.

The X-ray diffraction broadening (β) can be obtained by Warren's formula.

From Warren's formula:

$$\beta^2 = B_M^2 - B_S^2$$

$$\beta = \sqrt{B_M^2 - B_S^2}$$

Where B_M = The measured peak width in radians at half peak height.

B_S = The corresponding width of standard material.

Example: calculation of the crystallite sized of titania

The half-height width of 101 diffraction peak   =   0.93125°

=   0.01625 radian

The corresponding half-height width of peak of α- alumina = 0.004 radian

The pure width   = $\sqrt{B_M^2 - B_S^2}$

= $\sqrt{0.01625^2 - 0.004^2}$

=   0.01577 radian

B   =   0.01577 radian

2θ   =   25.30°

θ   =   12.65°

λ   =   1.5418 Å

The crystallite size   = $\dfrac{0.9 \times 1.5418}{0.01577 \cos 12.65}$ =   90.18 Å

=   9 nm
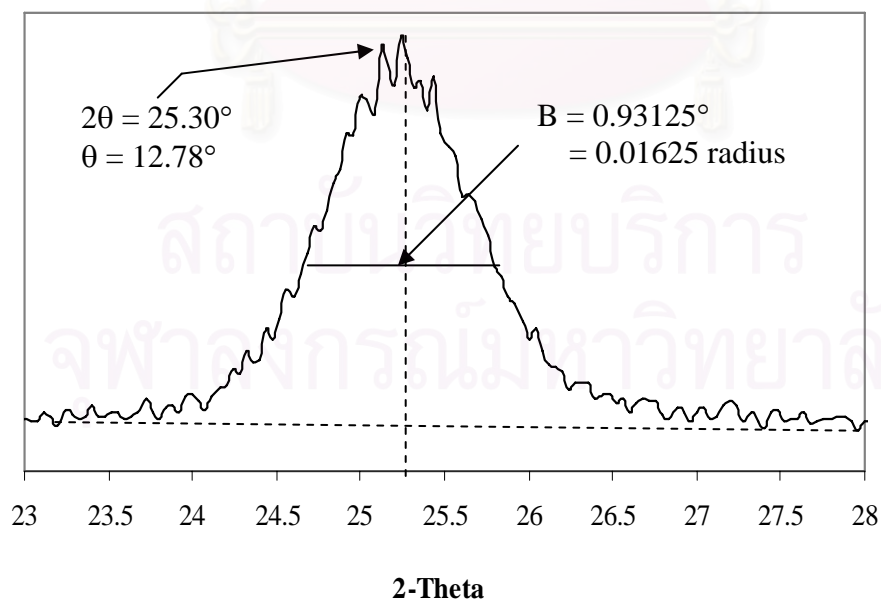
Figure B.1 the 101 diffraction peak of titania for calculation of the crystallite size.

APPENDIX B

APPEARANCE OF PHENYLUREA HERBICIDES IN 3-D VIEWS

1. Diuron

Figure B.1 Evaluation of intermediates generated during photocatalytic treatment of diuron by titania synthesized in 1,4-BG, in HPLC-retention time scale.

Figure B.2 Evaluation of intermediates generated during photocatalytic treatment of diuron by titania synthesized in toluene, in HPLC-retention time scale.

Figure B.3 Evaluation of intermediates generated during photocatalytic treatment of diuron by titania synthesized in mineral oil, in HPLC-retention time scale.

Figure B.4 Evaluation of intermediates generated during photocatalytic treatment of diuron by reference titania, HPLC-retention time scale.

Figure B.4 Evaluation of intermediates generated during photocatalytic treatment of diuron by reference titania, HPLC-retention time scale.

Figure B.5 Evaluation of intermediates generated during photocatalytic treatment of diuron in no titania used, HPLC-retention time scale.

Figure B.6 Intermediates generated during photocatalytic treatment of diuron, no catalyst use.

2. Isoproturon
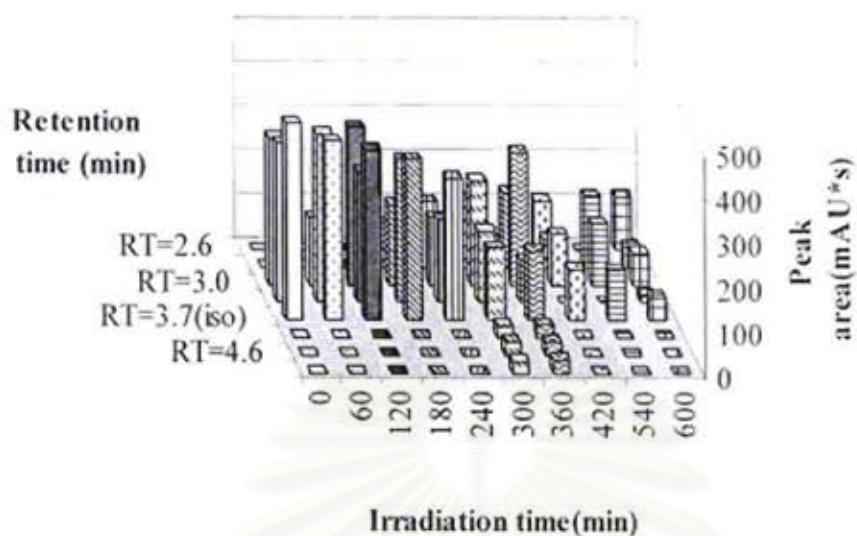
Figure B.7 Evaluation of intermediates generated during photocatalytic treatment of isoproturon by titania synthesized in 1,4-BG, in HPLC-retention time scale.
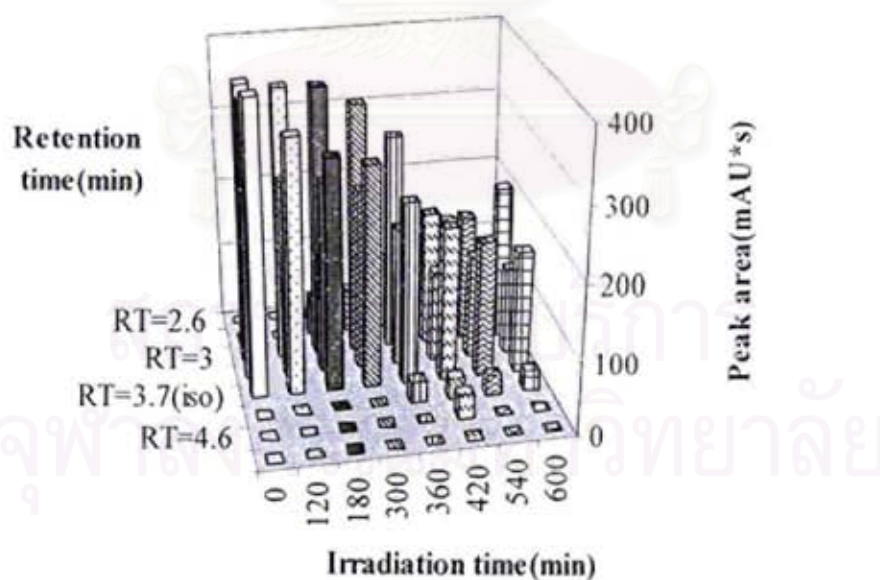
Figure B.8 Evaluation of intermediates generated during photocatalytic treatment of isoproturon by titania synthesized in toluene, in HPLC-retention time scale.
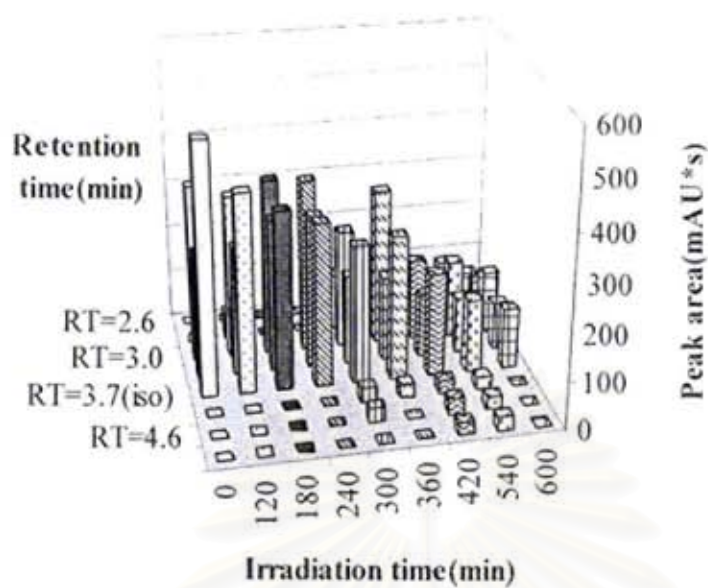
Figure B.9 Evaluation of intermediates generated during photocatalytic treatment of isoprturon by titania synthesized in mineral oil, in HPLC-retention time scale.
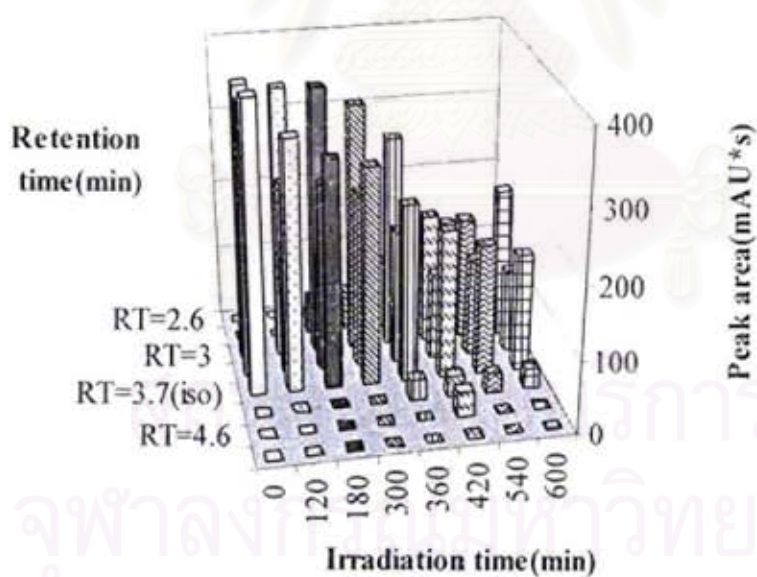
Figure B.10 Evaluation of intermediates generated during photocatalytic treatment of isoproturon by reference titania, in HPLC-retention time scale.
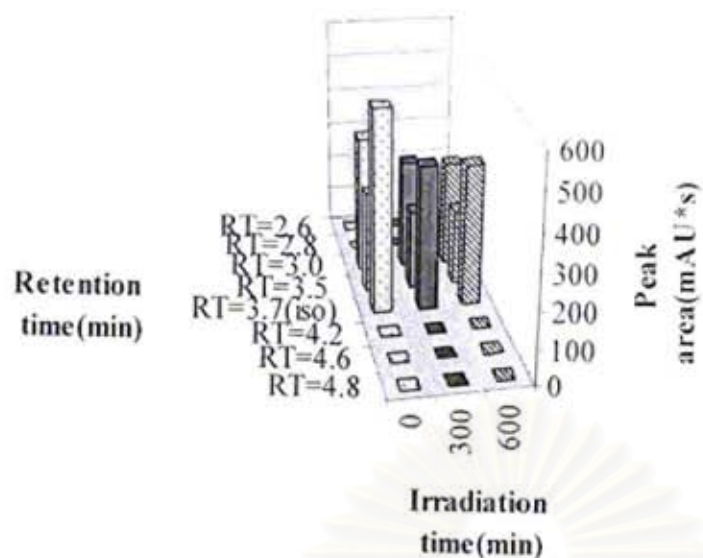
Figure B.11 Evaluation of intermediates generated during photocatalytic treatment of isoproturon in no titania used, HPLC-retention time scale.
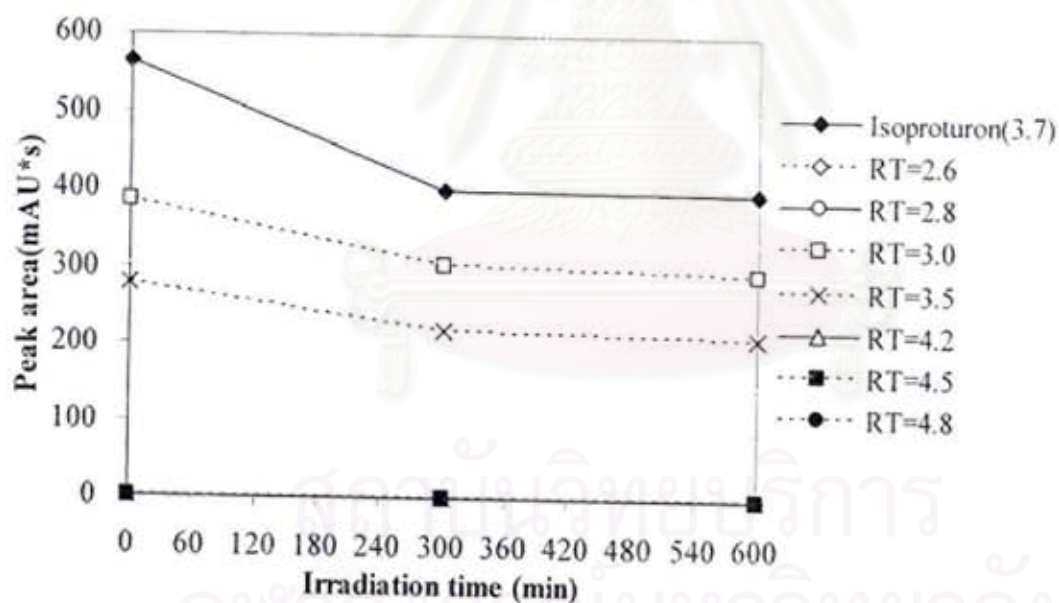
Figure B.12 Intermediates generated during photocatalytic treatment of isoproturon, no catalyst use
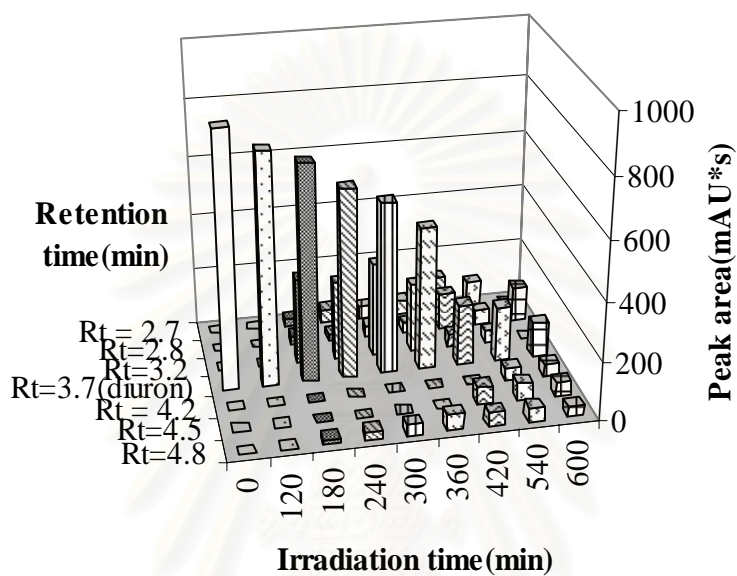
3. Linuron
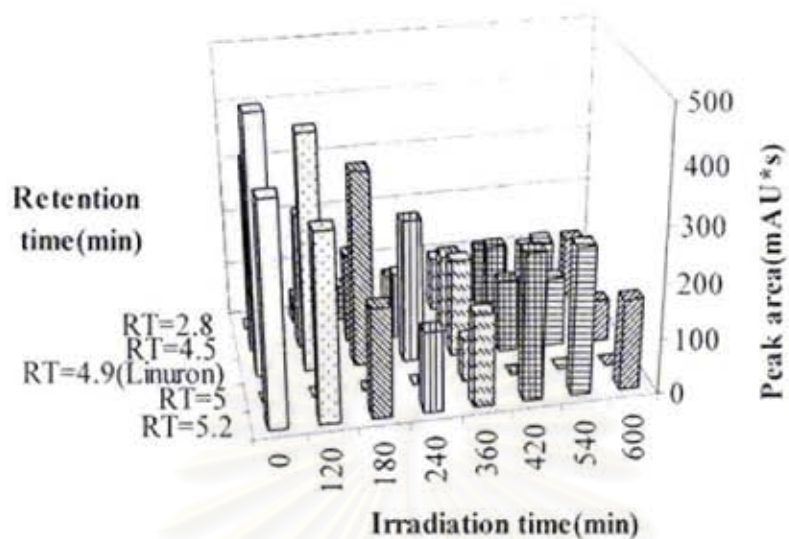
Figure B.13 Evaluation of intermediates generated during photocatalytic treatment of linuron by titania synthesized in 1,4-butanediol, in HPLC-retention time scale.
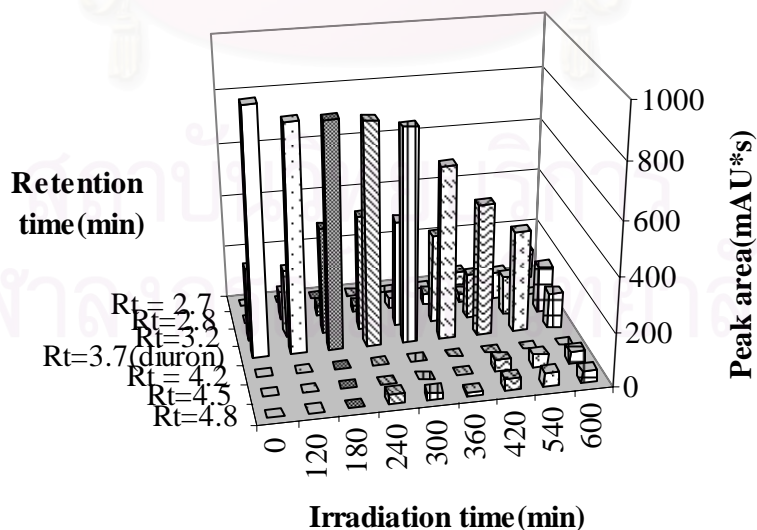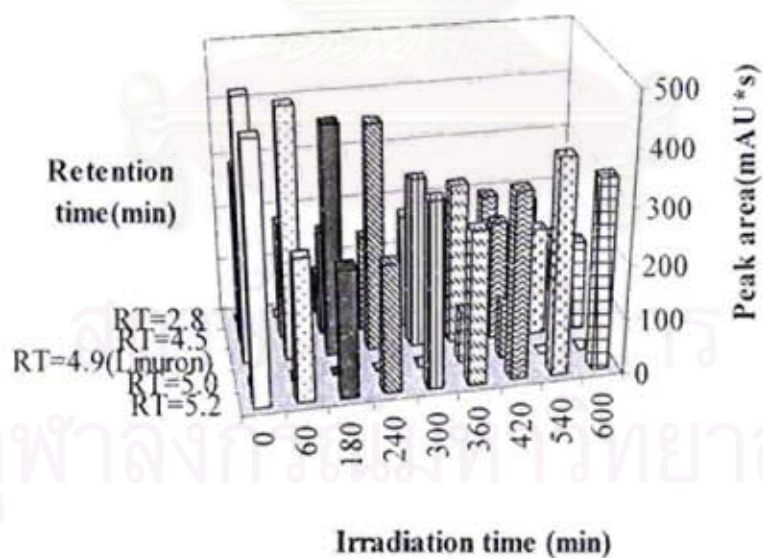

Figure B.14 Evaluation of intermediates generated during photocatalytic treatment of linuron by titania synthesized in toluene, in HPLC-retention time scale.
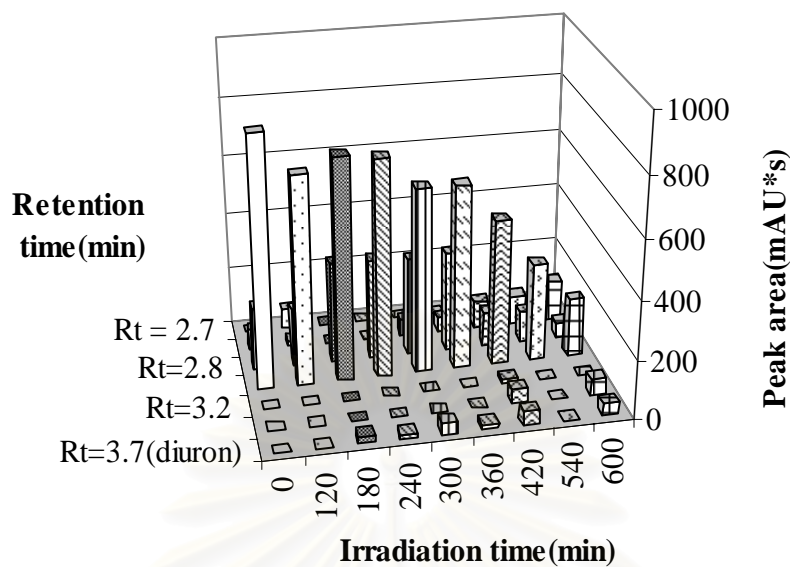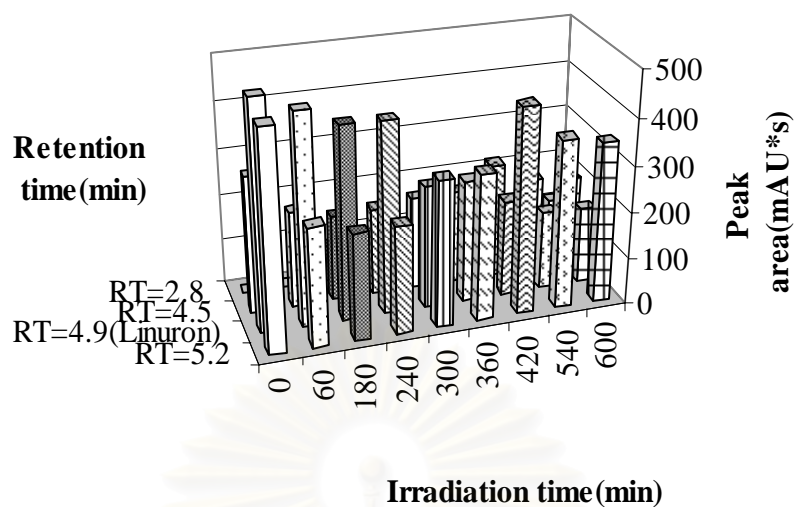
Figure B.15 Evaluation of intermediates generated during photocatalytic treatment of linuron by titania synthesized in mineral oil, in HPLC-retention time scale.
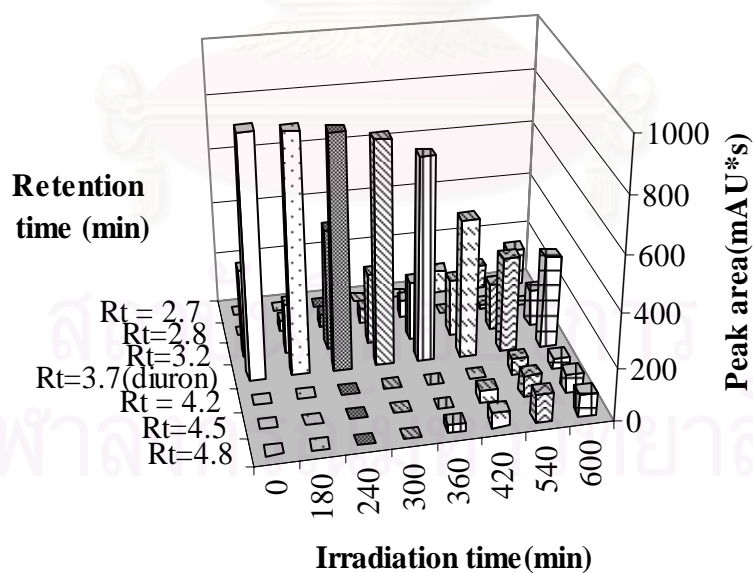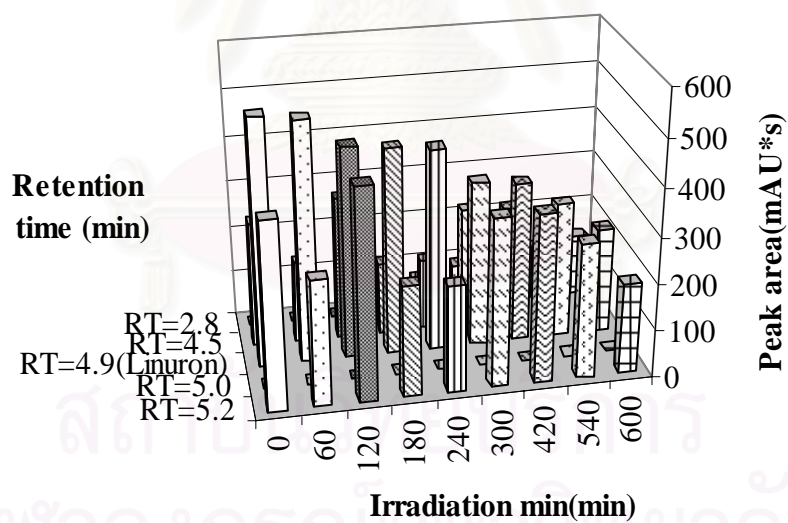

Figure B.16 Evaluation of intermediates generated during photocatalytic treatment of linuron by reference titania, in HPLC-retention time scale.
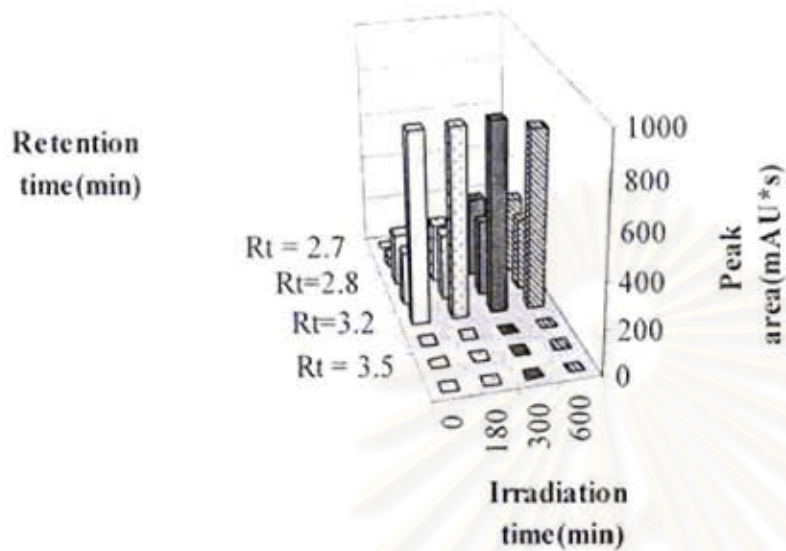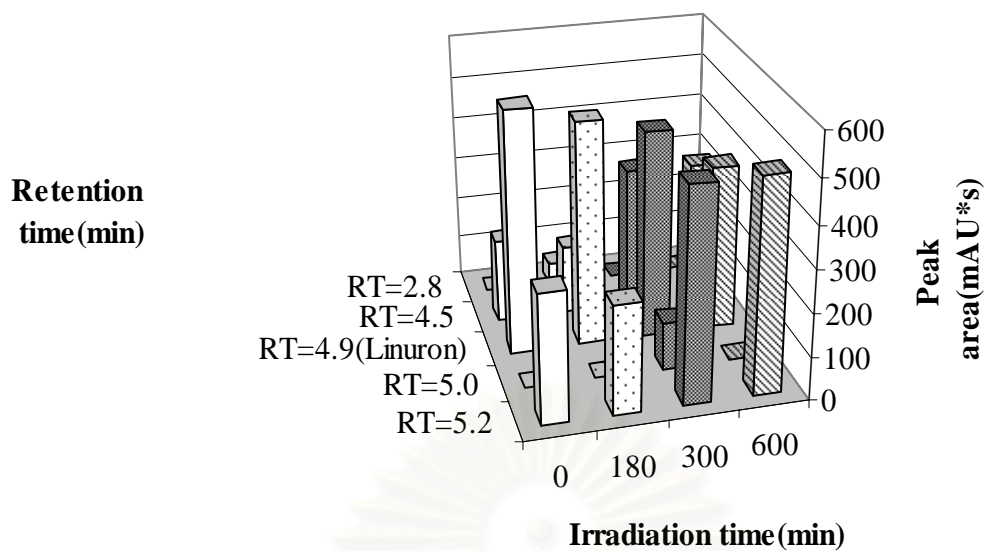
Figure B.17 Evaluation of intermediates generated during photocatalytic treatment of

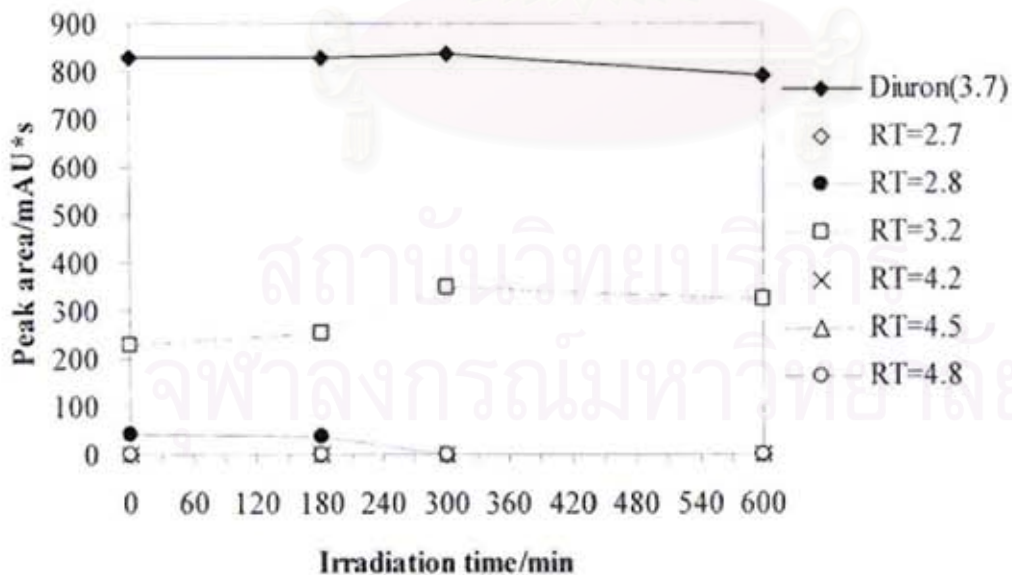linuron in no titania used, HPLC-retention time scale.
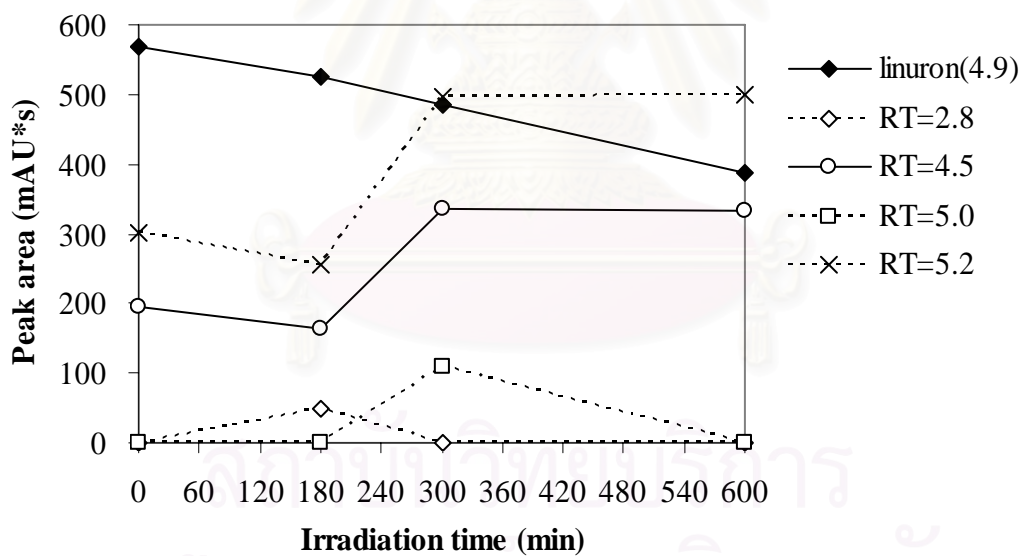
Figure B.18 Intermediates generated during photocatalytic treatment of linuron, no

catalyst use

APPENDIX C

MOLECULAR FRAGMENTATION OF GC/MS

1. Diuron

Figure C.1 Mass Spectra of intermediate generated from diuron for RT of HPLC at

2.7 min, in GC/MS at: (a) RT = 8.026 min, (b) RT = 9.853 min, (c) RT = 11.429 min,

(d) RT = 32.053 min, (e) RT= 50.894 min. The numerical values listed next to the

legend represent height of the GC/MS peaks.

Figure C.2 Mass Spectra of intermediate generated from diuron for RT of HPLC at 2.8 min, in GC/MS at: (a) RT = 7.451 min, (b) RT = 8.202 min, (c) RT = 9.872 min, (d) RT = 11.429 min, (e) RT = 20.925 min, (f) RT = 32.047 min. The numerical values listed next to the legend represent height of the GC/MS peaks.
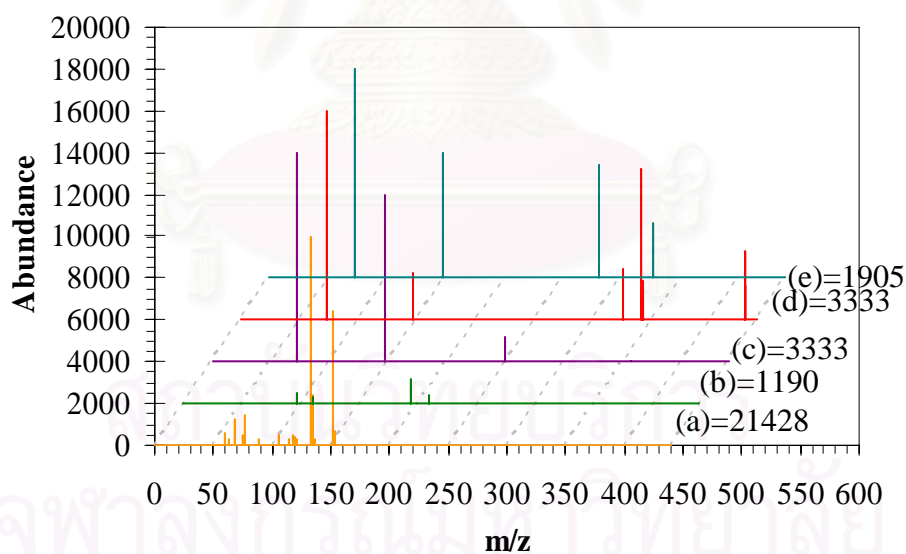
Figure C.3 Mass Spectra of intermediate generated from diuron for RT of HPLC at 3.2 min, in GC/MS at: (a) RT = 8.014 min, (b) RT = 9.872 min, (c) RT = 20.875 min, (d) RT = 32.047 min, (e) RT = 42.568 min. The numerical values listed next to the legend represent height of the GC/MS peaks.

Figure C.4 Mass Spectra of intermediate generated from diuron for RT of HPLC at 3.7 min, in GC/MS at: (a) RT = 8.026 min, (b)RT = 9.784 min, (c) RT = 18.982 min, (d) RT = 30.008 min, (e) RT = 42.556 min, (f) RT = 46.956 min. The numerical values listed next to the legend represent height of the GC/MS peaks.

Figure C.5 Mass Spectra of intermediate generated from diuron for RT of HPLC at 4.2 min, in GC/MS at: (a) RT = 11.404 min, (b) RT = 17.159 min, (c) RT = 20.919 min, (d) RT = 32.034 min, (e) RT = 42.556 min. The numerical values listed next to the legend represent height of the GC/MS peaks.

Figure C.6 Mass Spectra of intermediate generated from diuron for RT of HPLC at

4.5 min, in GC/MS at (a) RT = 5.849 min, (b) RT = 8.220 min, (c) RT = 9.853 min,

(d) RT = 17.309 min, (e) RT = 18.792 min, (f) RT = 20.912, (g) RT = 32.040 min.

The numerical values listed next to the legend represent height of the GC/MS peaks.

Figure C.7 Mass Spectra of intermediate generated from diuron for RT of HPLC at

4.8 min, in GC/MS at (a) RT = 5.524 min, (b) RT = 7.982 min, (c) RT = 11.467 min,

(d) RT = 20.937 min, (e) RT = 32.047 min, (f) RT = 42.568 min. The numerical

values listed next to the legend represent height of the GC/MS peaks.

2. Isoproturon Degradation

Figure C.8 Mass Spectra of intermediate generated from isoproturon for RT of HPLC

at 2.6 min, in GC/MS at: (a) RT = 7.895 min, (b) RT = 10.053 min, (c) RT = 18.717,

(d) RT = 20.900 min, (e) RT = 32.009 min, (f) RT = 51.676 min. The numerical

values listed next to the legend represent height of the GC/MS peaks.

Figure C.9 Mass Spectra of intermediate generated from isoproturon for RT of HPLC

at 2.8 min, in GC/MS at: (a) RT = 7.420 min, (b) RT = 9.709 min, (c) RT = 11.689

min, (d) RT = 20.856 min, (e) RT = 32.015 min, (f) RT = 44.545 min. The numerical

values listed next to the legend represent height of the GC/MS peaks.
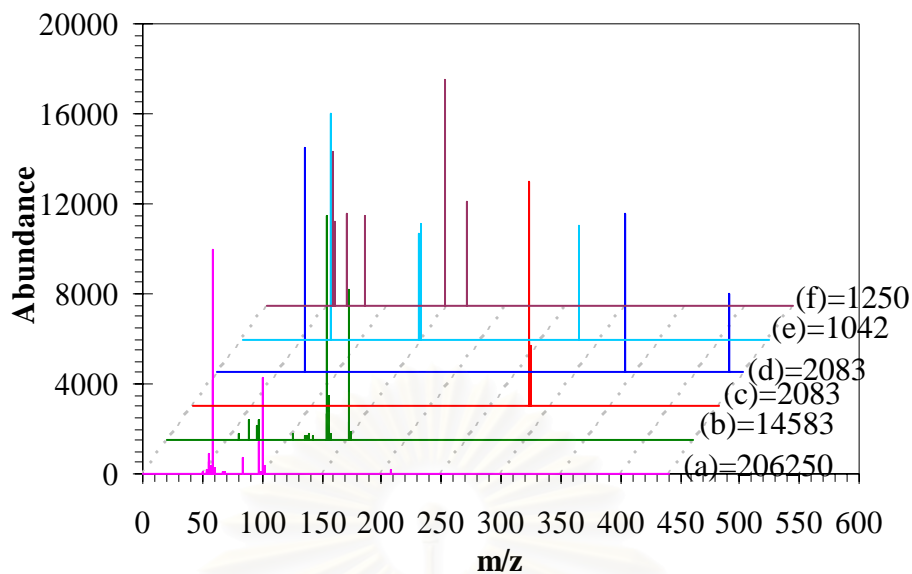
Figure C.10 Mass Spectra of intermediate generated from isoproturon for RT of HPLC at 3.0 min, in GC/MS at: (a) RT = 5.580 min, (b) RT = 7.901 min, (c) RT = 11.410 min, (d) RT = 32.028 min, (e) RT = 42.556 min, (f) RT = 51.038 min. The numerical values listed next to the legend represent height of the GC/MS peaks.
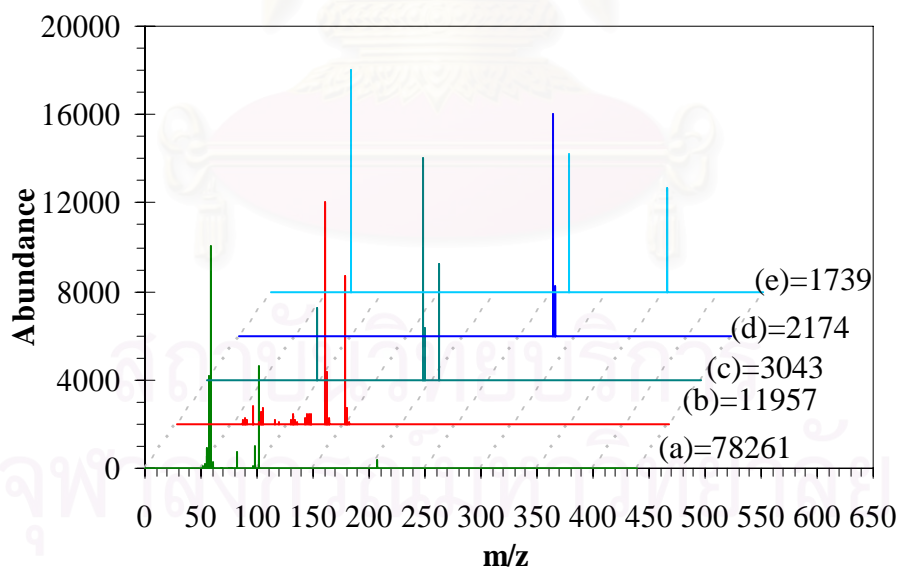
Figure C.11 Mass Spectra of intermediate generated from isoproturon for RT of HPLC at 3.5 min, in GC/MS at: (a) RT = 5.842 min, (b) RT = 8.102 min, (c) RT = 9.746 min, (d) RT = 11.435 min, (e) RT = 20.905 min. The numerical values listed next to the legend represent height of the GC/MS peaks.
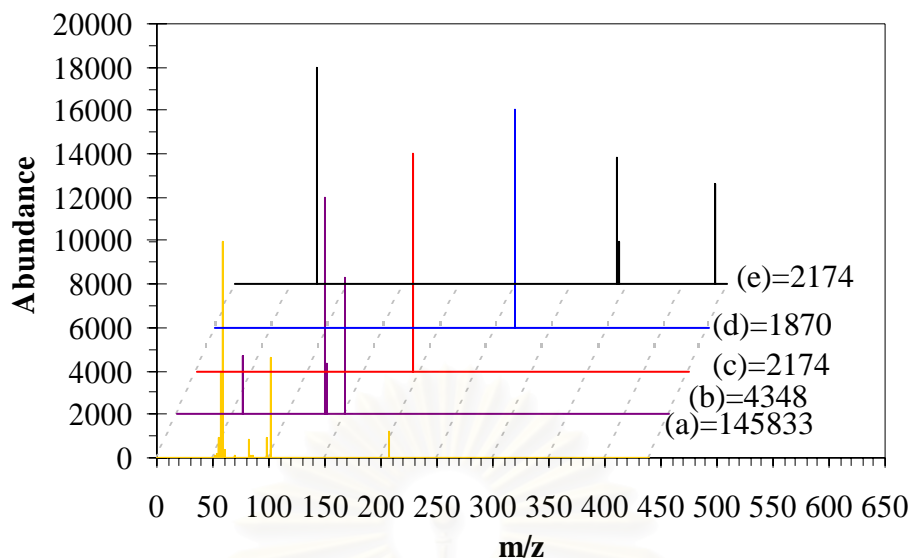
Figure C.12 Mass Spectra of intermediate generated from isoproturon for RT of

HPLC at 3.7 min, in GC/MS at: (a) RT = 5.606 min, (b) RT = 8.170 min, (c) RT =

10.022 min, (d) RT = 18.692 min, (e) RT = 32.015 min. The numerical values listed

next to the legend represent height of the GC/MS peaks.
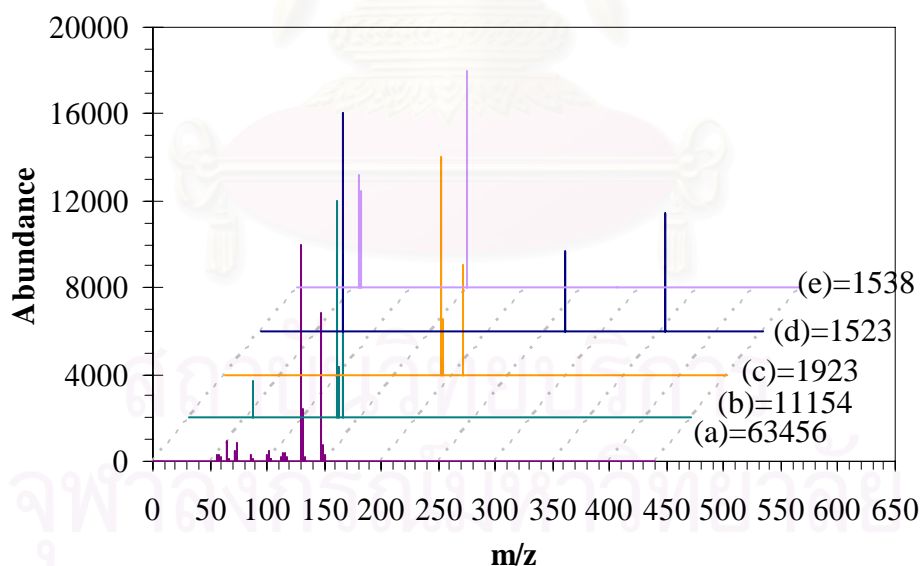
Figure C.13 Mass Spectra of intermediate generated from isoproturon for RT of

HPLC at 4.2 min, in GC/MS at: (a) RT = 8.029 min, (b) RT = 8.214 min, (c) RT =

9.750 min, (d) RT = 20.900 min, (e) RT = 47.873 min. The numerical values listed

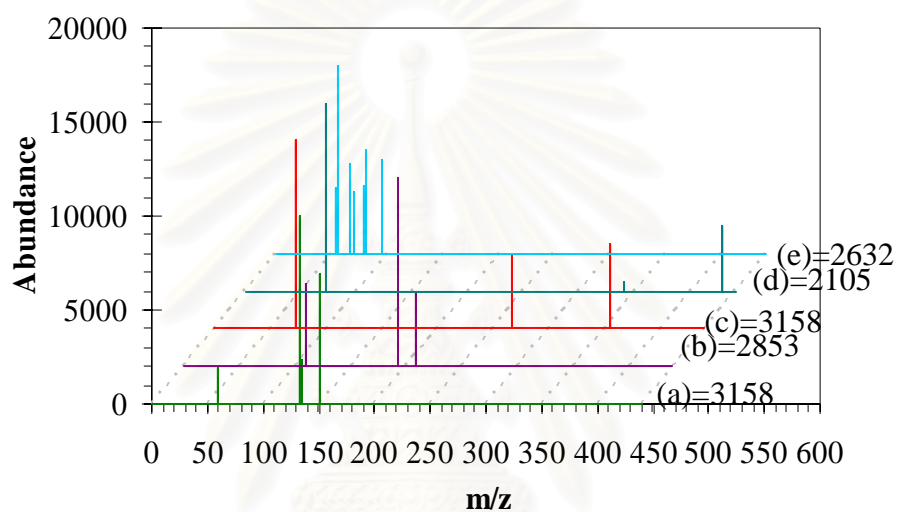next to the legend represent height of the GC/MS peaks.
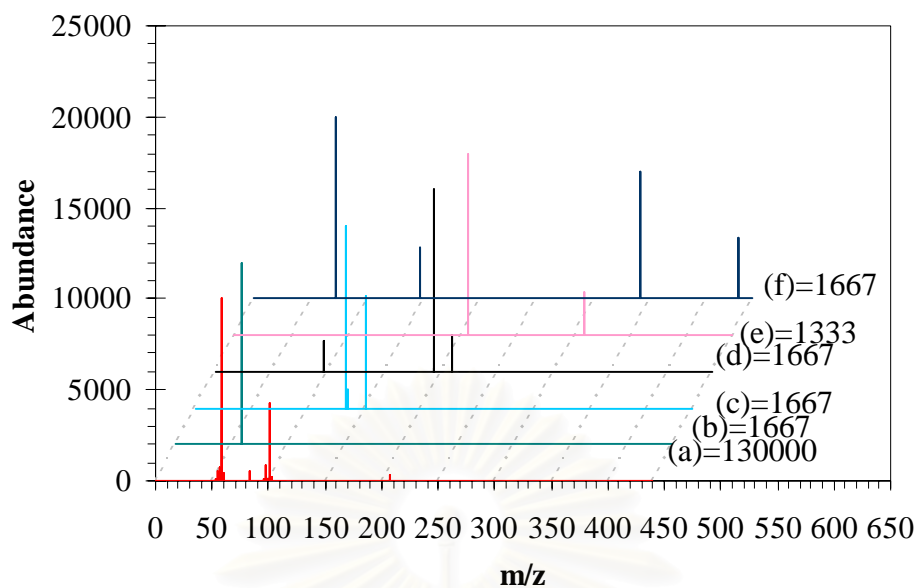
Figure C.14 Mass Spectra of intermediate generated from isoproturon for Rt of

HPLC at 4.5 min, in GC/MS at: (a) RT = 5.868 min, (b) RT = 6.857 min, (c) RT =

8.439 min, (d) RT = 9.728 min, (e) RT = 17.047 min, (f) RT = 32.016 min. The

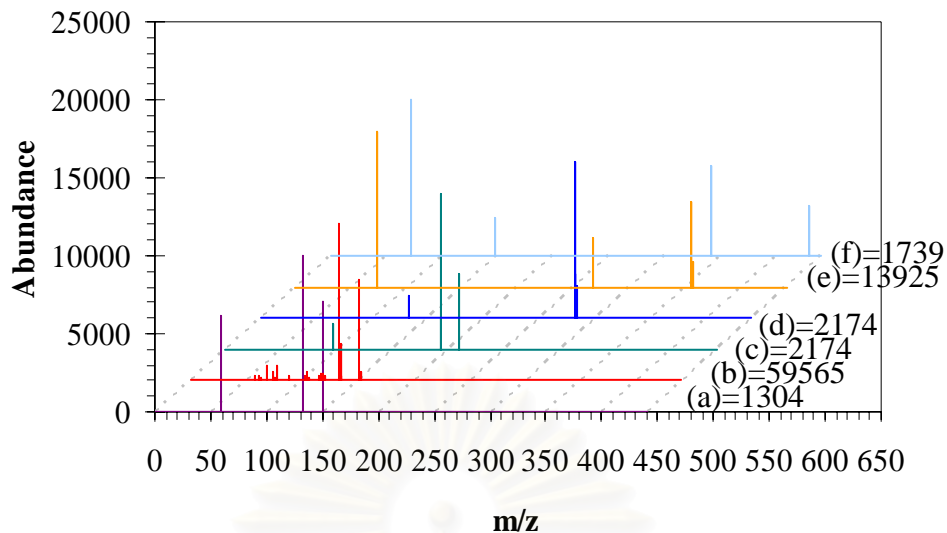numerical values listed next to the legend represent height of the GC/MS peaks.
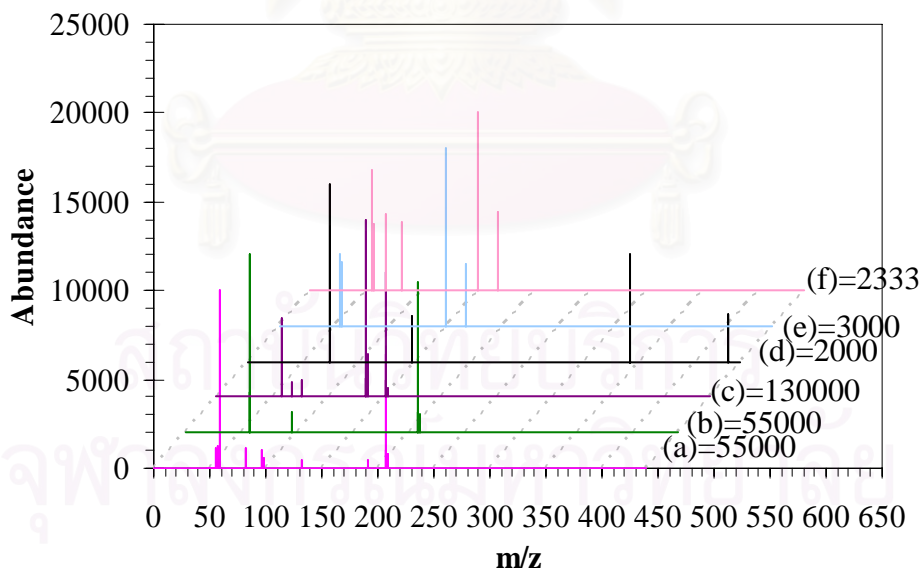
Figure C.15 Mass Spectra of intermediate generated from isoproturon for RT of

HPLC at 4.8 min, in GC/MS at: (a) RT = 4.761 min, (b) RT = 5.712 min, (c) RT =

7.814 min, (d) RT = 32.003 min, (e) RT = 48.792 min, (f) RT = 51.038 min. The

numerical values listed next to the legend represent height of the GC/MS peaks.

3. Linuron Degradation
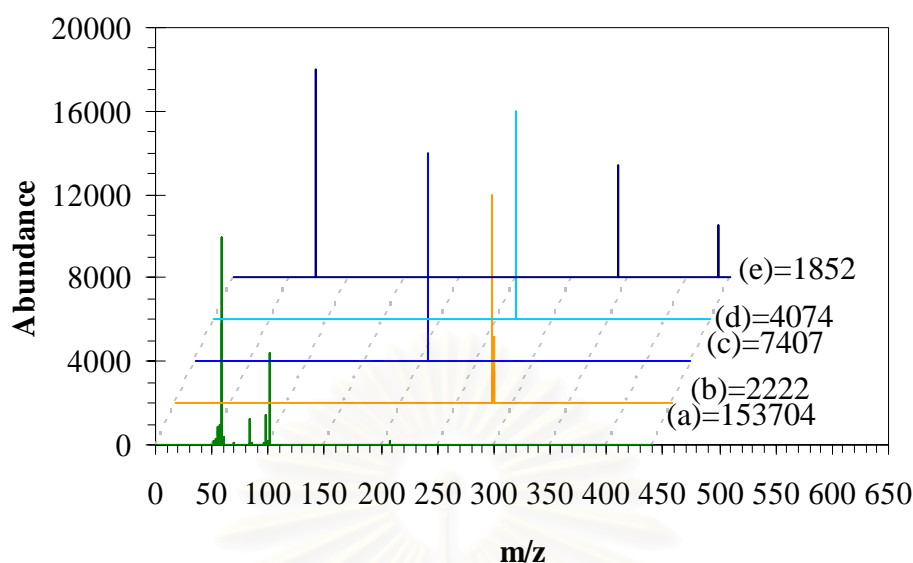
Figure C.16 Mass Spectra of intermediate generated from linuron for RT of HPLC at

2.8 min, in GC/MS at: (a) RT = 5.449 min, (b) RT = 11.404 min, (c) RT = 17.071

min, (d) RT = 18.742 min, (e) RT = 32.028 min. The numerical values listed next to

the legend represent height of the GC/MS peaks.
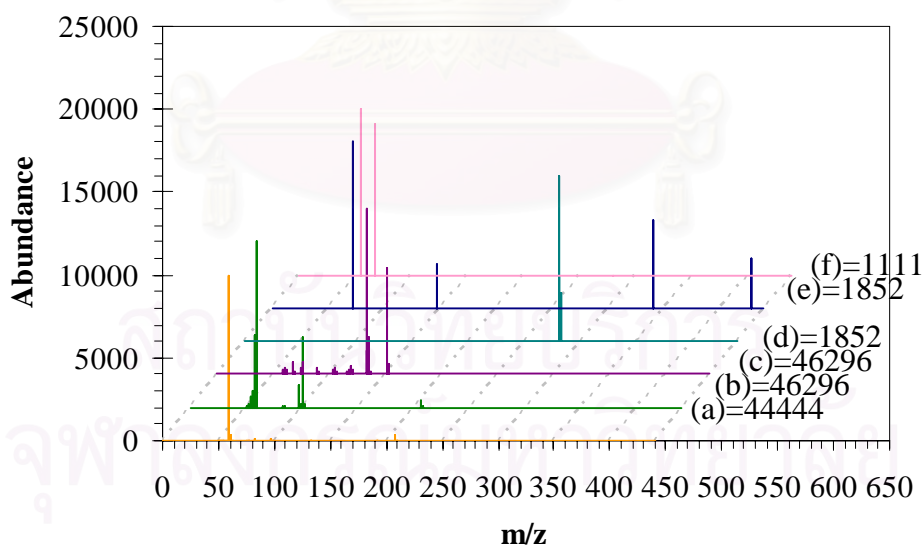
Figure C.17 Mass Spectra of intermediate generated from linuron for RT of HPLC at

4.5 min, in GC/MS at: (a) RT = 4.617 min, (b) RT = 5.614 min, (c) RT = 8.076 min,

(d) RT = 11.429 min, (e) RT = 32.028 min, (f) RT = 47.735 min. The numerical

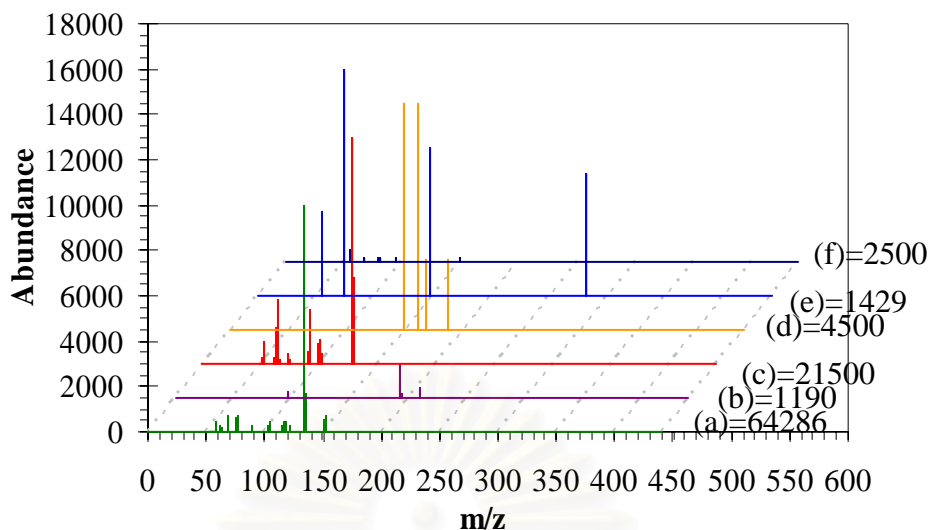values listed next to the legend represent height of the GC/MS peaks.
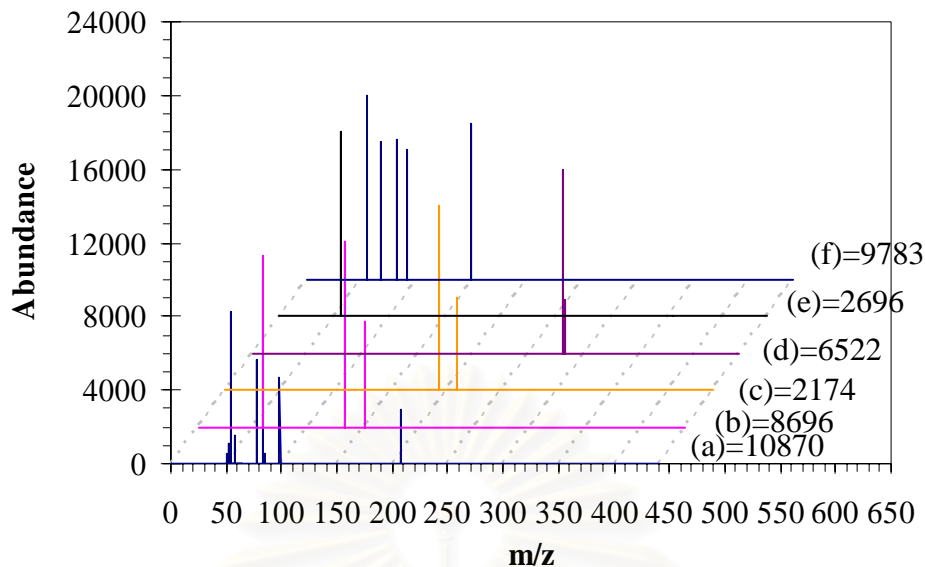
Figure C.18 Mass Spectra of intermediate generated from linuron for RT of HPLC at 4.9 min, in GC/MS at: (a) RT = 4.242 min, (b) RT = 7.176 min, (c) RT = 9.775 min, (d) RT = 11.398 min, (e) RT = 43.306 min, (f) RT = 9649 min. The numerical values listed next to the legend represent height of the GC/MS peaks.
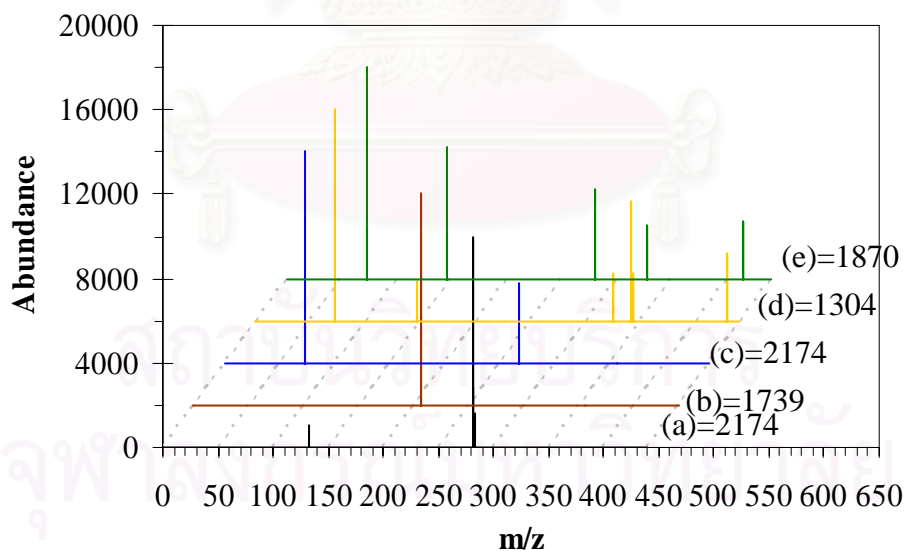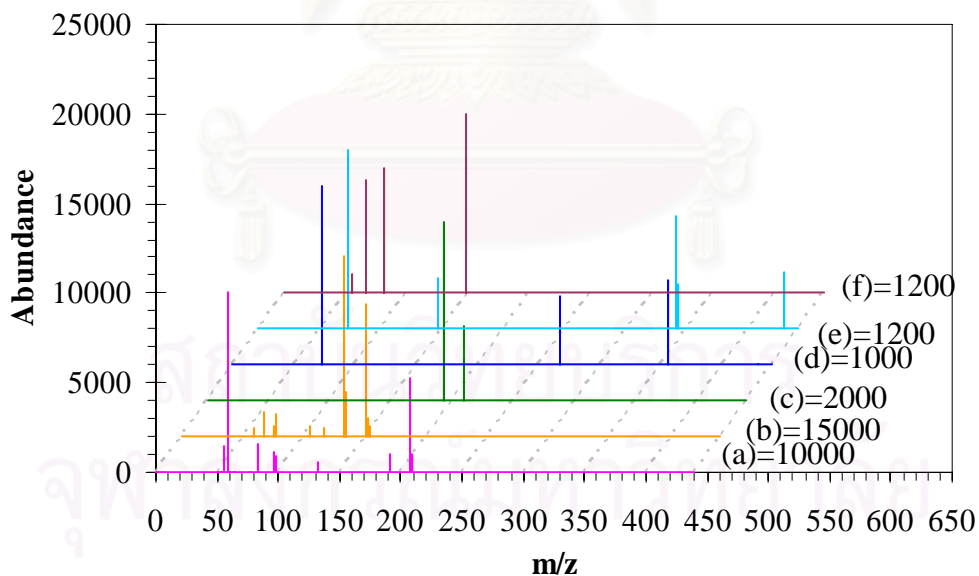

Figure C.19 Mass Spectra of intermediate generated from linuron for RT of HPLC at 5.0 min, in GC/MS at: (a) RT = 4.548 min, (b) RT = 7.932 min, (c) RT = 9.759 min, (d) RT = 20.912 min, (e) RT = 32.028 min, (f) RT = 50.200 min. The numerical values listed next to the legend represent height of the GC/MS peaks.
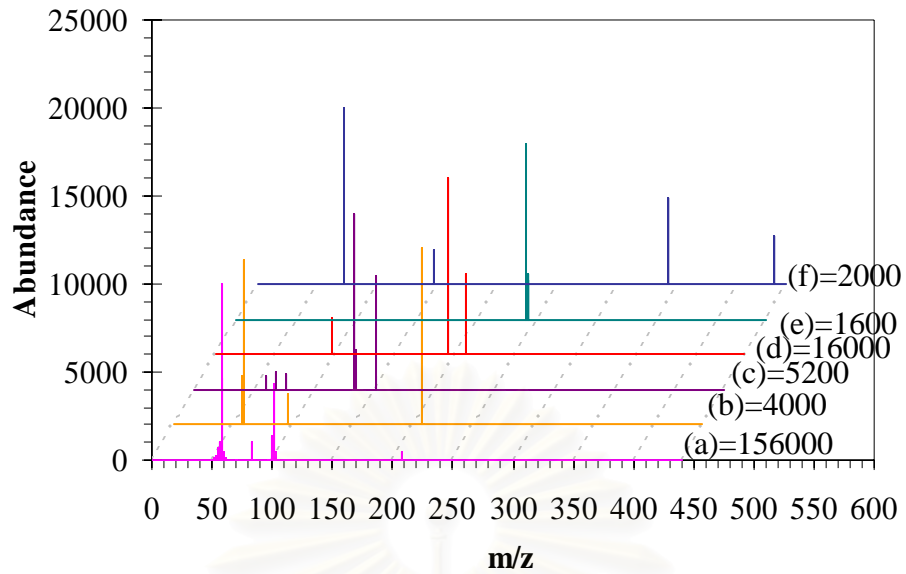
Figure C.20 Mass Spectra of intermediate generated from linuron for RT of HPLC at

5.2 min, in GC/MS at: (a) RT = 5.487 min, (b) RT = 5.931 min, (c) RT = 7.908 min,

(d) RT = 9.759 min, (e) RT = 11.404 min, (f) RT = 32.034 min. The numerical values

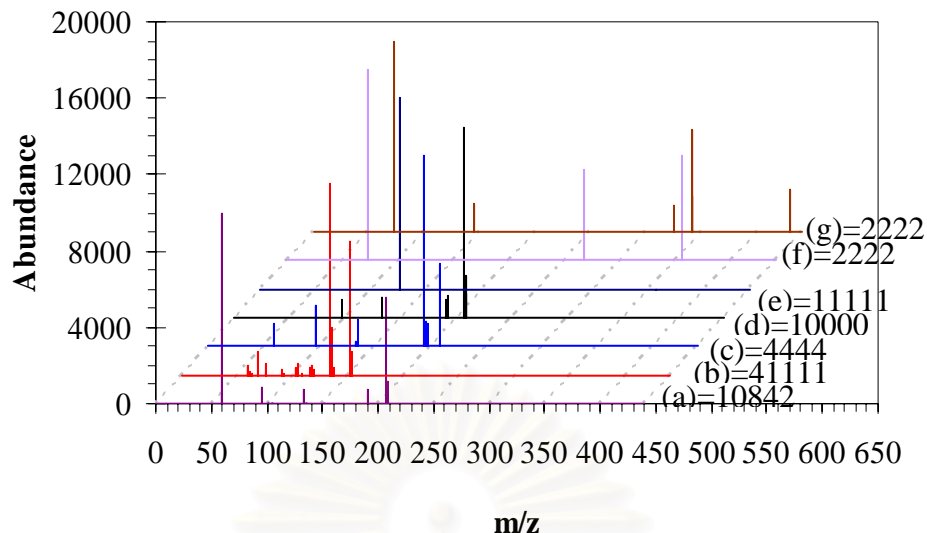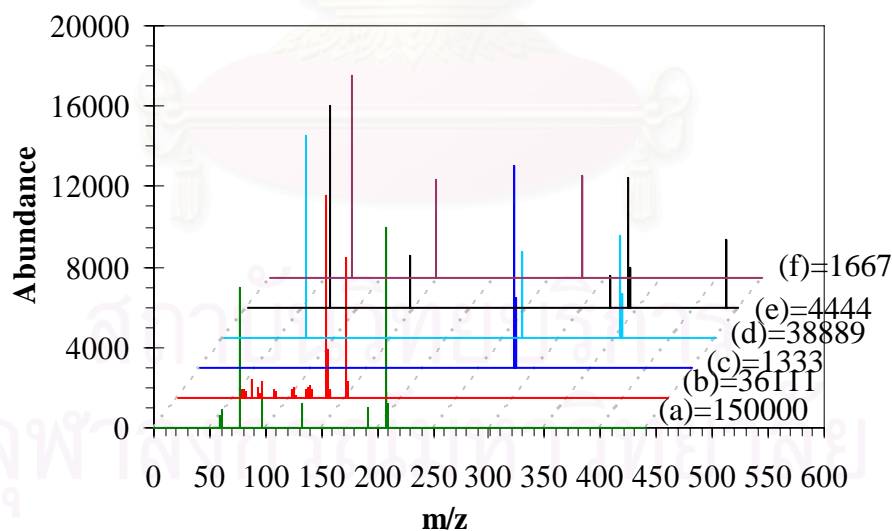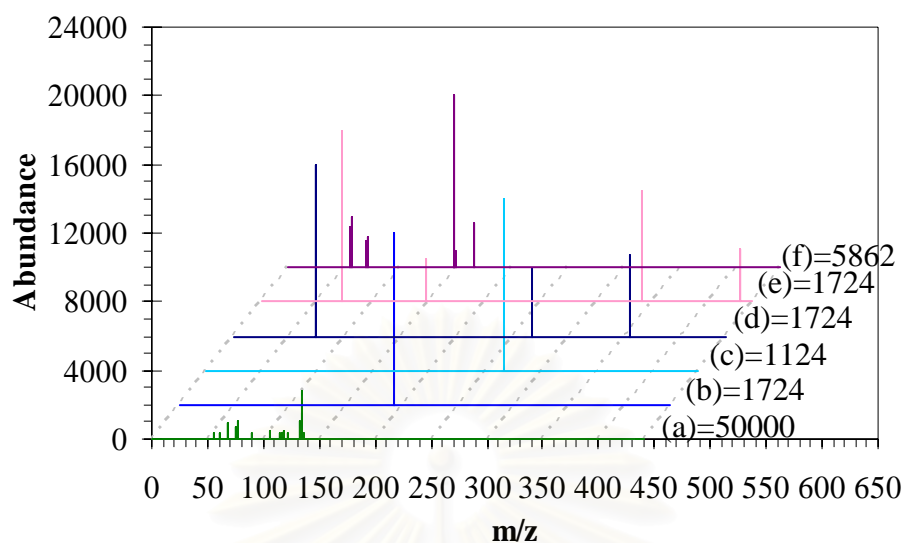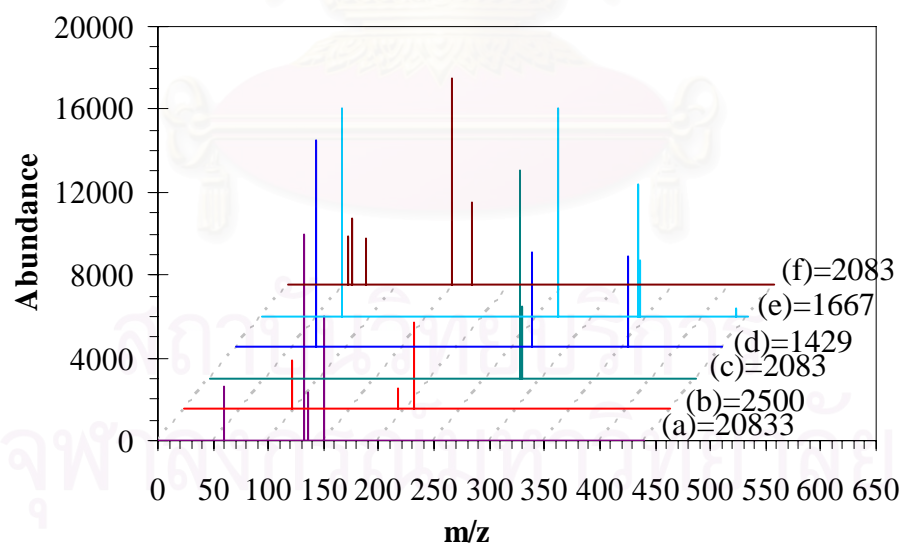listed next to the legend represent height of the GC/MS peaks.

APPENDIX D

ABUNDANCE OF GC-MS PEAK

1. **Diuron Degradation**

RT-MS	Abundance						
	Compound 1	Compound 2	Compound 3	Compound 4	Compound 5	Compound 6	Compound 7
	RT-HPLC=2.7	RT-HPLC=2.8	RT-HPLC=3.2	RT-HPLC=3.7	RT-HPLC=4.2	RT-HPLC=4.5	RT-HPLC=4.8
5.524	-	-	-	-	-	-	150000
5.849	-	-	-	-	-	10842	-
7.451	-	1304	-	-	-	-	-
8.014	3158	-	21428	64286	-	-	-
8.202	-	59565	-	-	-	41111	-
7.982	-	-	-	-	-	-	36111
9.872	2853	2174	1190	1190	-	4444	-
11.429	3158	2174	-	-	2174	-	1333
17.159	-	-	-	-	6522	-	-
17.309	-	-	-	-	-	10000	-
18.982	-	-	-	21500	-	11111	-
20.872	-	-	3333	-	-	-	-
20.937	-	13925	-	-	2174	2222	38889
30.008	-	-	-	4500	-	-	-
32.047	2105	1739	3333	-	1304	2222	4444
42.568	-	-	1905	1429	1870	-	1667
46.956	-	-	-	2500	-	-	-
50.894	2632	-	-	-	-	-	-

2. Isoproturon Degradation

| RT-MS | Abundance | | | | | | | |
| | Compound 1 | Compound 2 | Compound 3 | Compound 4 | Compound 5 | Compound 6 | Compound 7 | Compound 8 |
	RT-HPLC=2.7	RT-HPLC=2.8	RT-HPLC=3.0	RT-HPLC=3.5	RT-HPLC=3.7	RT-HPLC=4.2	RT-HPLC=4.5	RT-HPLC=4.8
4.761	-	-	-	-	-	-	-	55000
5.580	-	-	206250	-	-	-	-	-
5.606	-	-	-	-	145833	-	-	55000
5.842	-	-	-	78261	-	-	-	-
5.868	-	-	-	-	-	-	130000	-
6.857	-	-	-	-	-	-	1667	-
7.450	-	20833	-	-	-	-	-	-
7.814	-	-	-	-	-	-	-	130000
7.895	50000	-	-	-	-	-	-	-
7.901	-	-	14583	-	-	-	-	-
8.029	-	-	-	-	-	63465	-	-
8.102	-	-	-	11957	-	-	-	-
8.170	-	-	-	-	4348	-	-	-
8.214	-	-	-	-	-	11154	-	-
8.439	-	-	-	-	-	-	1667	-
9.705	-	2500	-	-	-	-	-	-
9.728	-	-	-	-	-	-	1667	-
9.750	-	-	-	3043	-	1923	-	-
10.053	1724	-	-	-	2174	-	-	-
11.410	-	-	2083	-	-	-	-	-
11.435	-	-	-	2174	-	-	-	-
11.689	-	2083	-	-	-	-	-	-
17.047	-	-	-	-	-	-	1333	-
18.692	1124	-	-	-	1870	-	-	-
20.852	-	1429	-	-	-	-	-	-
20.900	1724	-	-	1739	-	1523	-	-
32.015	1724	1667	2083	-	2174	-	1667	2000
42.556	-	-	1042	-	-	-	-	-
44.545	-	2083	-	-	-	-	-	-
47.873	-	-	-	-	-	1538	-	-
48.792	-	-	-	-	-	-	-	3000
51.038	-	-	1250	-	-	-	-	2333
51.676	5862	-	-	-	-	-	-	-

3. Linuron Degradation

RT-MS	Abundance				
	Compound 1	Compound 2	Compound 3	Compound 4	Compound 5
	RT-HPLC=2.8	RT-HPLC=4.5	RT-HPLC=4.9	RT-HPLC=5.0	RT-HPLC=5.2
4.548	-	-	-	10000	-
4.617	-	44444	-	-	-
5.449	153704	-	-	-	-
5.487	-	-	-	-	156000
5.654	-	46296	-	-	-
5.931	-	-	-	-	4000
7.176	-	-	8696	-	-
7.908	-	-	-	-	5200
7.932	-	-	-	9500	-
8.076	-	46296	-	-	-
9.759	-	-	-	2000	16000
11.398	-	-	6522	-	-
11.404	2222	-	-	-	1600
11.429	-	1852	-	-	-
17.071	7407	-	-	-	-
18.742	4074	-	-	-	-
20.912	-	-	-	1000	-
32.028	1852	1852	-	1200	-
32.034	-	-	-	-	2000
43.306	-	-	2696	-	-
47.735	-	1111	-	-	-
49.649	-	-	9783	-	-
50.200	-	-	-	1200	-

APPENDIX E

TEM CHARACTERISTIC OF REFERENCE TITANIA
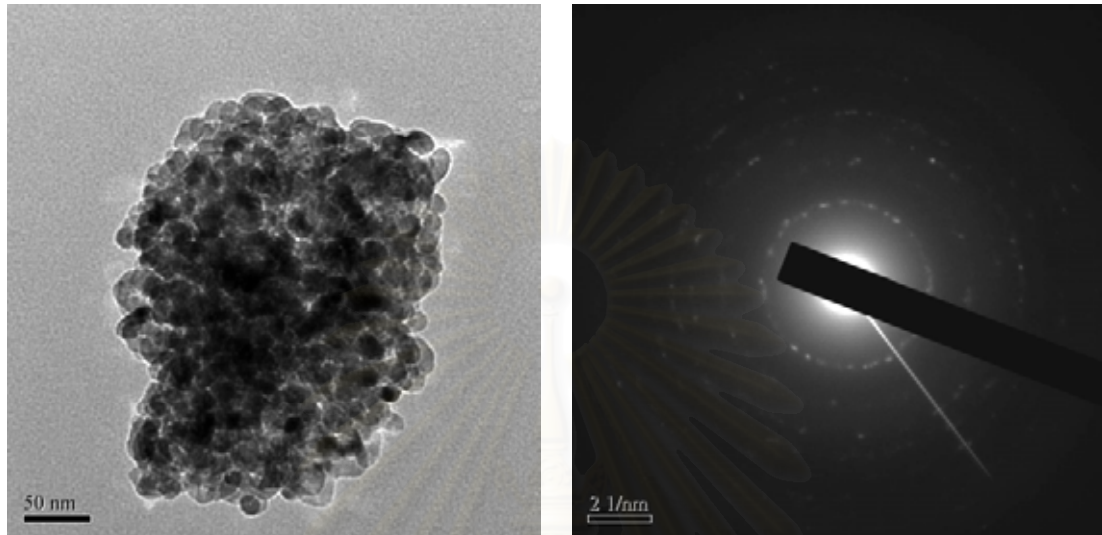
Figure E.1 TEM micrographs and SAED patterns of reference titania

LIST OF PUBLICATIONS

1. Jitlada Klongdee, Varong Pavarajarn, Okorn Mekasuwandumrong and Piyasan Praserthdam (2004). "Photocatalytic Degradation of Methylene Blue by TiO_2 Nanocrystals Synthesized via Thermal Decomposition of Titanium (IV) n-Butoxide in Organic Solvents." Regional Symposium on Chemical Engineering 2004: 200.

2. Klongdee, J., Petchkroh, W., Phuempoonsathaporn, K., Praserthdam, P., Vangnai, A.S., Pavarajarn, V (2005). "Activity of nanosized titania synthesized from thermal decomposition of titanium (IV) n-butoxide for the photocatalytic degradation of diuron." Science and Technology of Advanced Materials 6: 290-295.

Photocatalytic Degradation of Methylene Blue by TiO$_2$ Nanocrystals Synthesized via Thermal Decomposition of Titanium (IV) *n*-Butoxide in Organic Solvents

Jitlada Klongdee[1], Varong Pavarajarn[1], Okorn Mekasuwandumrong[2] , and Piyasan Praserthdam[1]*

[1] *Center of Excellence on Catalysis and Catalytic Reaction Engineering, Department of Chemical Engineering, Chulalongkorn University, Bangkok 10330*
[2] *Department of Chemical Engineering, Faculty of Engineering and Industrial Technology, Silpakorn University, Sanam Chandra Palace Campus, Nakhon Pathom 73000, Thailand*
*Corresponding author: (Phone +66-(0)2-2186890, Fax. +66-(0)2-2186877, E-mail: fchvpv@eng.chula.ac.th)

ABSTRACT

Nanocrystalline titania (TiO$_2$) was prepared by thermal decomposition of titanium (IV) *n*- butoxide in various organic solvents, i.e. 1,4-butanediol, toluene and mineral oil. The products obtained were anatase titania without contamination of other phases. The physical properties of samples were investigated by XRD, SEM, TEM and BET techniques. It was confirmed that the products were titania single crystals with crystallite size in the range of 12-13 nm. The photocatalytic activity of the products was investigated by using the UV-based photocatalytic decomposition of methylene blue. The reaction showed pseudo-first-order behavior. Rate constant for the reaction using each synthesized product as photocatalyst was determined and compared. The results were also compared with commercial TiO$_2$. The activity of TiO$_2$ prepared in 1,4-butanediol showed the best photocatalytic activity. It was also found that the photocatalytic activity was enhanced by calcination of the synthesized titania. The results suggested that the difference in photocatalytic activity of the nanocrystalline titania synthesized in various reaction mediums was the result from the difference in degree of agglomeration and different crystallinity of titania.

*Keywords***:** TiO$_2$, Photocatalytic activity, Nanocrystal.

INTRODUCTION

Titanium (IV) dioxide or titania (TiO$_2$) has been recognized as one of the commonly used metal-oxide in various industries because of its good physical and chemical properties, such as catalytic activity [1], photocatalytic activity [2], good stability toward adverse environment [3], sensitivity to humidity and gas [4], dielectric character [5], nonlinear optical characteristic [6] and photoluminescence [7]. Applications of titania are ranges in many fields including the use as catalysts, catalyst supports, electronics, cosmetics, pigments and filler coating. Nevertheless, photocatalyst is one of the most important uses of titania. Titania is known to have three natural polymorphs, i.e. rutile, anatase, and brookite. Rutile is thermodynamically stable polymorph, but anatase is more suitable form for catalytic applications.

There are many variables that influence the photocatalytic activity of titania, such as particle size, reactive surface area, crystal structure, as well as intensity and wavelength of the incident light. Among these factors, the crystal structure and crystallinity of titania are considered as important factors. Amorphous titania has negligible photocatalytic activity because of the recombination between the pair of photoexcited electron and hole in the amorphous structure [8]. For crystalline titania, only anatase is generally accepted to have significant photocatalytic activity [9-11].

Nanocrystalline titania can be synthesized by many methods, such as sol-gel method, hydrothermal method, vapor-phase hydrolysis, laser-induced decomposition, chemical vapor decomposition and molten salt method. In this work, nanocrystalline anatase titania was synthesized via the thermal decomposition of titanium alkoxide in organic solvent. This method has been used to successfully synthesize various type of nanosized metal oxides with large surface area, high crystallinity and high thermal stability [12-17]. However, it has been reported that organic solvent, which is used as the reaction medium, influences both the decomposition mechanism and physical properties of titania synthesized [18]. In this work, the effects of the reaction medium, i.e. organic solvent, on the photocatalytic activity of the titania obtained are investigated by using the degradation of methylene blue (MB) aqueous solution. The results are also compared with the degradation using the Japanese Reference Catalyst titania (JRC-TIO-1).

EXPERIMENTAL

Synthesis of Titania

Titanium (IV) *n*-butoxide (TNB) was used as starting material for titania synthesis. 15 g of TNB was suspended in 100 ml of organic solvent, i.e. 1,4-butanediol, toluene or mineral oil, in a test tube, which was then placed in a 300 ml autoclave. The gap between the test tube and the autoclave wall was filled with 30 ml of the same solvent used in the test tube. The autoclave was purged completely by nitrogen before heating up to 300°C at a rate of 2.5°C/min. Autogeneous pressure during the reaction gradually increased as the temperature was raised. Once the prescribed temperature was reached, the temperature was held constant for 2 h, before the system was cooled down to room temperature. After the system was cool, the resulting powders were repeatedly washed with methanol and dried in air. The obtained product was then calcined at 500°C for 2 h in a box furnace with a heating rate of 10°C/min.

Titania Characterization

Powder X-ray diffraction (XRD) analysis was done by using a SIEMENS D5000 diffractometer with CuKα radiation. The crystallite size of the product was determined from the broadening of its main peak, using the Scherrer equation. Morphology of the products was observed on JEOL Scanning Electron Microscope and JEOL TEM-200cx Transmission Electron Microscope. Specific surface area of the samples was measured by using the BET multipoint method.

Photocatalytic Experiments

The photodegradation of methylene blue (MB) was employed to evaluate photocatalytic activity of titania synthesized. For each condition, 23mg of titania was dispersed in 230 ml of 10 ppm MB aqueous solution. The mixed solution was transferred into test tubes and kept in the dark. The photocatalytic reaction was initiated by exposing test tubes to the sunlight at room temperature. The experiments were conducted for 4 hours at the middle of the day to get approximately same intensity of light for the whole experiment. It should be noted that the photocatalytic activity evaluation for all titania investigated was tested at the same time, so all samples had experienced same lighting conditions. The decomposition of MB was periodically monitored by measuring the absorbance of the solution at 665 nm using UV-Visible scanning spectrophotometer.

RESULTS AND DISCUSSION

Formation of titania in different solvents

Nanocrystalline titania was successfully synthesized by using thermal decomposition of TNB in all organic solvents investigated. The XRD patterns, as shown in Figure 1, confirm that the products obtained are anatase titania without contamination of other phases, e.g. rutile or brookite. TEM micrographs of the as-synthesized products prepared in all solvents are shown in Figure 2. The crystallite sizes of products calculated from the Scherrer equation are in the range of 12 to 13 nm, which agree with the TEM observation. Therefore, it is suggested that each primary particle observed by TEM is a nanosized single crystal titania.
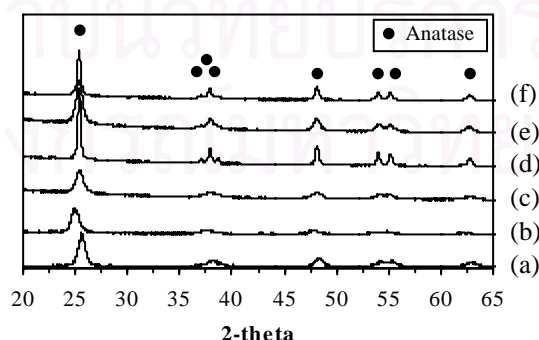
Figure 1. The XRD patterns of titania synthesized by the reaction in various organic mediums: (a) in mineral oil, (b) in mineral oil and subsequently calcined at 500°C, (c) in toluene, (d) in toluene and subsequently calcined at 500°C, (e) in 1,4-butanediol, (f) in 1,4-butanediol and subsequently calcined 500°C.
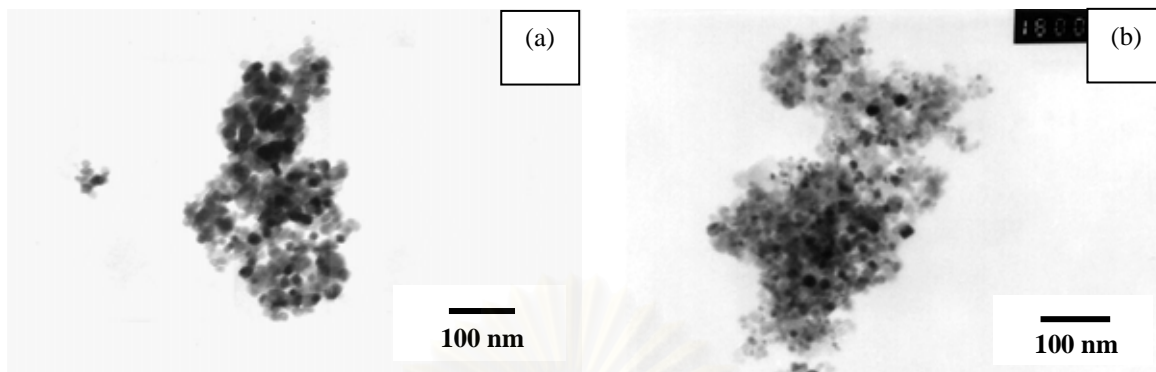
Figure 2.   TEM micrographs of the as-synthesized products prepared in: (a) 1,4-butanediol, (b) toluene.
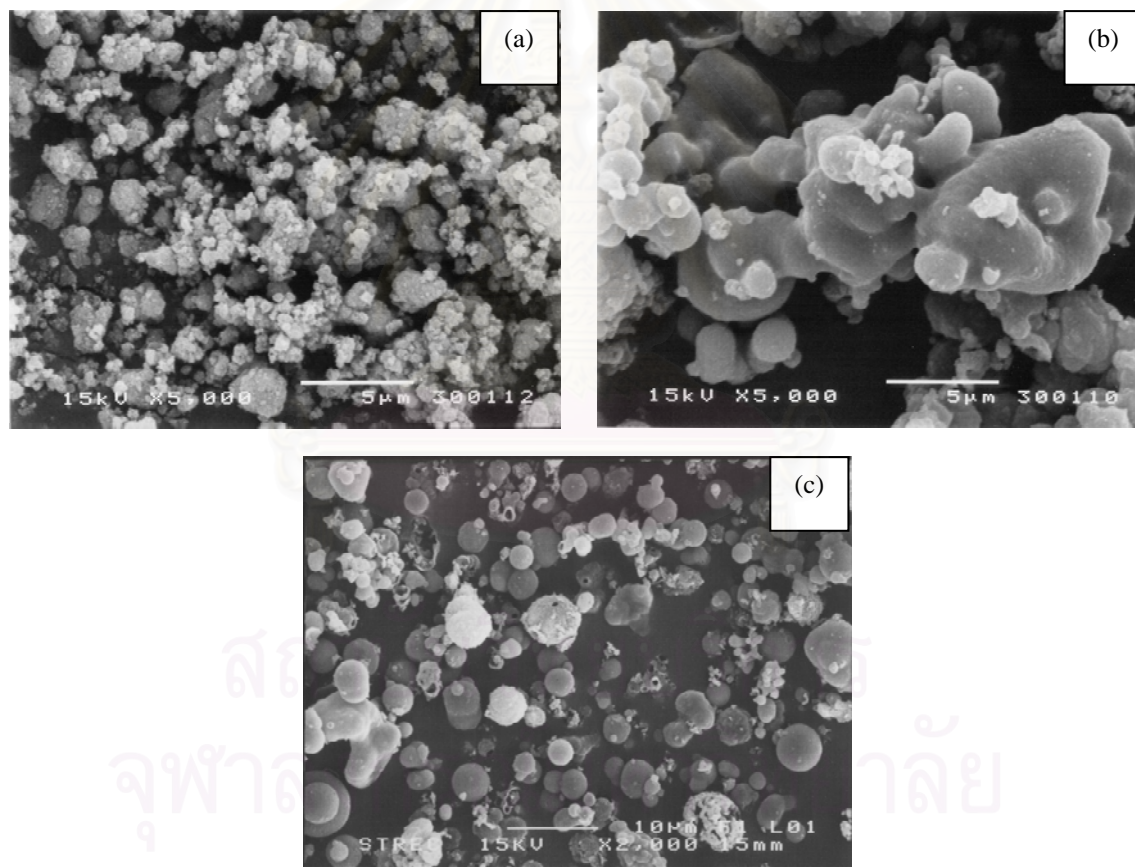
Figure 3.   SEM micrographs of the as-synthesized products prepared in: (a) 1,4-butanediol, (b) toluene, (c) mineral oil.

SEM micrographs reveal that the morphology of the products obtained from 1,4-butanediol, toluene and mineral oil are different (see Figure 3). The products synthesized in toluene and mineral oil agglomerate into micron-size particles, which are called secondary particles. Although the secondary particles formed in both toluene and mineral oil are similar in size, ones synthesized in toluene are more spherical in shape. On the other hand, for the reaction in 1,4-butanediol, irregular aggregates made up of nanometer-sized particles are observed. These differences in morphologies of titania can be explained by difference in the colloidal stability of the precipitate in different reaction medium [19]. As reported by Park et al., the repulsive force between two particles depends upon many parameters, including dielectric constant of the continuous phase, particle size and particle surface potential [19]. Since other parameters indicated by Park et al. were controlled in this work, agglomeration of the precipitates in this study was the result mainly from the dielectric constant of the reaction medium. For instance, particles in mineral oil, which has quite low dielectric constant, would become agglomerated and form spherical secondary particles.

Physical properties of titania synthesized in various solvents are shown in Table 1, including BET surface area (S_{BET}) measured by nitrogen adsorption and the surface area calculated from a crystallite size (S_{XRD}). The ratio between S_{BET} and S_{XRD} is referred as the degree of agglomeration. The degree of agglomeration of titania prepared in 1,4-butanediol and toluene are nearly 1, indicating that each primary particle exposes its entire surface to the adsorbate molecules. However, the degree of agglomeration of product prepared in mineral oil are lower, suggesting more packing of titania crystals in the spherical secondary particles.

Table 1. Physical properties of titania synthesized at 300°C for 2 h in various organic solvents.

Solvent	Crystallite size, d (nm)	S_{BET} (m²/g)	S_{XRD}[a] (m²/g)	S_{BET}/S_{XRD}
1,4-butanediol	13	110	120	0.92
toluene	12	145	130	1.11
mineral oil	12	93	130	0.72

[a] Calculated surface area assuming that the particles are nonporous spheres and using the density of anatase (3.84 g/cm³).

Photocatalytic activity for the degradation of MB aqueous solution

Figure 4 illustrates the effects of the reaction medium used for titania synthesis on the photocatalytic activity of synthesized titania. It was found that the disappearance of MB, using various synthesized titania as catalyst, follows the pseudo-first-order kinetics. The transformed first order plots are given in Figure 5, whereas the slopes are rate constants of the degradation. The rate constant for each catalyst is shown in Table 2.

(a)   (b)
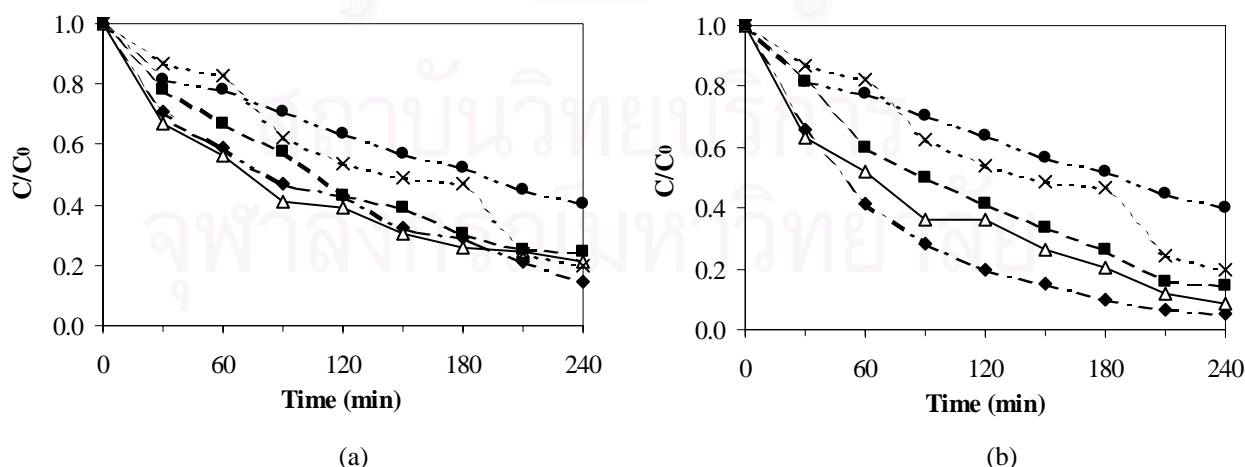
Figure 4. Disappearance of MB by photooxidation using (a) as-synthesized titania, (b) titania calcined at 500°C:

(a)

(b)
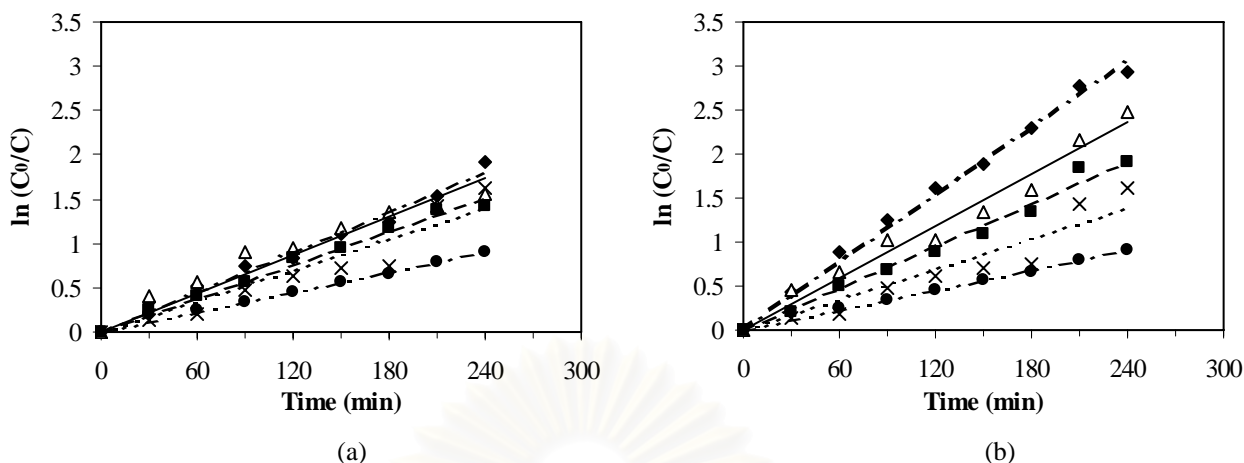
Figure 5. Pseudo-first-order transforms of disappearance of MB by photooxidation using (a) as-synthesized titania, (b) titania calcined at 500°C: (— ···) synthesized in 1,4-butanediol, (——) synthesized in toluene, (- - -) synthesized in mineral oil, (··········) reference catalyst JRC-TIO-1, (— · −) no titania used.

In this work, the photodegradation of MB aqueous solution using synthesized titania were compared with that of the Japanese Reference Catalyst titania (JRC-TIO-1). The results show that all titania synthesized in this work exhibited higher photocatalytic activity than the JRC-TIO-1. Moreover, it is also shown that titania, which has experienced the calcination, exhibits higher activity than the as-synthesized catalyst. This result can be explained by the increasing in crystallinity of titania after heat treatment at high temperature [8].

Table 2: Rate constants of the photocatalytic degradation reaction of MB using titania synthesized in various solvents.

Titania preparation		Rate constant
Solvent used	Condition	(min^{-1})
1,4-butanediol	as-synthesized	7.53×10^{-3}
	calcined at 500°C	1.28×10^{-2}
toluene	as-synthesized	7.26×10^{-3}
	calcined at 500°C	9.82×10^{-3}
mineral oil	as-synthesized	6.34×10^{-3}
	calcined at 500°C	7.95×10^{-3}
JRC-TIO-1		5.792×10^{-3}
no catalyst used		3.781×10^{-3}

Nevertheless, it is evident that type of the solvent employed as the medium for the thermal decomposition of TNB also affects the photocatalytic activity of titania obtained. The activity of titania synthesized in the organic solvent investigated is in the following order: 1,4-butanediol > toluene > mineral oil. This difference in the activity might be the result from two possible causes, i.e. degree of agglomeration and structure of crystal formed, since titania synthesized in all reaction medium are in the same crystalline phase with relatively same

active area for photooxidation reaction. Therefore, titania synthesized in mineral oil, which is highly agglomerated (see Figure 3), has less activity than more dispersed titania such as one synthesized in 1,4-butanediol. The other factor affecting the activity of titania is the structure of the crystal formed, or the crystallinity. As reported in our earlier work, crystallization mechanism of titania in the thermal decomposition of titanium alkoxide process depends upon the reaction medium [20]. When 1,4-butanediol is employed as reaction medium, anatase crystals are formed via direct crystallization when the temperature in the autoclave reaches approximately 250°C, which is lower than the temperature of the operation (300°C). Subsequent heating only results in growth of the crystals. On the other hand, for the reaction in toluene, anatase titania is formed from the solid state transformation of amorphous intermediate, which is initially precipitated from the solution [20]. The difference in the formation mechanism of titania reflects the difference in crystallinity of obtained particles and therefore affects their photocatalytic activity. Since it has been accepted that the decrease in crystal defects generally improves the photocatalytic activity of titania [21-23], the results in this work supports the mechanisms in our previous work, as discussed earlier. Furthermore, it is also suggested that titania synthesized in 1,4-butanediol has higher crystallinity than those synthesized in toluene and mineral oil.

CONCLUSION

Nanocrystalline anatase titania can be prepared via thermal decomposition of TNB in organic solvents. The photocatalytic degradation of MB aqueous solution is employed to investigate the activity of obtained titania. It is found that type of the solvent employed for the synthesis of titania in the thermal decomposition of titanium alkoxide process affects the photocatalytic activity of titania obtained. The activity of titania are shown in the following order: 1,4-butanediol>toluene>mineral oil. This result can be explained by the lower degree of agglomeration in mineral oil and different crystallinity obtained from different reaction mechanism.

ACKNOWLEDGEMENT

REFERENCES

[1] Coulter, K. E. and Sault, A. G., 'Effects of Activation on the Surface-Properties of Silica-Supported Cobalt Catalysts', *Journal of Catalysis*, **154 (1)**, pp 56-64, (1995).

[2] Wakanabe, T., Kitamura, A., Kojima, E., Nakayama, C., Hashimoto, K. and Fujishima, A., Photocatalytic Purification and Treatment of Water and Air, in: Olis, D. E. and Al-Ekabi, H. (Eds.), Elsevier, Amsterdam, pp 747, (1993).

[3] Tonejc, A. M., Goti, M., Grzeta, B., Music, S., Popovi, S., Trojko, R., Turkovi, A. and MuSevic, I., 'Transmission Electron Microscopy Studies of Nanophase Tio2', *Materials Science and Engineering B-Solid State Materials for Advanced Technology*, **40 (2-3)**, pp 177-184, (1996).

[4] Traversa, E., Gnappi, G., Montenero, A. and Gusmano, G., 'Ceramic Thin Films by Sol-Gel Processing as Novel Materials for Integrated Humidity Sensors', *Sensors and Actuators B-Chemical*, **31 (1-2)**, pp 59-70, (1996).

[5] Ohtani, B. and Nishimoto, S., 'Effect of Surface Adsorptions of Aliphatic-Alcohols and Silver Ion on the Photocatalytic Activity of Tio2 Suspended in Aqueous-Solutions', *Journal of Physical Chemistry*, **97 (4)**, pp 920-926, (1993).

[6] O'Regan, B. and Gratzel, M., 'A Low-Cost, High-Efficiency Solar Cell Based on Dye-Sensitized Colloidal TiO_2 Films', *Nature*, **353 (6346)**, pp 737, (1991).

[7] Liu, Y. J. and Claus, R. O., 'Blue Light Emitting Nanosized Tio2 Colloids', *Journal of the American Chemical Society*, **119 (22)**, pp 5273-5274, (1997).

[8] Ohtani, B., Ogawa, Y. and Nishimoto, S., 'Photocatalytic Activity of Amorphous-Anatase Mixture of Titanium(IV) Oxide Particles Suspended in Aqueous Solutions', *Journal of Physical Chemistry B*, **101 (19)**, pp 3746-3752, (1997).

[9] Nishimoto, S.-i., Ohtani, B., Kajiwara, H. and Kagiya, T., 'Correlation of the Crystal Structure of Titanium Dioxide Prepared from Titanium Tetra-2-Propoxide with the Photocatalytic Activity for Redox Reactions in Aqueous Propan-2-Ol and Silver Salt Solutions', *Journal of the Chemical Society - Faraday Transactions 1*, **81 (1)**, pp 61-68, (1985).

[10] Fox, M. A. and Dulay, M. T., 'Heterogeneous Photocatalysis', *Chemical Reviews*, **93 (1)**, pp 341-357, (1993).

[1]   Coulter, K. E. and Sault, A. G., 'Effects of Activation on the Surface-Properties of Silica-Supported Cobalt Catalysts', *Journal of Catalysis*, **154 (1)**, pp 56-64, (1995).

[2]   Wakanabe, T., Kitamura, A., Kojima, E., Nakayama, C., Hashimoto, K. and Fujishima, A., Photocatalytic Purification and Treatment of Water and Air, in: Olis, D. E. and Al-Ekabi, H. (Eds.), Elsevier, Amsterdam, pp 747, (1993).

[3]   Tonejc, A. M., Goti, M., Grzeta, B., Music, S., Popovi, S., Trojko, R., Turkovi, A. and MuSevic, I., 'Transmission Electron Microscopy Studies of Nanophase Tio2', *Materials Science and Engineering B-Solid State Materials for Advanced Technology*, **40 (2-3)**, pp 177-184, (1996).

[4]   Traversa, E., Gnappi, G., Montenero, A. and Gusmano, G., 'Ceramic Thin Films by Sol-Gel Processing as Novel Materials for Integrated Humidity Sensors', *Sensors and Actuators B-Chemical*, **31 (1-2)**, pp 59-70, (1996).

[5]   Ohtani, B. and Nishimoto, S., 'Effect of Surface Adsorptions of Aliphatic-Alcohols and Silver Ion on the Photocatalytic Activity of Tio2 Suspended in Aqueous-Solutions', *Journal of Physical Chemistry*, **97 (4)**, pp 920-926, (1993).

[6]   O'Regan, B. and Gratzel, M., 'A Low-Cost, High-Efficiency Solar Cell Based on Dye-Sensitized Colloidal TiO_2 Films', *Nature*, **353 (6346)**, pp 737, (1991).

[7]   Liu, Y. J. and Claus, R. O., 'Blue Light Emitting Nanosized Tio2 Colloids', *Journal of the American Chemical Society*, **119 (22)**, pp 5273-5274, (1997).

[8]   Ohtani, B., Ogawa, Y. and Nishimoto, S., 'Photocatalytic Activity of Amorphous-Anatase Mixture of Titanium(IV) Oxide Particles Suspended in Aqueous Solutions', *Journal of Physical Chemistry B*, **101 (19)**, pp 3746-3752, (1997).

[9]   Nishimoto, S.-i., Ohtani, B., Kajiwara, H. and Kagiya, T., 'Correlation of the Crystal Structure of Titanium Dioxide Prepared from Titanium Tetra-2-Propoxide with the Photocatalytic Activity for Redox Reactions in Aqueous Propan-2-Ol and Silver Salt Solutions', *Journal of the Chemical Society - Faraday Transactions 1*, **81 (1)**, pp 61-68, (1985).

[10] Fox, M. A. and Dulay, M. T., 'Heterogeneous Photocatalysis', *Chemical Reviews*, **93 (1)**, pp 341-357, (1993).

[11] Tanaka, K., Hisanaga, T. and Rivera, A. P., in: Photocatalytic Purification and Treatment of Water and Air Ollis, D. F. and Al-Ekabi, H. (Eds.), Elsevier, Amsterdam, pp 169, (1993).

[12] Inoue, M., Kondo, Y. and Inui, T., *Inorganic Chemistry*, **27** pp 215-221, (1988).

[13] Inoue, M., Kominami, H. and Inui, T., *Journal of the American Ceramic Society*, **75** pp 2597-2598, (1992).

[14] Inoue, M., Kominami, H. and Inui, T., 'Novel Synthetic Method for the Catalytic Use of Thermally Stable Zirconia - Thermal Decomposition of Zirconium Alkoxides in Organic Media', *Applied Catalysis A - General*, **97 (2)**, pp L25-L30, (1993).

[15] Kominami, H., Kato, J., Murakami, S., Kera, Y., Inoue, M., Inui, T. and Ohtani, B., 'Synthesis of Titanium(IV) Oxide of Ultra-High Photocatalytic Activity: High-Temperature Hydrolysis of Titanium Alkoxides with Water Liberated Homogeneously from Solvent Alcohols', *Journal of Molecular Catalysis a-Chemical*, **144 (1)**, pp 165-171, (1999).

[16] Kongwudthiti, S., Praserthdam, P., Silveston, P. and Inoue, M., 'Influence of Synthesis Conditions on the Preparation of Zirconia Powder by the Glycothermal Method', *Ceramics International*, **29 (7)**, pp 807-814, (2003).

[17] Mekasuwandumrong, O., Silveston, P. L., Praserthdam, P., Inoue, M., Pavarajarn, V. and Tanakulrungsank, W., 'Synthesis of Thermally Stable Micro Spherical Chi-Alumina by Thermal Decomposition of Aluminum Isopropoxide in Mineral Oil', *Inorganic Chemistry Communications*, **6 (7)**, pp 930-934, (2003).

[18] Kominami, H., Kato, J., Takada, Y., Doushi, Y., Ohtani, B., Nishimoto, S., Inoue, M., Inui, T. and Kera, Y., 'Novel Synthesis of Microcrystalline Titanium(IV) Oxide Having High Thermal Stability and Ultra-High Photocatalytic Activity: Thermal Decomposition of Titanium(IV) Alkoxide in Organic Solvents', *Catalysis Letters*, **46 (3-4)**, pp 235-240, (1997).

[19] Park, H. K., Kim, D. K. and Kim, C. H., 'Effect of Solvent on Titania Particle Formation and Morphology in Thermal Hydrolysis of Ticl4', *Journal of the American Ceramic Society*, **80 (3)**, pp 743-749, (1997).

[20] Payakgul, W., Mekasuwandumrong, O., Pavarajarn, V. and Praserthdam, P., 'Effects of Reaction Medium on the Synthesis of TiO_2 Nanocrystals by Thermal Decomposition of Titanium (IV) *n*-Butoxide', *Ceramics International*, (in press).

[21] Anpo, M., Shima, T., Kodama, S. and Kubokawa, Y., 'Photocatalytic Hydrogenation of CH_3CCH with H_2O on Small-Particle TiO_2: Size Quantization Effects and Reaction Intermediates', *Journal of Physical Chemistry*, **91** pp 4305-4310, (1987).

ELSEVIER

SCIENCE AND
TECHNOLOGY OF
ADVANCED
MATERIALS

www.elsevier.com/locate/stam

Activity of nanosized titania synthesized from thermal decomposition of titanium (IV) *n*-butoxide for the photocatalytic degradation of diuron

Jitlada Klongdee[a], Wansiri Petchkroh[b], Kosin Phuempoonsathaporn[c],
Piyasan Praserthdam[a], Alisa S. Vangnai[b,d], Varong Pavarajarn[a,*]

[a]*Department of Chemical Engineering, Faculty of Engineering, Center of Excellence on Catalysis and Catalytic Reaction Engineering,
Chulalongkorn University, Bangkok 10330, Thailand*
[b]*National Research Center for Environmental and Hazardous Waste Management (NRC-EHWM), Chulalongkorn University, Bangkok 10330, Thailand*
[c]*Biotechnology Graduate Program, Faculty of Science, Chulalongkorn University, Bangkok 10330, Thailand*
[d]*Department of Biochemistry, Faculty of Science, Chulalongkorn University, Bangkok 10330, Thailand*

Abstract

Nanoparticles of anatase titania were synthesized by the thermal decomposition of titanium (IV) *n*-butoxide in 1,4-butanediol. The powder obtained was characterized by various characterization techniques, such as XRD, BET, SEM and TEM, to confirm that it was a collection of single crystal anatase with particle size smaller than 15 nm. The synthesized titania was employed as catalyst for the photodegradation of diuron, a herbicide belonging to the phenylurea family, which has been considered as a biologically active pollutant in soil and water. Although diuron is chemically stable, degradation of diuron by photocatalyzed oxidation was found possible. The conversions achieved by titania prepared were in the range of 70–80% within 6 h of reaction, using standard UV lamps, while over 99% conversion was achieved under solar irradiation. The photocatalytic activity was compared with that of the Japanese Reference Catalyst (JRC-TIO-1) titania from the Catalysis Society of Japan. The synthesized titania exhibited higher rate and efficiency in diuron degradation than reference catalyst. The results from the investigations by controlling various reaction parameters, such as oxygen dissolved in the solution, diuron concentration, as well as light source, suggested that the enhanced photocatalytic activity was the result from higher crystallinity of the synthesized titania. © 2005 Elsevier Ltd. All rights reserved.

Keywords: Titania; Thermal decomposition; Nanoparticle; Photocatalytic activity; Diuron; Degradation

1. Introduction

Titanium (IV) dioxide or titania (TiO_2) is one of the most common metal-oxides recognized in various industries. Due to its good physical and chemical properties, such as catalytic activity [1], photocatalytic activity [2], good stability toward adverse environment [3], sensitivity to humidity and gas [4], dielectric character [5], nonlinear optical characteristic [6] and photoluminescence [7], titania has been used in many fields of application including the use as catalysts, catalyst supports, electronics, cosmetics, pigments and filler coating. Nevertheless, photocatalyst is one of the most important applications of titania. Although titania is known to have three natural polymorphs, i.e. rutile, anatase, and brookite, only anatase is generally accepted to have significant photocatalytic activity [8–10].

Many factors affect the photocatalytic activity of titania. Particle size is one of the most important factors. It has been reported that photocatalytic activity is increased with the decrease in titania particle size, especially into nanometer-scale, because of high surface area and short interface migration distances for photoinduced holes and electrons [11–13]. Nanocrystalline titania can be synthesized by many methods, such as sol-gel method, hydrothermal method, vapor-phase hydrolysis, laser-induced decomposition, chemical vapor decomposition and molten salt method. In this work, nanocrystalline anatase titania was synthesized via the thermal decomposition of titanium alkoxide in organic solvent, which has been employed to synthesize various nanocrystalline metal-oxides [14–19]. It has been

---

* Corresponding author. Tel.: +66 2 2186 890; fax: +66 2 2186 877.
E-mail address: fchvpv@eng.chula.ac.th (V. Pavarajarn).

demonstrated that the activity of titania synthesized by this method is much higher than those of commercially available titania for photocatalytic decomposition of simple compound, such as acetic acid, in aqueous solutions [20]. However, it has never been used for the decomposition of more complex substance. In this study, photodegradation of complex substance, i.e. diuron [3-(3,4-dichlorophynyl)-1,1-dimethylurea], is employed to investigate the activity of titania prepared by this method.

Diuron has been one of the most commonly used herbicides for more than 40 years. It is bio-recalcitrant and chemically stable with half-life in soil over 300 days. Since, diuron is slightly soluble (solubility of 36.4 mg/l at 25 °C), it can slowly penetrates through soil and contaminates underground water. Photodegradation using titania as catalyst is therefore one potential option for contaminated water remediation.

2. Materials and methods

2.1. Synthesis of titania

Titanium (IV) *n*-butoxide (TNB) was used as starting material for titania synthesis. 15 g of TNB was suspended in 100 ml of 1,4-butanediol, which was used as reaction medium, in a test tube. The test tube was then placed in a 300 ml autoclave. The gap between the test tube and the autoclave wall was also filled with 1,4-butanediol. The autoclave was purged completely by nitrogen before heating up to 300 °C at a rate of 2.5 °C/min. Autogeneous pressure during the reaction gradually increased as the temperature was raised. The system was held at 300 °C for 2 h before cooling down to room temperature. The resulting powders in the test tube were repeatedly washed with methanol and dried in 110 °C oven overnight. Subsequently, the obtained product was calcined at 500 °C for 2 h in a box furnace with a heating rate of 10 °C/min.

Synthesized powders were characterized by various techniques, i.e. powder X-ray diffraction (XRD), scanning electron microscope (SEM) and transmission electron microscope (TEM). Powder X-ray diffraction (XRD) analysis was done by using a SIEMENS D5000 diffractometer with CuKα radiation. The crystallite size of the product was determined from the broadening of its main peak, using the Scherrer equation. Specific surface area of the samples was also measured by using the BET multipoint method.

2.2. Photocatalytic experiments

Photodegradation of diuron in aqueous solution was employed to investigate the photocatalytic activity of the synthesized titania. The initial concentrations of diuron used were 1 and 10 ppm, respectively. The solution was mixed with titania in the ratio of 1 mg titania to 10 ml of solution

and kept in the dark for at least 15 min to allow the complete adsorption of diuron on the surface of titania. The photocatalytic reaction was initiated by exposing test tubes to light from UV lamps (Phillips Cleo 15 W). Diuron degradation was periodically monitored by using a reverse phase HPLC system. The HPLC system included Hyperclone column (150×8 mm inner diameter; 5 μm particle size) (Phenomenex, USA) with a mobile phase of 70% acetonitrile–29.5% water–0.5% phosphoric acid; a flow rate of 0.5 ml/min and a UV detector at 254 nm. The photocatalytic activity of the synthesized catalyst was compared with that of the Japanese Reference Catalyst titania, JRC-TIO-1, which is also pure nanocrystalline anatase.

3. Results and discussion

3.1. Properties of synthesized titania

The particles obtained from the decomposition of TNB in 1,4-butanediol at 300 °C was confirmed to be titania. The XRD analysis, as shown in Fig. 1, revealed that the synthesized product before calcination was already anatase phase. This result was in agreement with the results from our previous work that anatase crystals were formed by crystallization when the temperature in the autoclave reached 250 °C [21]. The crystallite size of the as-synthesized product calculated from the Scherrer equation was approximately 13 nm, while that of the calcined product was 15 nm. It should be noted that the crystallite sizes calculated were in agreement with TEM observation (Fig. 2). Therefore, it was suggested that the synthesized product synthesized was nanosized single crystal titania.

As shown in Table 1, the BET surface area measured by nitrogen adsorption (S_{BET}) of the as-synthesized products was comparable with the surface area calculated from the particle size (S_{XRD}), which was assumed that the particles were spherical and nonporous. It was therefore suggested
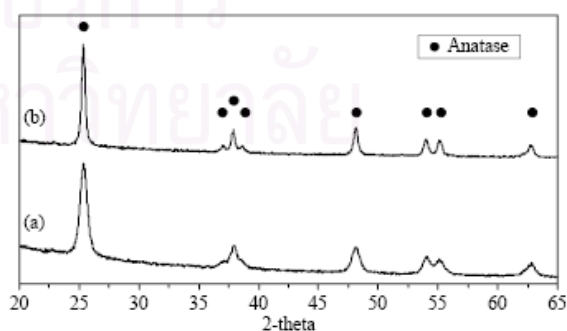

Fig. 1. XRD patterns of synthesized titania: (a) before calcination, (b) after calcination.
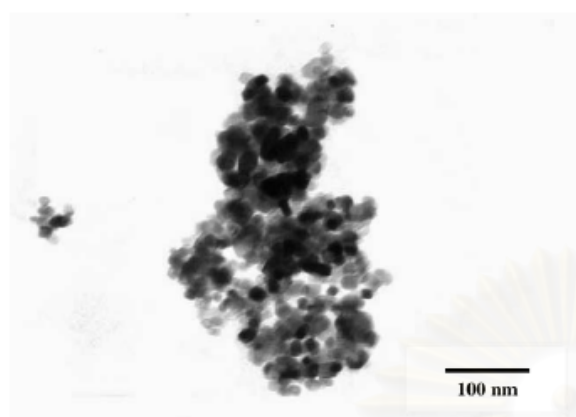
Fig. 2. TEM micrograph of as-synthesized titania.

that the primary particles were not heavily agglomerated. It was also confirmed by SEM micrographs (Fig. 3a) that the synthesized powder was an irregular aggregates of nanometer particles. According to Park et al. [22], agglomeration of the precipitates is influenced by dielectric constant of the reaction medium. The lower the dielectric constant, the higher the degree of agglomeration. Since, 1,4-butanediol has quite high dielectric constant ($\varepsilon = 32$ at 25 °C [23]), the repulsive force between anatase particles formed in this reaction medium is more pronounced than the attraction force, resulting in low degree of agglomeration.

After calcination at 500 °C, the calcined powder was still in anatase phase, as previously proved that anatase synthesized by this method is thermally stable [21]. Nevertheless, the crystallite size of titania increased due to crystal growth. Agglomeration of primary particles was also observed, according to the fact that the BET surface area was notably decreased. Despite of the smaller surface area, calcined titania has shown higher photocatalytic activity than as-synthesized titania. This is due to the fact that the crystallinity of titania was improved by calcination and the crystallinity predominantly influenced the activity rather than surface area [24].

3.2. Photodegradation of diuron

It has been reported that titania synthesized by the thermal decomposition of titanium alkoxide in organic

Table 1
Crystallite size and surface area of the synthesized products

	Crystallite size[a], d (nm)	S_{BET} (m^2/g)	S_{XRD} (m^2/g)
Synthesized titania			
Before calcination	13	113	120
After calcination	15	68	103
Reference titania	9	53	174

[a] Crystallite size calculated from XRD peak broadening.
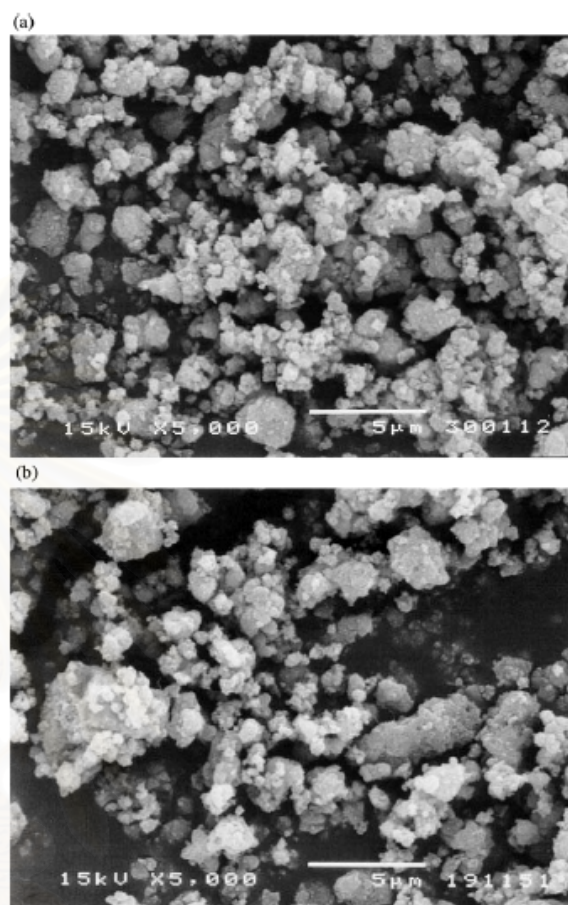
Fig. 3. SEM micrographs of synthesized titania: (a) before calcination, (b) after calcination.

solvent has high activity in photocatalytic decomposition of various compounds [20]. In this work, titania synthesized by this method was employed as catalyst in the photodegradation of diuron, which is chemically stable pollutant. Since, the photocatalytic activity depends upon the conditions of the reaction, such as temperature, light intensity, initial concentration of the compound to be degraded and amount of catalyst used, it is difficult to directly compare the results obtained in this work to those reported in literatures. Therefore, in order to investigate activity of the in-house synthesized catalyst, the results were compared to that of the reference catalyst (JRC-TIO-1) from the Catalysis Society of Japan. It should be noted that mass of the reference catalyst used was the same as the mass of the in-house synthesized catalyst.

Fig. 4 shows the disappearance of diuron by photocatalytic degradation using the synthesized titania or reference titania as catalyst. It should be noted that C is the concentration of diuron at time t, while C_0 is the initial diuron concentration. The results shown in Fig. 4a indicate

Fig. 4. Results for photocatalytic degradation of 1 ppm diuron aqueous solution: (a) in oxygen saturated solution, (b) in nitrogen-purged solution; (■) synthesized titania, (◇) reference titania.
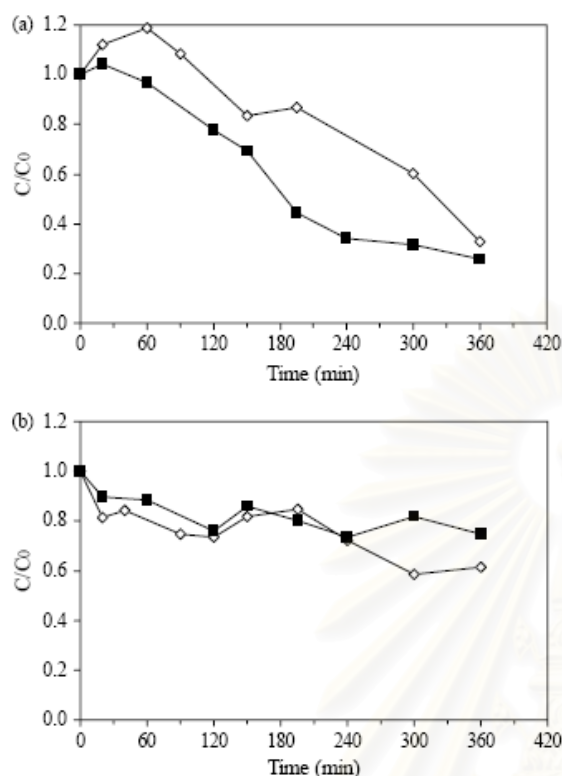
the activity. Crystallinity, including quality and quantity of both bulk and surface crystal defects, is one factor that affects the electron-hole separation [25]. It has been reported that negligible photocatalytic activity of amorphous titania is attributable to the facilitated recombination of photoexcited electrons and holes in the amorphous structure. Therefore, the result in Fig. 4a suggests that titania synthesized by thermal decomposition of TNB in 1,4-butanediol has structure with high crystallinity that prevents electron-hole recombination. This result supports the findings in our previous work that titania synthesized by this method was formed via crystallization pathway [21].

When all oxygen dissolved in the solution was purged by thoroughly bubbling with nitrogen gas, the conversion of diuron photodegradation dramatically decreased. As shown in Fig. 4(b), only about 30% of diuron was degraded within 6 h of the reaction with either the synthesized or the reference catalyst. This is in agreement with the generally accepted mechanism of the photocatalytic reaction that the presence of oxygen as an electron scavenger in the system is required for the course of the reaction [26–28]. Without electron scavenger, the electron-hole recombination spontaneously took place on the surface of titania. The enhanced effect from crystallinity of the synthesized titania was therefore compromised and the progress of the photocatalytic reactions from both catalysts were roughly the same. However, regardless of the depletion of dissolved oxygen in the solution, the reaction still slowly progressed. This was expected to be the results from chlorine radicals produced from diuron degradation. Several studies involving photocatalytic decomposition of chlorinated organic materials have proposed that chlorine radicals may be generated during photocatalysis [29] and these radicals participate in radical chain reactions [30–32].

Further, investigations on the enhanced activity of the synthesized titania were conducted by using solar irradiation, which had much higher light intensity than UV lamps. It should be noted that the concentration of

that although both catalysts yielded approximately the same degradation after the reaction time of 6 h, the synthesized titania showed almost twice as much in the initial degradation rate than the reference catalyst. The amount of diuron was reduced to 30% of its initial value within 4 h of the reaction using the synthesized catalyst, while almost 6 h was required for the reference catalyst.

It has been recognized that the efficiency of titania in photocatalytic reaction is influenced by many factors such as crystallinity of the anatase phase [9], particle size [11] and surface area [11]. Since, the synthesized and reference titania are both anatase with roughly same particle size and surface area, the main factor accountable for the enhanced activity of the synthesized titania is its crystallinity. Although there has been no consensus on the detailed mechanism of the photocatalytic reaction on titania, it is generally agreed that the reaction involves generation of electron-hole pairs upon illumination of UV light on titania. The photogenerated holes can be subsequently scavenged by oxidizing species such as H_2O or OH^- and result in highly reactive hydroxyl radicals, which are the key for decomposition of most organic contaminants. Therefore, the separation of the photogenerated electron-hole pairs is considered to have a predominant role in photocatalytic reaction. The longer the separation period, the higher
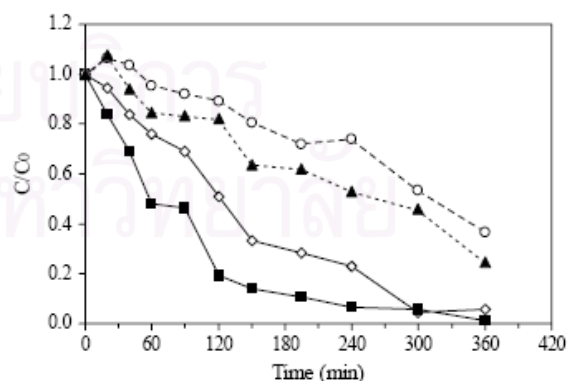

Fig. 5. Results for photocatalytic degradation of 10 ppm diuron aqueous solution: (- - -) using UV lamps, (—) using solar radiation; (■), (▲) synthesized titania, (◇), (○) reference titania.

Fig. 6. First-order linear transforms of the degradation of 10 ppm diuron aqueous solution: (- - -) using UV lamps, (—) using solar radiation; (■), (▲) synthesized titania, (◇), (○) reference titania.
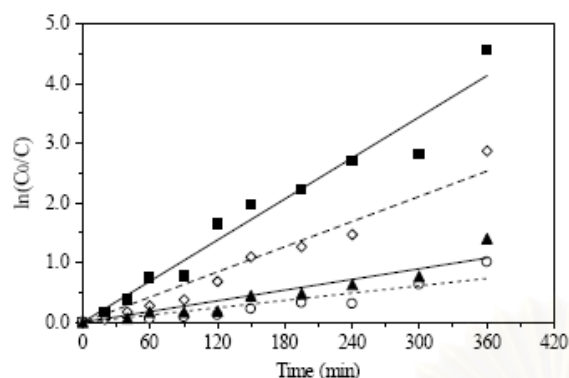
diuron employed was increased to 10 ppm in order to investigate the effect of the initial concentration as well. Fig. 5 shows the results comparing the photodegradation using sunlight to that using UV lamps. Furthermore, since rates of photooxidation of various organic contaminants over illuminated titania have been suggested to follow the Langmuir–Hinshelwood kinetics model [27,33,34], which can be simplified to the apparent first-order kinetics at low concentration, the plot of $\ln (C_0/C)$ versus time was expected to be a straight line with the slope equal to the apparent rate constant, k_{app}, of the degradation. The first-order linear transforms of the results shown in Fig. 5 are given in Fig. 6 and the rate constants are reported in Table 2.

Regarding the effect of diuron concentration, it was found that the degradation rate under UV light shown in Fig. 5 ($C_0 = 10$ ppm) was only slightly less than that was given in Fig. 4 ($C_0 = 1$ ppm). This is in general agreement with the pseudo first-order nature, according to the Langmuir–Hinshelwood kinetics, of the photooxidation on titania.

It can be seen from Figs. 5 and 6 that titania synthesized from thermal decomposition of titanium alkoxide has higher photocatalytic activity than the reference catalyst, especially under solar irradiation. Although it was not surprise to observe higher degradation rate under higher light intensity, it was particularly interesting to find that the enhancement in the activity from the synthesized titania

increased with an increase in light intensity. According to Table 2, the reaction rate constant obtained from the synthesized titania was roughly 45% higher than that of the reference titania, when UV lamps were used. On the other hand, the rate from the synthesized titania was about 60% higher, under solar irradiation.

In general, under higher light intensity, more photo-electron-hole pairs are generated. However, it has been reported that a rate of the electron-hole recombination increases with increasing light intensity more progress-ively than the rates of charge transfer reaction [35]. Therefore, titania with high crystallinity, which prolongs the separation lifetime of the photogenerated electron-hole pairs, would utilize these greater amount of photoexcited electrons and holes with higher efficiency. Consequently, the enhancement in the photocatalytic activity under high light intensity is more pronounced than that from titania with lower crystallinity. This feature supports the afore-mentioned discussion that thermal decomposition of titanium alkoxide resulted in anatase titania with much higher crystallinity than the conventional preparation techniques.

Results discussed above have demonstrated that titania synthesized by thermal decomposition of TNB in 1,4-butanediol is potentially applicable for the photodegrada-tion of diuron. However, the operating conditions for photocatalytic reaction in this work have not been optimized. Further, investigation on effects of degradation parameters on the degradation efficiency as well as the intermediates resulted from diuron degradation will be discussed in our next paper.

4. Conclusion

Nanocrystalline anatase titania can be prepared via thermal decomposition of TNB in 1,4-butanediol. The synthesized titania has shown higher photocatalytic activity comparing to the reference catalyst. It is suggested that the enhanced activity is resulted from high crystallinity of the synthesized powder, which consequently reduces the recombination of photogenerated electron-hole pairs. The synthesized titania also shows the potential for the degradation of chemically stable compound such as diuron. Nevertheless, conditions for photodecomposition need to be optimized.

Acknowledgements

Table 2
Rate constants and half-life of the photocatalytic degradation reaction of diuron

	k_{app} (min^{-1})	$t_{1/2}$ (min)
Degradation using UV lamps		
Synthesized titania	3.003×10^{-3}	230.8
Reference titania	2.042×10^{-3}	339.5
Degradation using solar irradiation		
Synthesized titania	1.145×10^{-2}	60.5
Reference titania	7.027×10^{-3}	98.6

155

References

[1] K.E. Coulter, A.G. Sault, Effects of activation on the surface-properties of silica-supported cobalt catalysts, Journal of Catalysis 154 (1995) 56–64.

[2] T. Wakanabe, A. Kitamura, E. Kojima, C. Nakayama, K. Hashimoto, A. Fuijishima, in: D.E. Olis, H. Al-Ekabi (Eds.), Photocatalytic Purification and Treatment of Water and Air, Elsevier, Amsterdam, 1993, p. 747.

[3] A.M. Tonejc, M. Goti, B. Grzeta, S. Music, S. Popovi, R. Trojko, A. Turkovi, I. MuSevic, Transmission electron microscopy studies of nanophase TiO_2, Materials Science and Engineering B-Solid State Materials for Advanced Technology 40 (1996) 177–184.

[4] E. Traversa, G. Gnappi, A. Montenero, G. Gusmano, Ceramic thin films by sol–gel processing as novel materials for integrated humidity sensors, Sensors and Actuators B-Chemical 31 (1996) 59–70.

[5] B. Ohtani, S. Nishimoto, Effect of surface adsorptions of aliphatic-alcohols and silver ion on the photocatalytic activity of TiO_2 suspended in aqueous-solutions, Journal of Physical Chemistry 97 (1993) 920–926.

[6] B. O'Regan, M. Gratzel, A low-cost, high-efficiency solar cell based on dye-sensitized colloidal TiO_2 films, Nature 353 (1991) 737.

[7] Y.J. Liu, R.O. Claus, Blue light emitting nanosized TiO_2 colloids, Journal of the American Chemical Society 119 (1997) 5273–5274.

[8] S. Nishimoto, B. Ohtani, H. Kajiwara, T. Kagiya, Correlation of the crystal structure of titanium dioxide prepared from titanium tetra-2-propoxide with the photocatalytic activity for redox reactions in aqueous propan-2-ol and silver salt solutions, Journal of the Chemical Society-Faraday Transactions 1 (81) (1985) 61–68.

[9] M.A. Fox, M.T. Dulay, Heterogeneous photocatalysis, Chemical Reviews 93 (1993) 341–357.

[10] K. Tanaka, T. Hisanaga, A.P. Rivera, in: D.F. Ollis, H. Al-Ekabi (Eds.), Photocatalytic Purification and Treatment of Water and Air, Elsevier, Amsterdam, 1993, p. 169.

[11] N.P. Xu, Z.F. Shi, Y.Q. Fan, J.H. Dong, J. Shi, M.Z.C. Hu, Effects of particle size of TiO_2 on photocatalytic degradation of methylene blue in aqueous suspensions, Industrial and Engineering Chemistry Research 38 (1999) 373–379.

[12] T. Sato, Y. Yamamoto, Y. Fujishiro, S. Uchida, Intercalation of iron oxide in layered $H_2Ti_4O_9$ and $H_4Nb_6O_{17}$: visible-light induced photocatalytic properties, Journal of the Chemical Society-Faraday Transactions 92 (1996) 5089–5092.

[13] S. Uchida, Y. Yamamoto, Y. Fujishiro, A. Watanabe, O. Ito, T. Sato, Intercalation of titanium oxide in layered $H_2Ti_4O_9$ and $H_4Nb_6O_{17}$ and photocatalytic water cleavage with $H_2Ti_4O_9/(TiO_2, Pt)$ and $H_4Nb_6O_{17}/(TiO_2, Pt)$ nanocomposites, Journal of the Chemical Society-Faraday Transactions 93 (1997) 3229–3234.

[14] M. Inoue, Y. Kondo, T. Inui, An ethylene glycol derivative of boehmite, Inorganic Chemistry 27 (1988) 215–221.

[15] M. Inoue, H. Kominami, T. Inui, Thermal transformation of chi-alumina formed by thermal decomposition of aluminum alkoxide in organic media, Journal of the American Ceramic Society 75 (1992) 2597–2598.

[16] M. Inoue, H. Kominami, T. Inui, Novel synthetic method for the catalytic use of thermally stable zirconia—thermal decomposition of zirconium alkoxides in organic media, Applied Catalysis A-General 97 (1993) L25–L30.

[17] H. Kominami, J. Kato, S. Murakami, Y. Kera, M. Inoue, T. Inui, B. Ohtani, Synthesis of titanium (IV) oxide of ultra-high photo-catalytic activity: high-temperature hydrolysis of titanium alkoxides with water liberated homogeneously from solvent alcohols, Journal of Molecular Catalysis A-Chemical 144 (1999) 165–171.

[18] S. Kongwudthiti, P. Praserthdam, P. Silveston, M. Inoue, Influence of synthesis conditions on the preparation of zirconia powder by the glycothermal method, Ceramics International 29 (2003) 807–814.

[19] O. Mekasuwandumrong, P.L. Silveston, P. Praserthdam, M. Inoue, V. Pavarajarn, W. Tanakulrungsank, Synthesis of thermally stable micro spherical chi-alumina by thermal decomposition of aluminum isopropoxide in mineral oil, Inorganic Chemistry Communications 6 (2003) 930–934.

[20] H. Kominami, J. Kato, Y. Takada, Y. Doushi, B. Ohtani, S. Nishimoto, M. Inoue, T. Inui, Y. Kera, Novel synthesis of microcrystalline titanium (IV) oxide having high thermal stability and ultra-high photocatalytic activity: thermal decomposition of titanium (IV) alkoxide in organic solvents, Catalysis Letters 46 (1997) 235–240.

[21] W. Payakgul, O. Mekasuwandumrong, V. Pavarajarn, P. Praserthdam, Effects of reaction medium on the synthesis of TiO_2 nanocrystals by thermal decomposition of titanium (IV) *n*-butoxide, Ceramics International 31 (2005) 391–397.

[22] H.K. Park, D.K. Kim, C.H. Kim, Effect of solvent on titania particle formation and morphology in thermal hydrolysis of $TiCl_4$, Journal of the American Ceramic Society 80 (1997) 743–749.

[23] J.A. Dean, Lange's Handbook of Chemistry, McGraw-Hill, New York, 1999.

[24] H. Kominami, S. Murakami, Y. Kera, B. Ohtani, Titanium (IV) oxide photocatalyst of ultra-high activity: a new preparation process allowing compatibility of high adsorptivity and low electron-hole recombination probability, Catalysis Letters 56 (1998) 125–129.

[25] S.J. Tsai, S. Cheng, Effect of TiO_2 crystalline structure in photocatalytic degradation of phenolic contaminants, Catalysis Today 33 (1997) 227–237.

[26] C. Kormann, D.W. Bahnemann, M.R. Hoffmann, Photocatalytic production of hydrogen peroxides and organic peroxides in aqueous suspensions of titanium dioxide, zinc oxide, and desert sand, Environmental Science & Technology 22 (1988) 798–806.

[27] A. Houas, H. Lachheb, M. Ksibi, E. Elaloui, C. Guillard, J.M. Herrmann, Photocatalytic degradation pathway of methylene blue in water, Applied Catalysis B-Environmental 31 (2001) 145–157.

[28] H.-S. Son, S.-J. Lee, I.-H. Cho, K.-D. Zoh, Kinetics and mechanism of TNT degradation in TiO_2 photocatalysis, Chemosphere 57 (2004) 309–317.

[29] M.R. Nimlos, W.A. Jacoby, D.M. Blake, T.A. Milne, Direct mass spectrometric studies of the destruction of hazardous wastes. 2. Gas-phase photocatalytic oxidation of trichloroethylene over TiO_2: products and mechanisms, Environmental Science & Technology 27 (1993) 732–740.

[30] Y. Luo, D.F. Ollis, Heterogeneous photocatalytic oxidation of trichloroethylene and toluene mixtures in air: kinetic promotion and inhibition, time-dependent catalyst activity, Journal of Catalysis 163 (1996) 1–11.

[31] O. dHennezel, D.F. Ollis, Trichloroethylene-promoted photocatalytic oxidation of air contaminants, Journal of Catalysis 167 (1997) 118–126.

[32] M. Lewandowski, D.F. Ollis, Halide acid pretreatments of photocatalysts for oxidation of aromatic air contaminants: rate enhancement, rate inhibition, and a thermodynamic rationale, Journal of Catalysis 217 (2003) 38–46.

[33] W.Z. Tang, H. An, Photocatalytic degradation kinetics and mechanism of acid-blue-40 by TiO_2/UV in aqueous-solution, Chemosphere 31 (1995) 4171–4183.

[34] I.K. Konstantinou, V.A. Sakkas, T.A. Albanis, Photocatalytic degradation of propachlor in aqueous TiO_2 suspensions. Determination of the reaction pathway and identification of intermediate products by various analytical methods, Water Research 36 (2002) 2733–2742.

[35] M.R. Hoffmann, S.T. Martin, W.Y. Choi, D.W. Bahnemann, Environmental applications of semiconductor photocatalysis, Chemical Reviews 95 (1995) 69–96.

VITA

Miss Jitlada Klongdee was born on September 6, 1979 in Mukdahan Province, Thailand. She received the Bachelor Degree of Science (Industrial Chemistry) from Faculty of Science and Technology, Prince of Songkla University in 2003. She continued her Master's study at Chulalongkorn University in June, 2003.